Supporting Information

Development of a novel highly anti-proliferative family of gold complexes: Au(I)-phosphonium-phosphines

Benjamin Rousselle,[a] Florence Bouyer,[b] Jérôme Bayardon,[a] Myriam Laly,[a] François Ghiringhelli,[b] Yoann Rousselin,[a] Ewen Bodio,*[a] and Raluca Malacea-Kabbara*[a]

[a] ICMUB UMR6302, CNRS, Univ. Bourgogne Franche-Comté, F-21000 Dijon, France

[b] INSERM UMR 1231, Dijon, France

ewen.bodio@u-bourgogne.fr, raluca.malacea@u-bourgogne.fr

Table of content

1. ^{1}H, $^{13}C\{^{1}H\}$ and $^{31}P\{^{1}H\}$ NMR spectra of compound **2** p. 2
2. ^{1}H, $^{13}C\{^{1}H\}$ and $^{31}P\{^{1}H\}$ NMR spectra of compound **3** p. 4
3. ^{1}H, $^{13}C\{^{1}H\}$ and $^{31}P\{^{1}H\}$ NMR spectra of compound **4** p. 6
4. ^{1}H, $^{13}C\{^{1}H\}$ and $^{31}P\{^{1}H\}$ NMR spectra of compound **5a** p. 8
5. ^{1}H, $^{13}C\{^{1}H\}$ and $^{31}P\{^{1}H\}$ NMR spectra of compound **5b** p. 10
6. ^{1}H, $^{13}C\{^{1}H\}$ and $^{31}P\{^{1}H\}$ NMR spectra of compound **5c** p. 12
7. ^{1}H, $^{13}C\{^{1}H\}$ and $^{31}P\{^{1}H\}$ NMR spectra of compound **5d** p. 14
8. ^{1}H, $^{13}C\{^{1}H\}$ and $^{31}P\{^{1}H\}$ NMR spectra of compound **5e** p. 16
9. ^{1}H, $^{13}C\{^{1}H\}$ and $^{31}P\{^{1}H\}$ NMR spectra of compound **5f** p. 18
10. ^{1}H, $^{13}C\{^{1}H\}$ and $^{31}P\{^{1}H\}$ NMR spectra of compound **Ia** p. 20
11. ^{1}H, $^{13}C\{^{1}H\}$ and $^{31}P\{^{1}H\}$ NMR spectra of compound **Ib** p. 22
12. ^{1}H, $^{13}C\{^{1}H\}$ and $^{31}P\{^{1}H\}$ NMR spectra of compound **Ic** p. 24
13. ^{1}H, $^{13}C\{^{1}H\}$ and $^{31}P\{^{1}H\}$ NMR spectra of compound **Id** p. 26
14. ^{1}H, $^{13}C\{^{1}H\}$ and $^{31}P\{^{1}H\}$ NMR spectra of compound **Ie** p. 28
15. ^{1}H, $^{13}C\{^{1}H\}$ and $^{31}P\{^{1}H\}$ NMR spectra of compound **If** p. 30
16. ^{1}H, $^{13}C\{^{1}H\}$ and $^{31}P\{^{1}H\}$ NMR spectra of compound **Ig** p. 32
17. Crystal structure and table of crystal data of compound **Ie** p. 33
18. Crystal structure and table of crystal data of compound **If** p. 43
19. Stability studies of compounds **Ia-f** in DMSO and in presence of water p. 50
20. Water solubility evaluation of compounds **Ia-g** determined by ICP-AES p. 64
21. Cells cytotoxity curves of **Ia-g**, DMSO, oxaliplatin, 5-FU, paclitaxel (A549) p. 65
22. Cells cytotoxity curves of **Ia-g**, DMSO, oxaliplatin, 5-FU, paclitaxel (MDA) p. 66
23. Cells cytotoxity curves of **Ia-g**, DMSO, oxaliplatin, 5-FU, paclitaxel (SW480) p. 67

1. ^{1}H, $^{13}C\{^{1}H\}$ and $^{31}P\{^{1}H\}$ NMR spectra of compound **2**

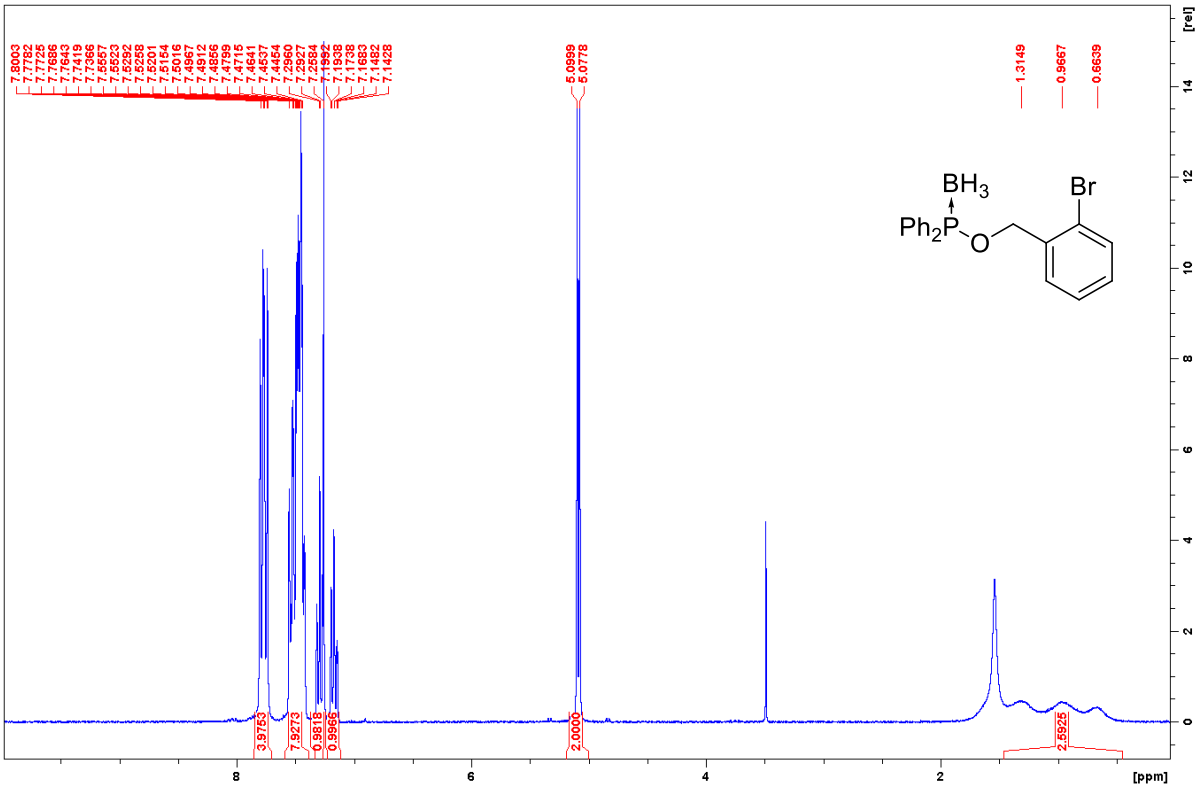

^{1}H NMR (300 MHz, Chloroform-*d*)

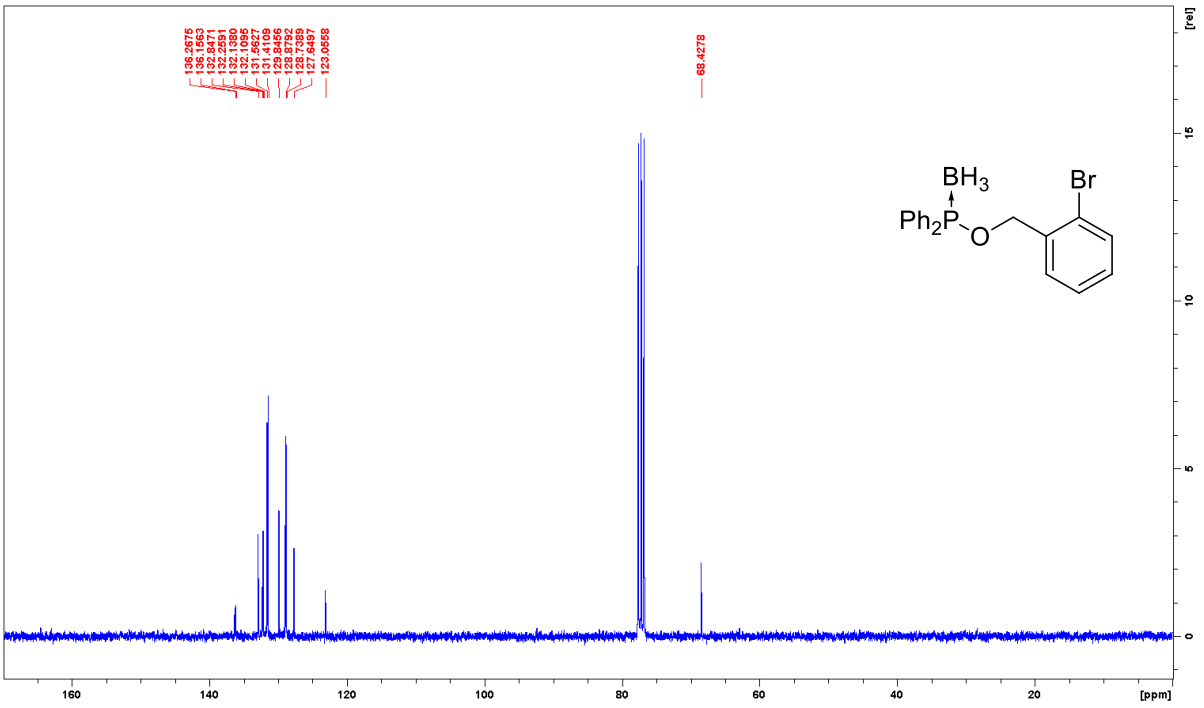

$^{13}C\{^{1}H\}$ NMR (75 MHz, Chloroform-*d*)

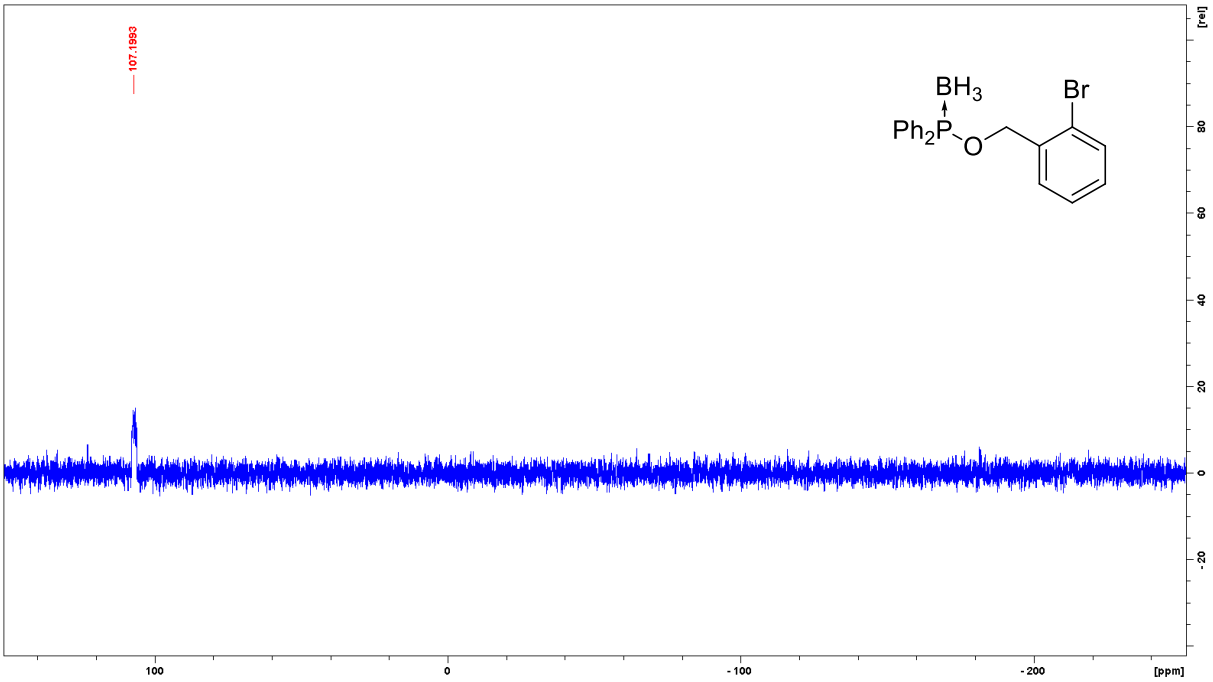

$^{31}P\{^{1}H\}$ NMR (202 MHz, Methylene Chloride-d_2)

2. ^{1}H, $^{13}C\{^{1}H\}$ and $^{31}P\{^{1}H\}$ NMR spectra of compound **3**

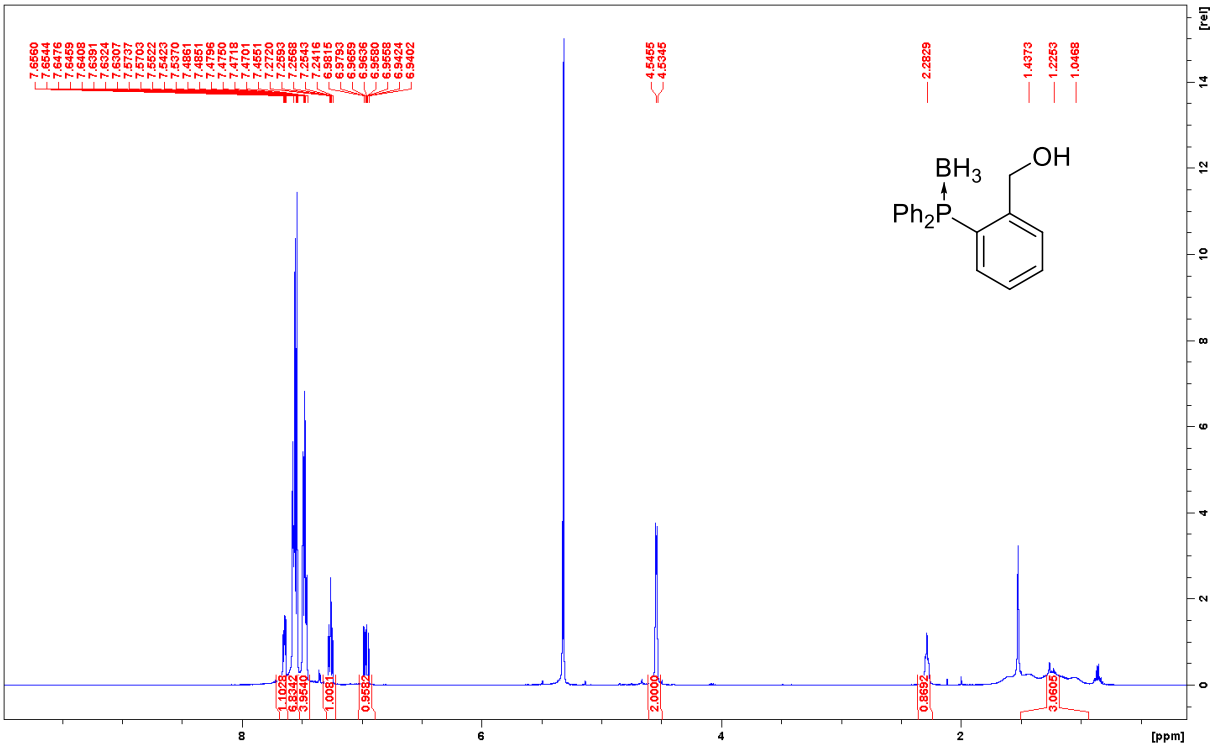

^{1}H NMR (500 MHz, Methylene Chloride-d_2)

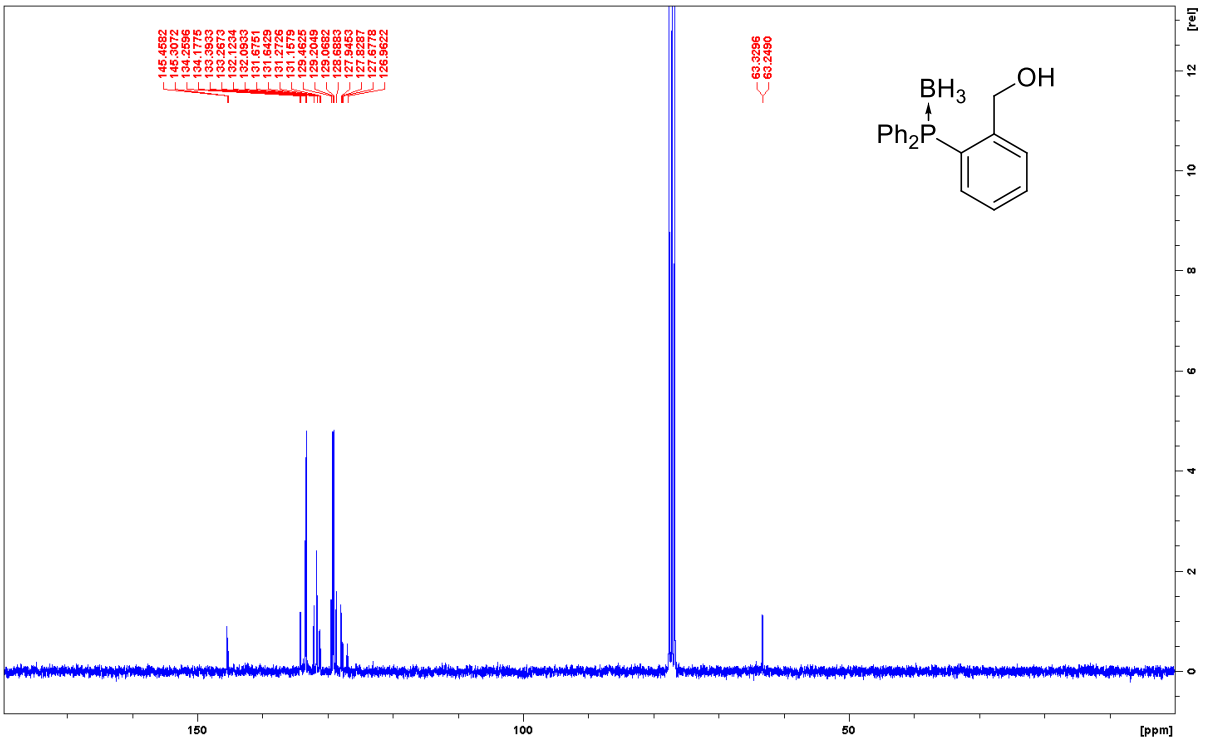

$^{13}C\{^{1}H\}$ NMR (75 MHz, Chloroform-*d*)

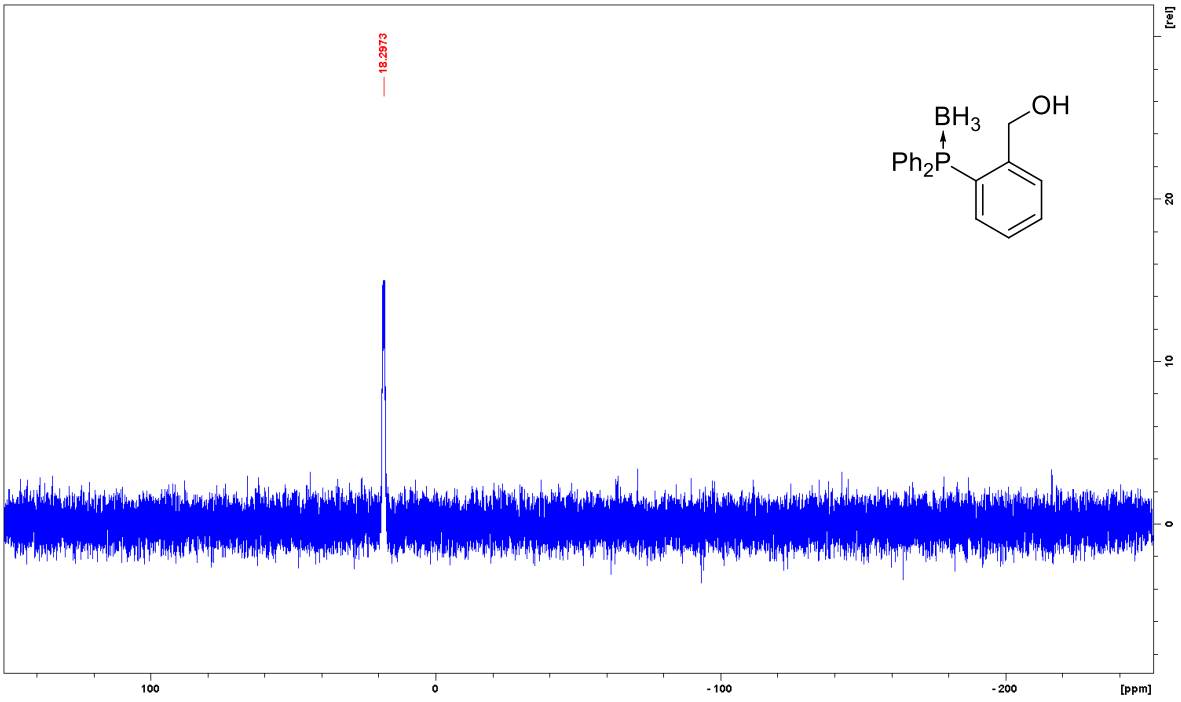

$^{31}P\{^{1}H\}$ NMR (202 MHz, Methylene Chloride-d_2)

3. ^{1}H, $^{13}C\{^{1}H\}$ and $^{31}P\{^{1}H\}$ NMR spectra of compound **4**

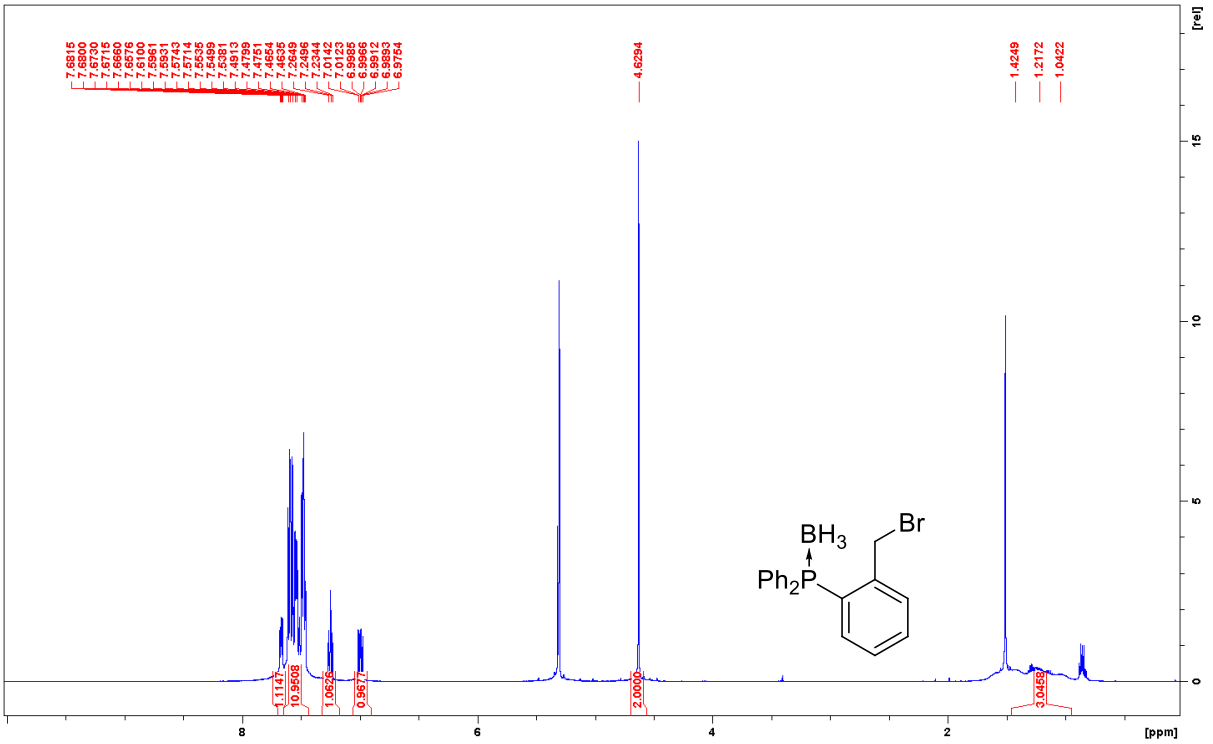

^{1}H NMR (500 MHz, Methylene Chloride-d_2)

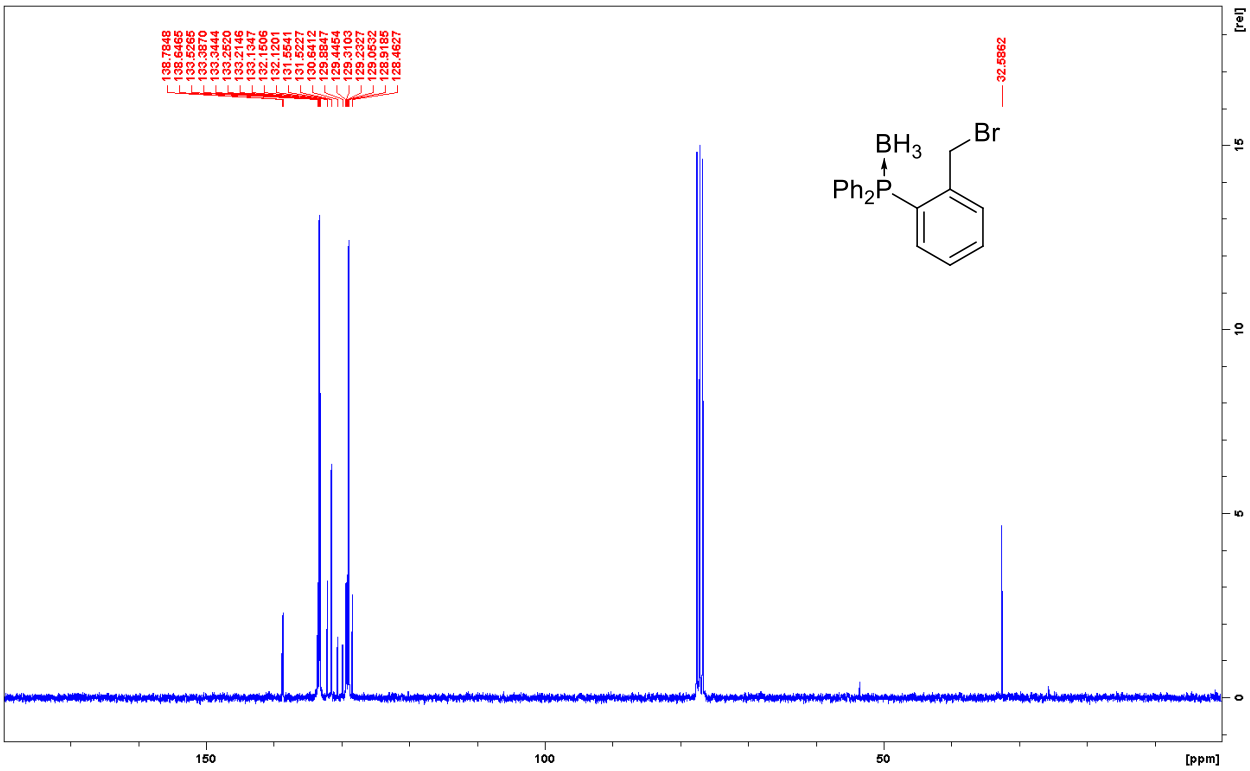

$^{13}C\{^{1}H\}$ NMR (75 MHz, Chloroform-*d*)

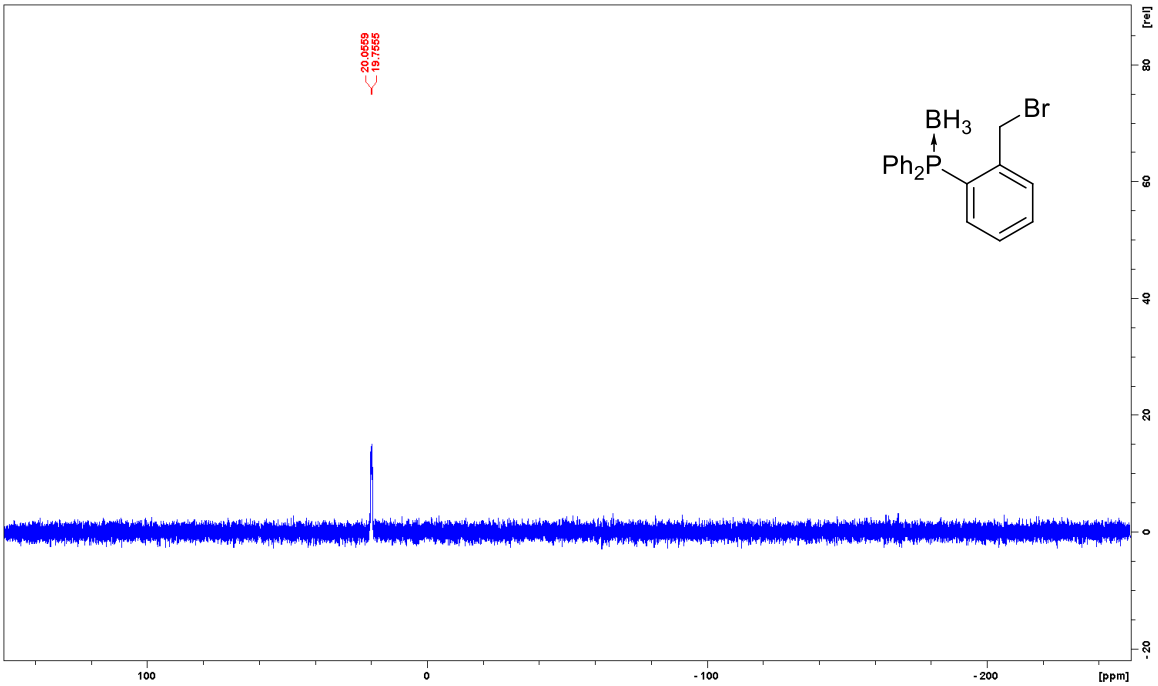

$^{31}P\{^{1}H\}$ NMR (202 MHz, Methylene Chloride-d_2)

4. ^{1}H, $^{13}C\{^{1}H\}$ and $^{31}P\{^{1}H\}$ NMR spectra of compound **5a**

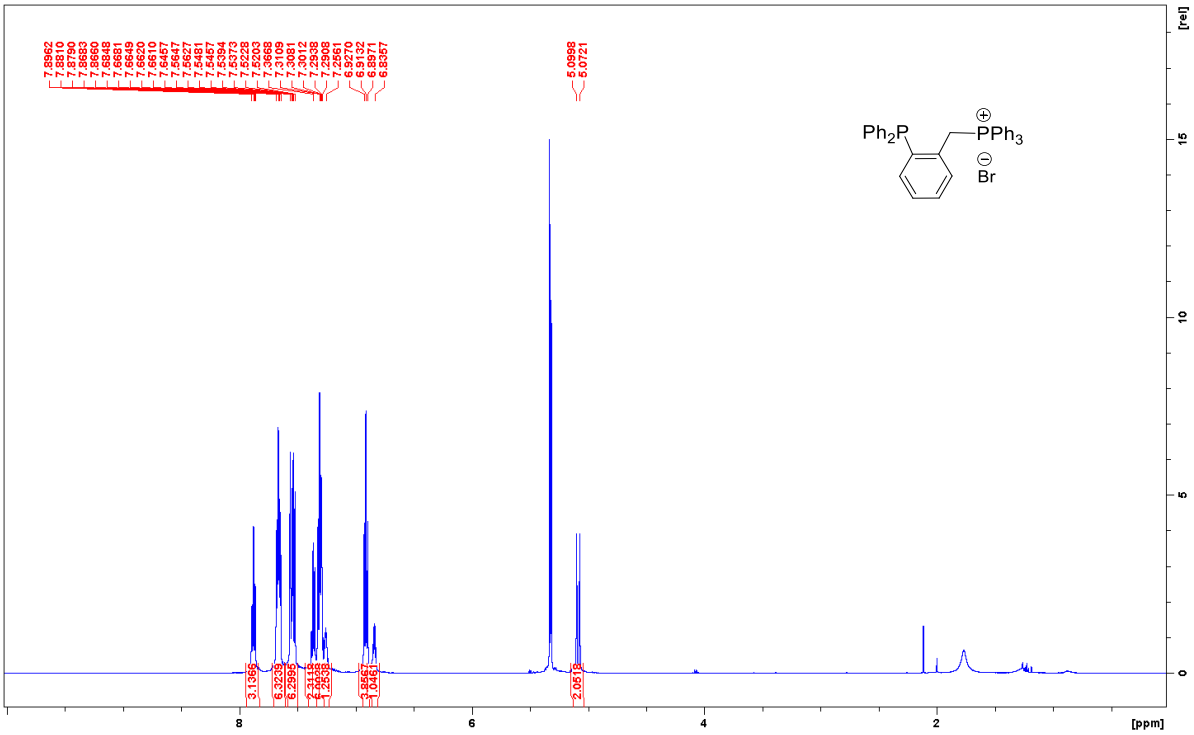

^{1}H NMR (500 MHz, Methylene Chloride-d_2)

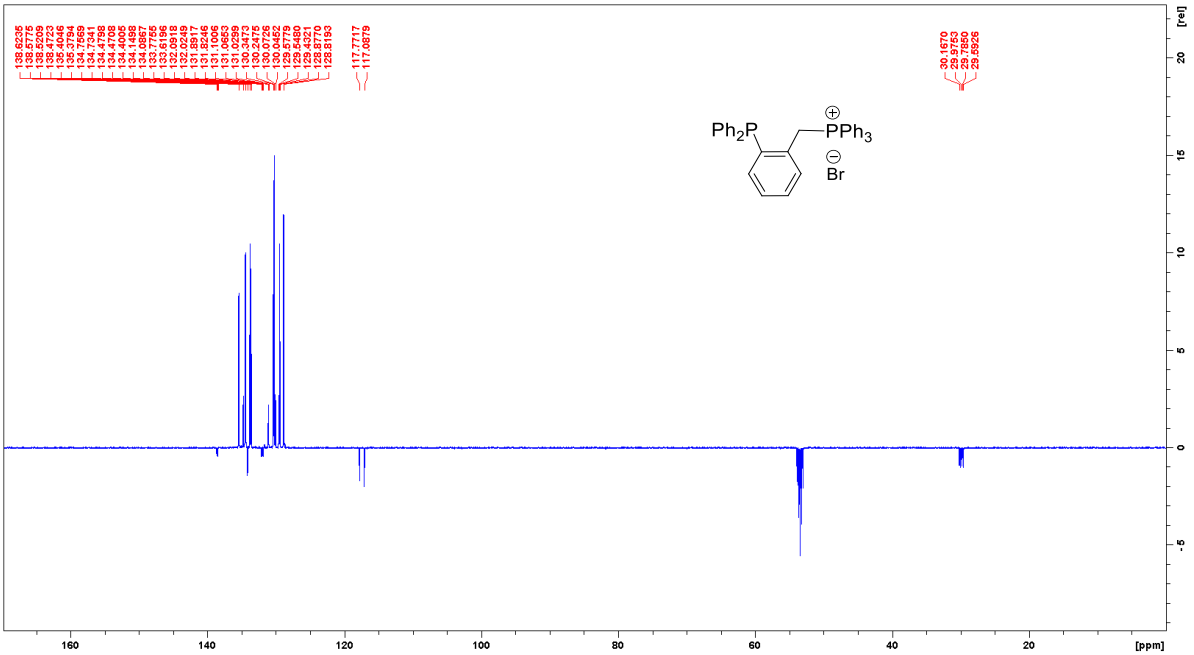

$^{13}C\{^{1}H\}$ J-mod NMR (75 MHz, Methylene Chloride-d_2)

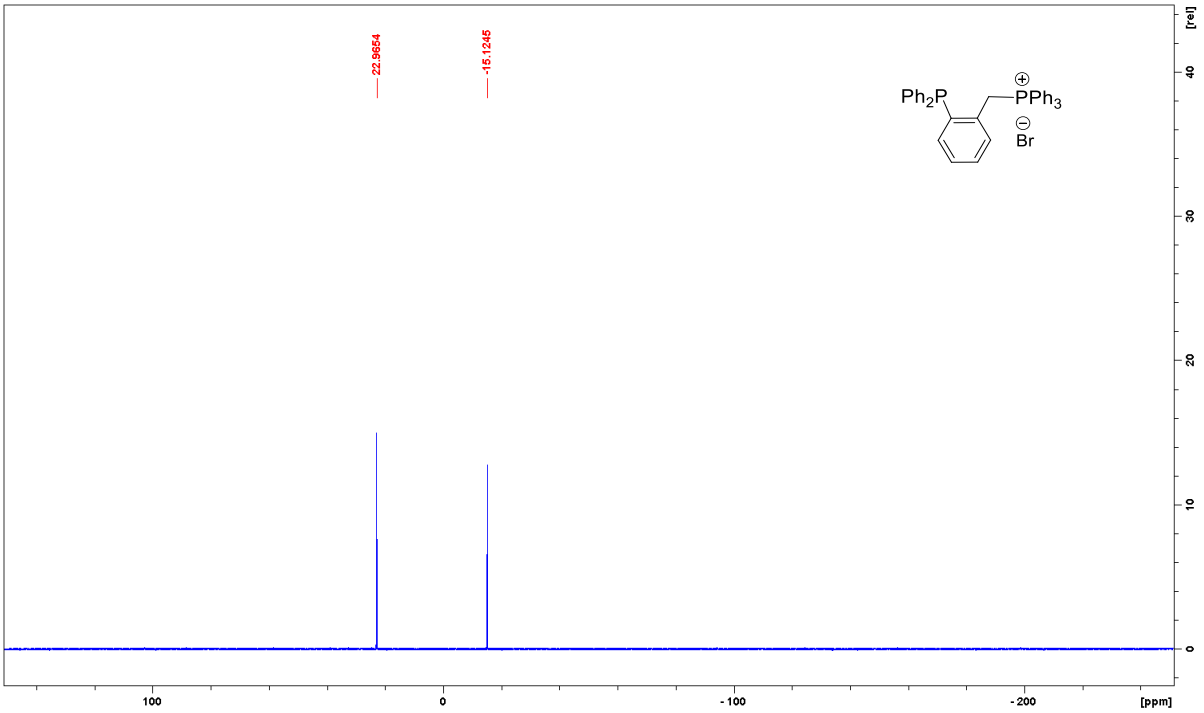

$^{31}P\{^{1}H\}$ NMR (202 MHz, Methylene Chloride-d_2)

5. ^{1}H, $^{13}C\{^{1}H\}$ and $^{31}P\{^{1}H\}$ NMR spectra of compound **5b**

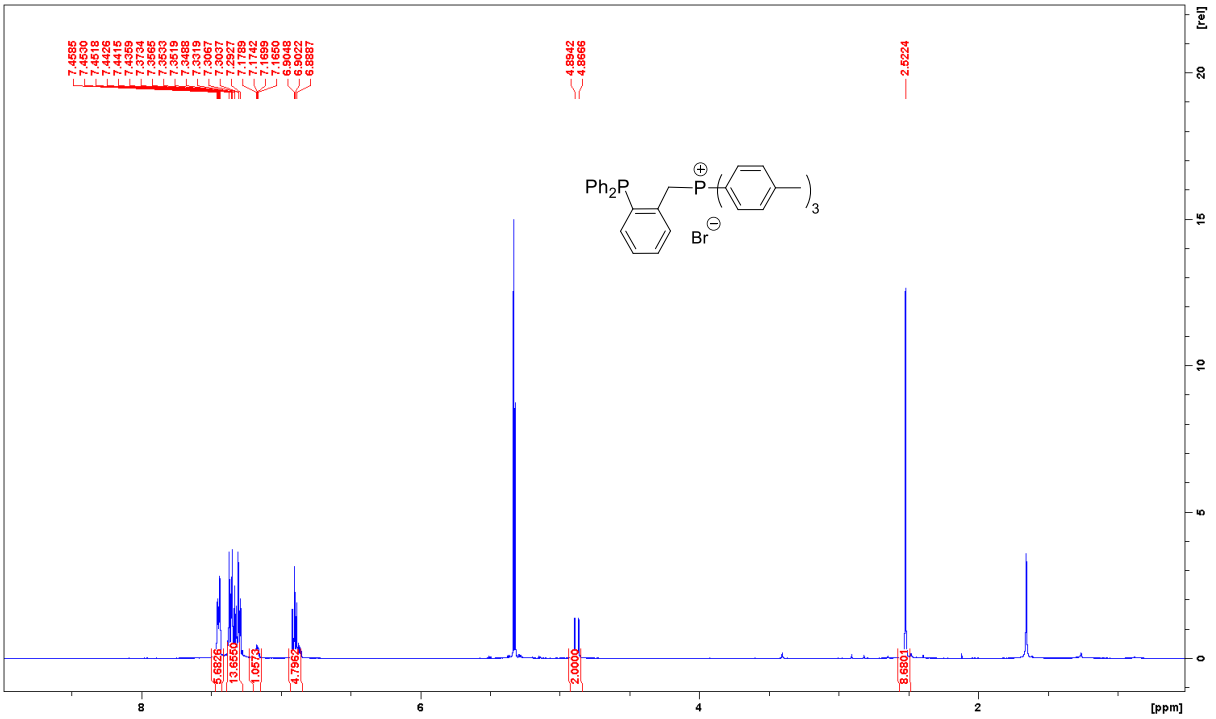

^{1}H NMR (500 MHz, Methylene Chloride-d_2)

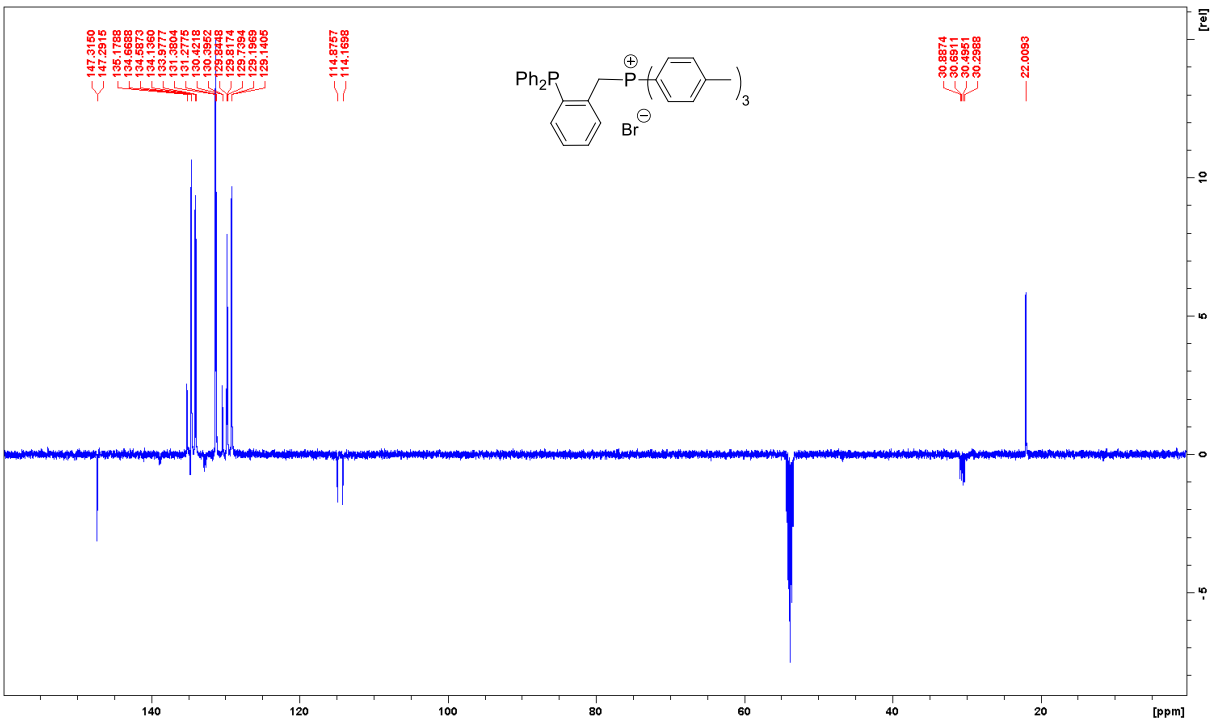

$^{13}C\{^{1}H\}$ J-mod NMR (75 MHz, Methylene Chloride-d_2)

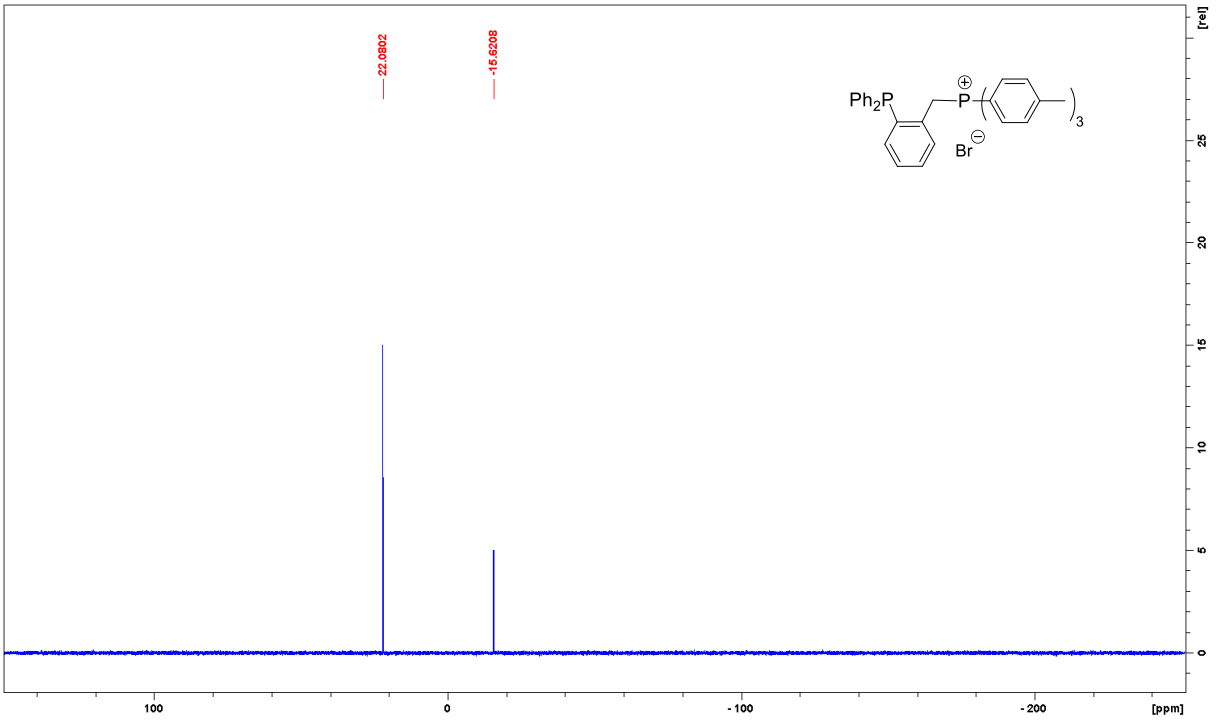

$^{31}P\{^{1}H\}$ NMR (202 MHz, Methylene Chloride-d_2)

6. ^{1}H, $^{13}C\{^{1}H\}$ and $^{31}P\{^{1}H\}$ NMR spectra of compound **5c**

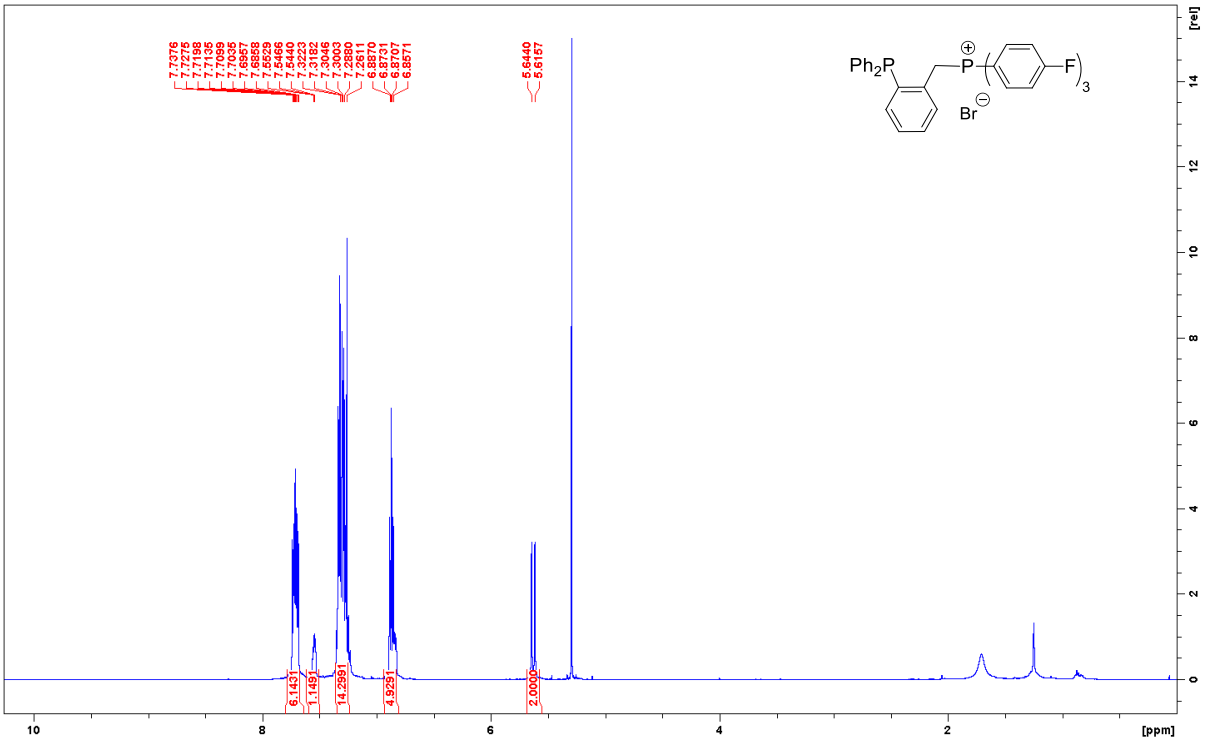

^{1}H NMR (500 MHz, Methylene Chloride-d_2)

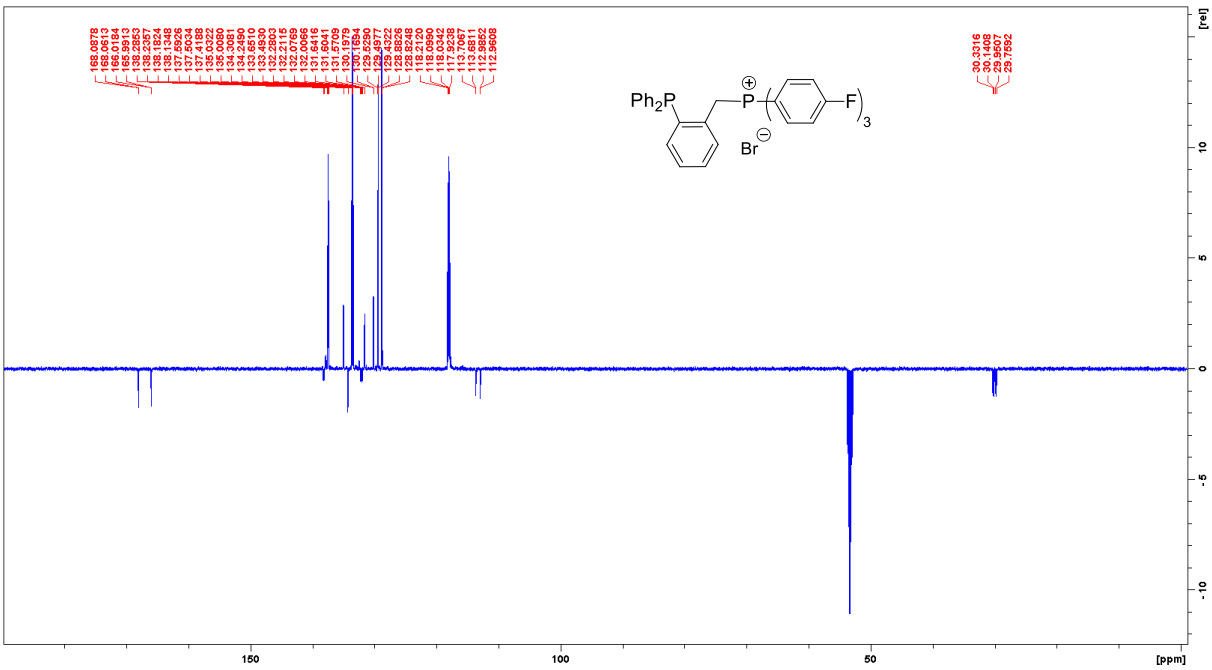

$^{13}C\{^{1}H\}$ J-mod NMR (75 MHz, Methylene Chloride-d_2)

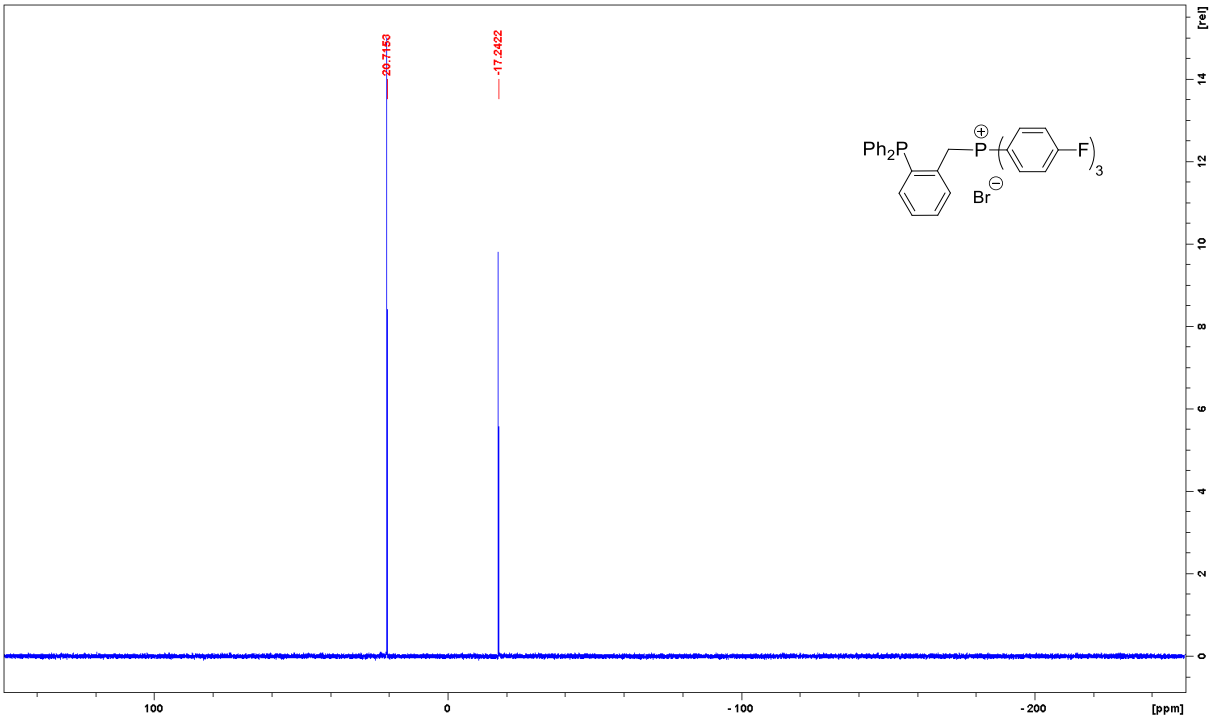

$^{31}P\{^{1}H\}$ NMR (202 MHz, Methylene Chloride-d_2)

7. ^{1}H, $^{13}C\{^{1}H\}$ and $^{31}P\{^{1}H\}$ NMR spectra of compound **5d**

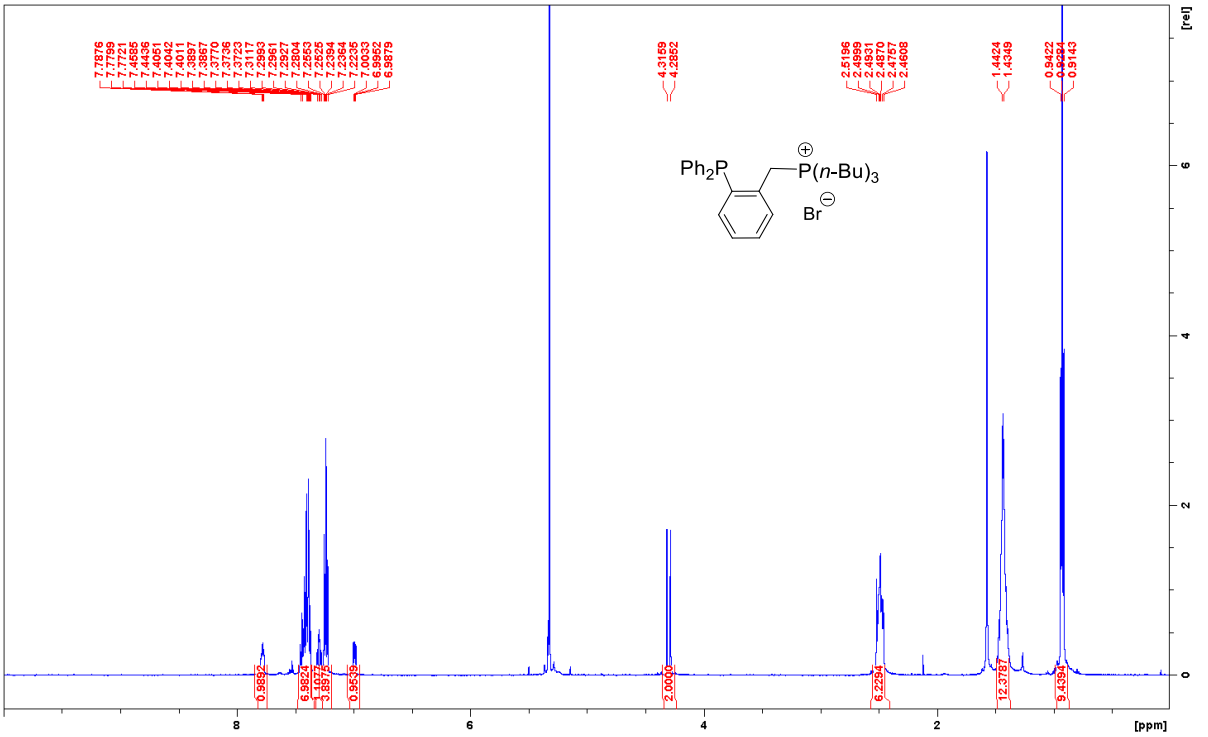

^{1}H NMR (500 MHz, Methylene Chloride-d_2)

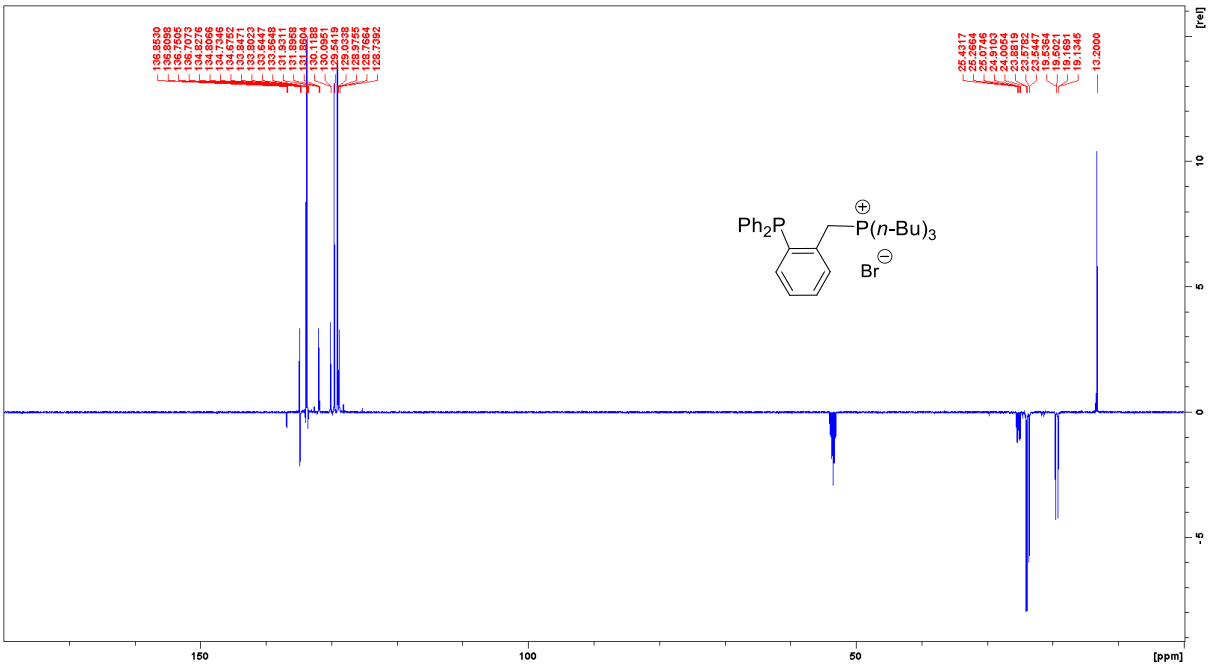

$^{13}C\{^{1}H\}$ J-mod NMR (75 MHz, Methylene Chloride-d_2)

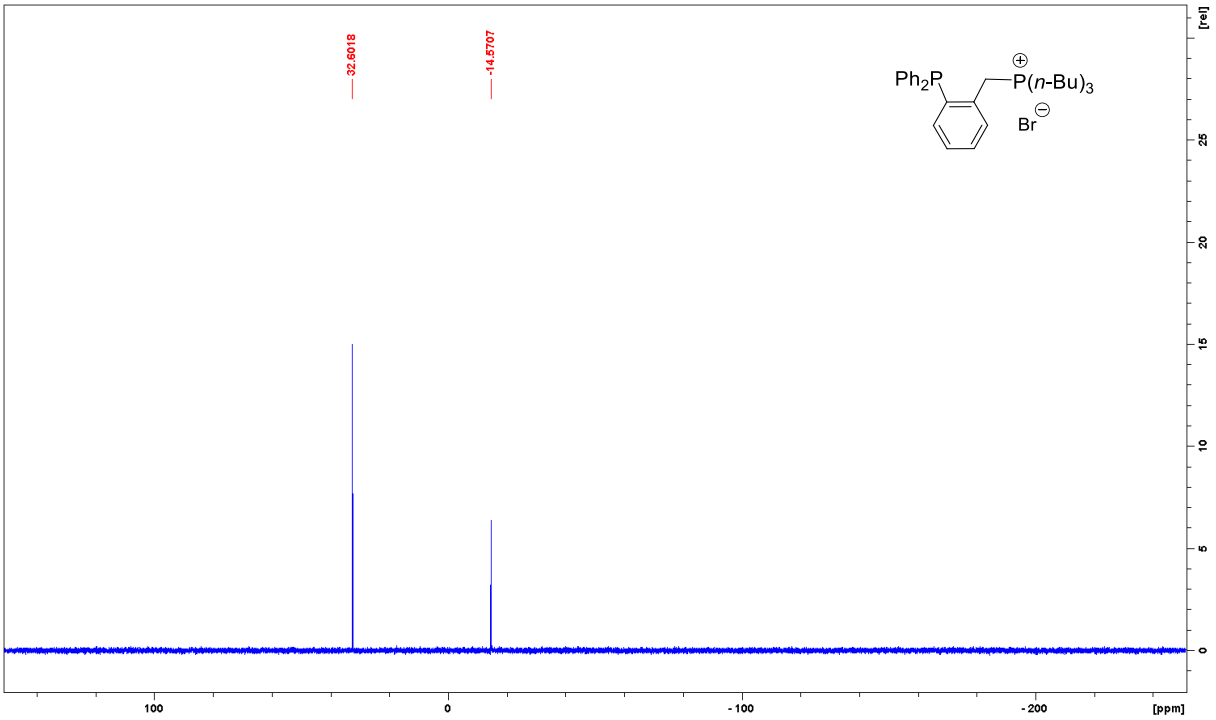

$^{31}P\{^{1}H\}$ NMR (202 MHz, Methylene Chloride-d_2)

8. ^{1}H, $^{13}C\{^{1}H\}$ and $^{31}P\{^{1}H\}$ NMR spectra of compound **5e**

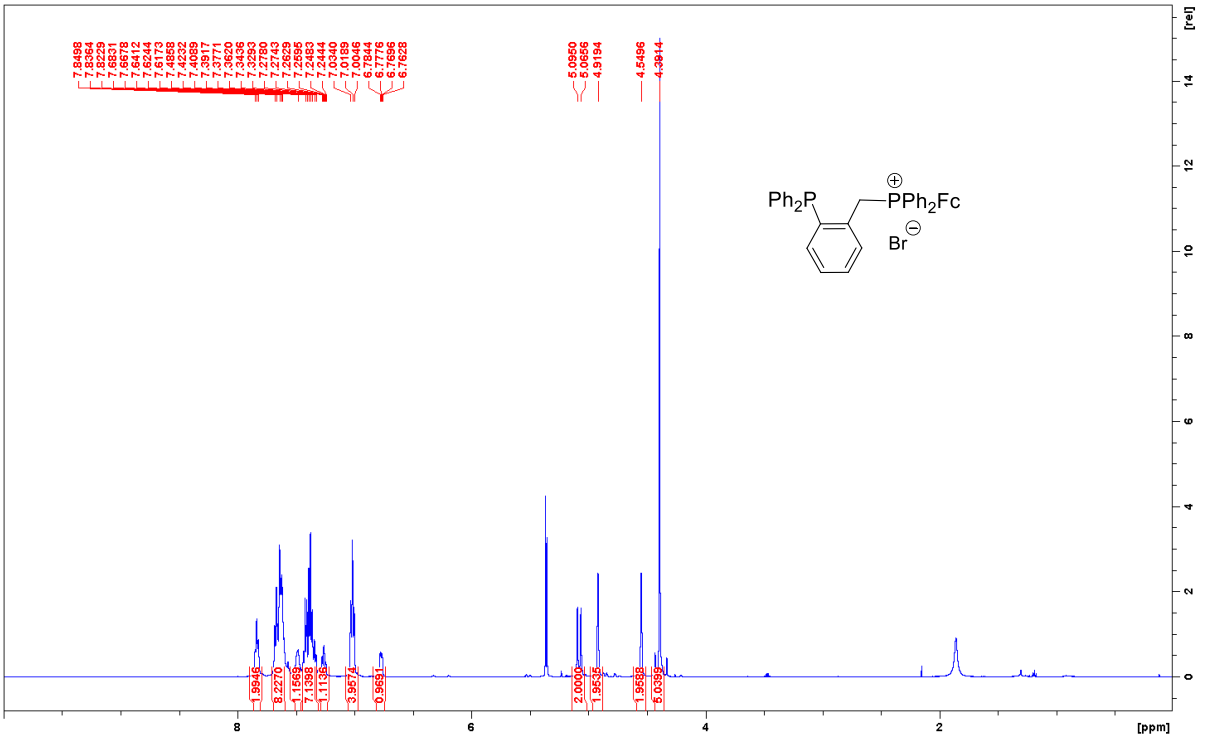

^{1}H NMR (500 MHz, Methylene Chloride-d_2)

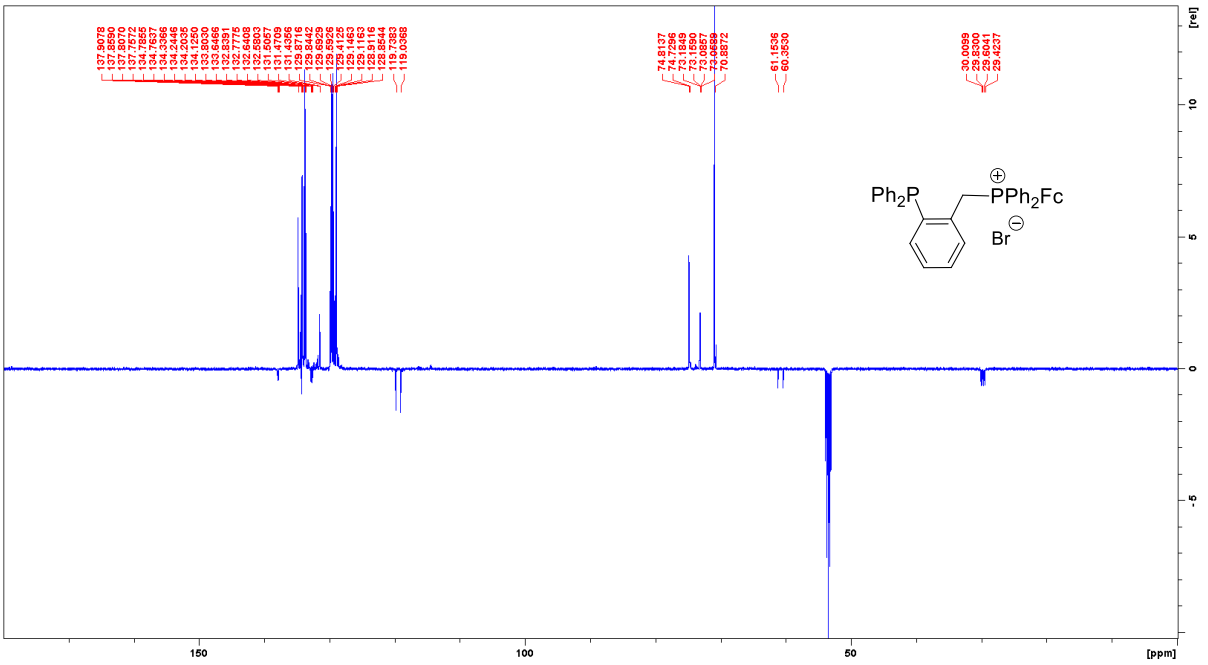

$^{13}C\{^{1}H\}$ J-mod NMR (75 MHz, Methylene Chloride-d_2)

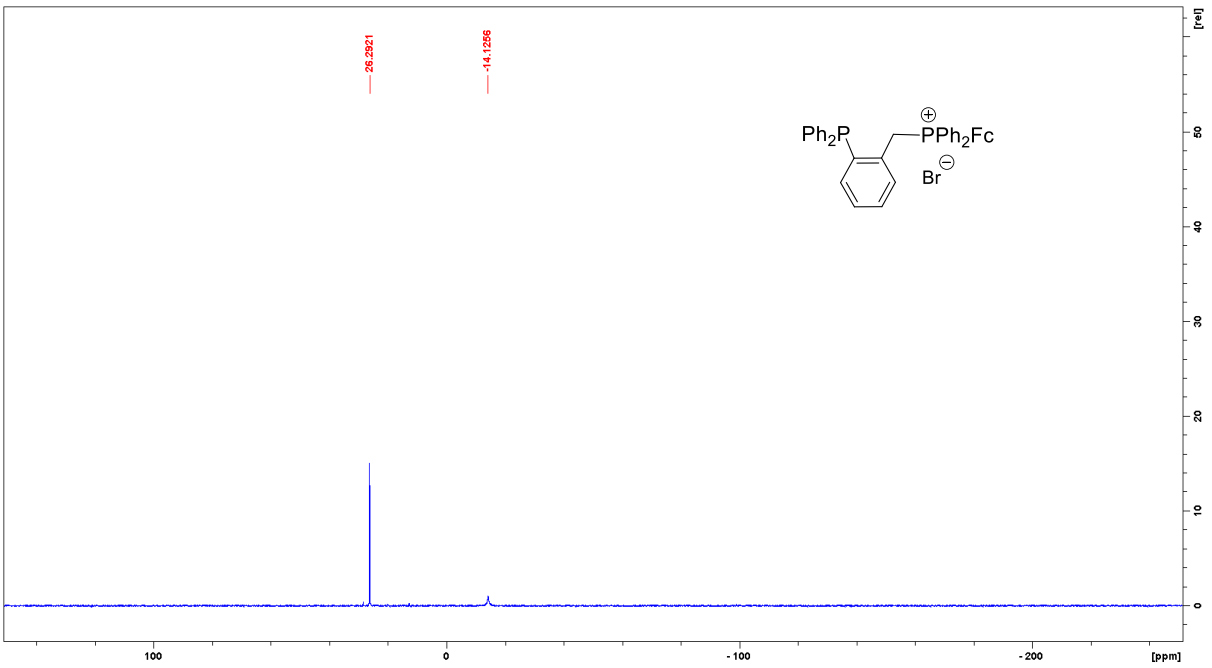

$^{31}P\{^{1}H\}$ NMR (202 MHz, Methylene Chloride-d_2)

9. ^{1}H, $^{13}C\{^{1}H\}$ and $^{31}P\{^{1}H\}$ NMR spectra of compound **5f**

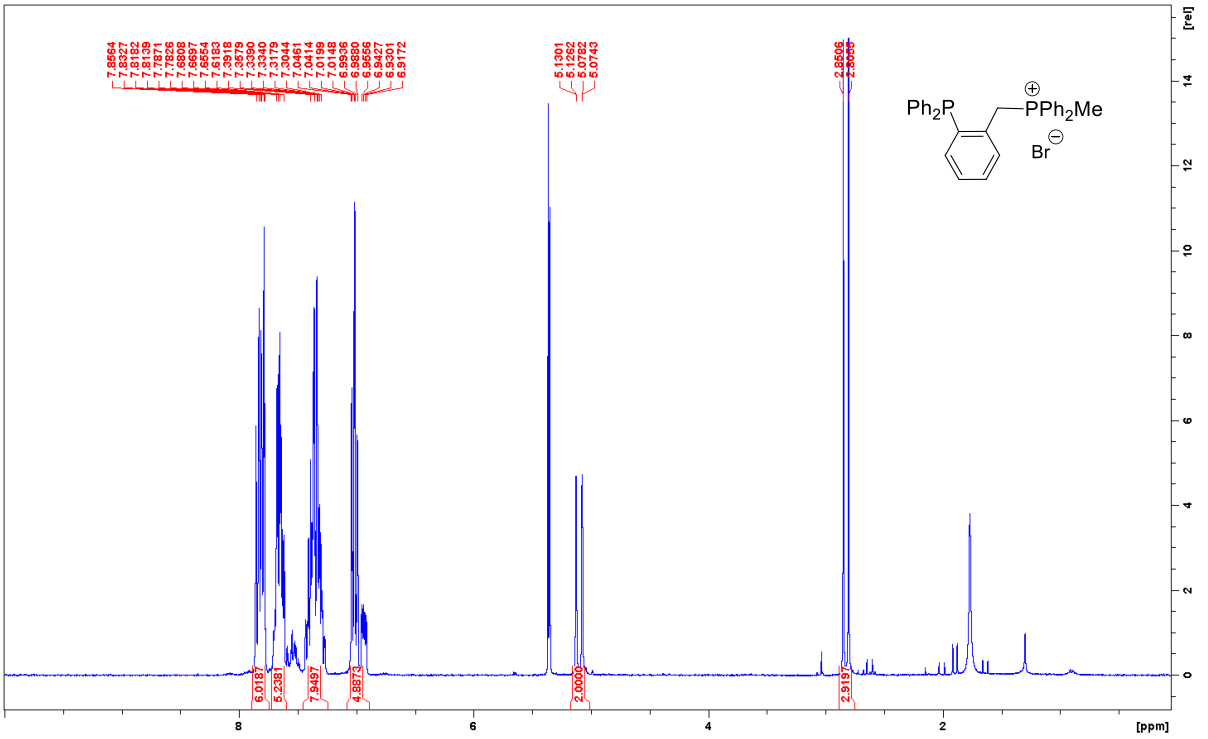

^{1}H NMR (300 MHz, Methylene Chloride-d_2)

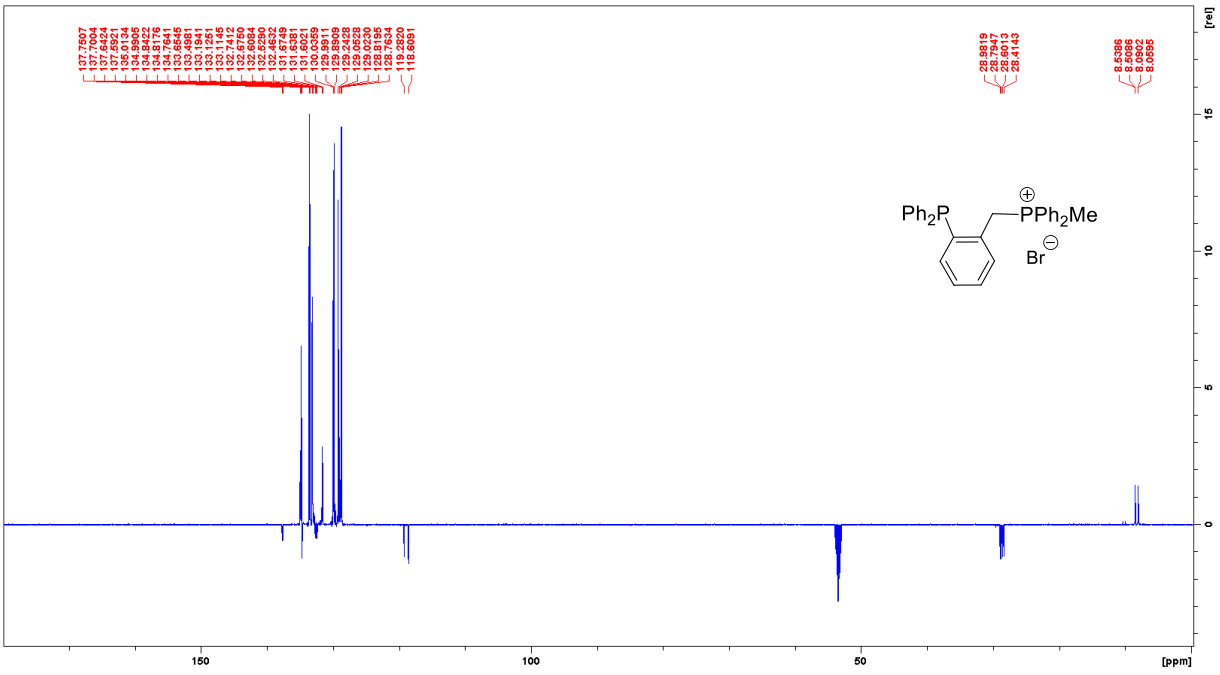

$^{13}C\{^{1}H\}$ J-mod NMR (125.7 MHz, Methylene Chloride-d_2)

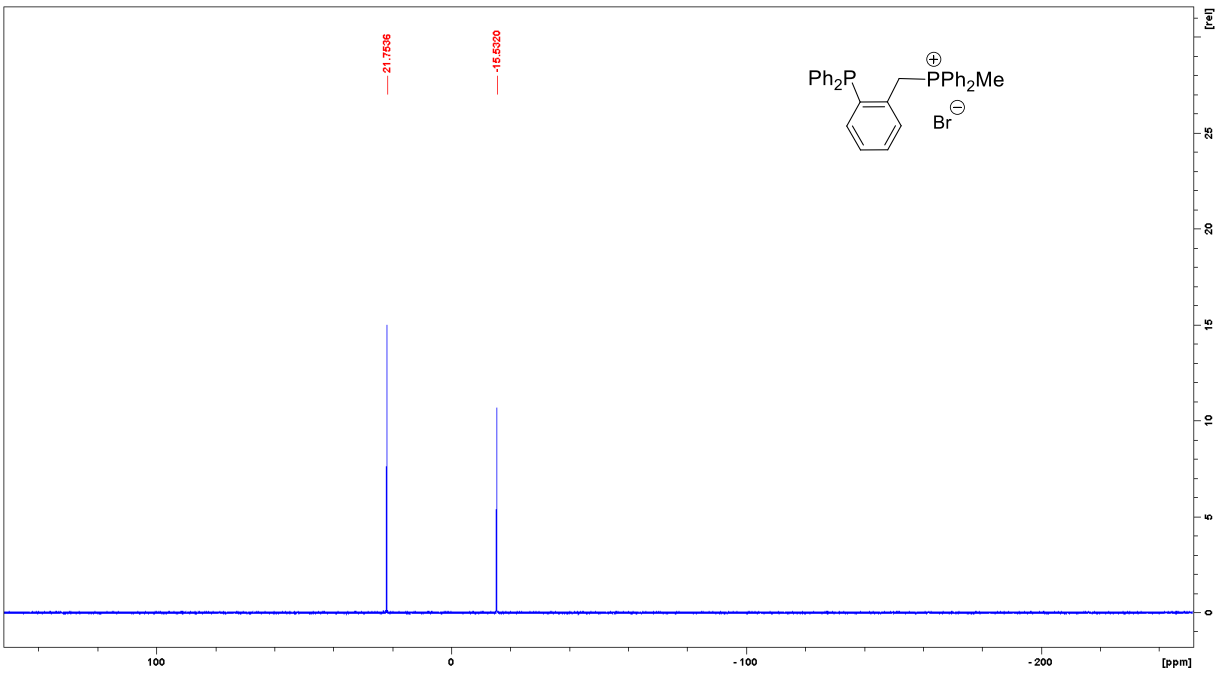

$^{31}P\{^{1}H\}$ NMR (121.5 MHz, Methylene Chloride-d_2)

10. ^{1}H, $^{13}C\{^{1}H\}$ and $^{31}P\{^{1}H\}$ NMR spectra of compound **Ia**

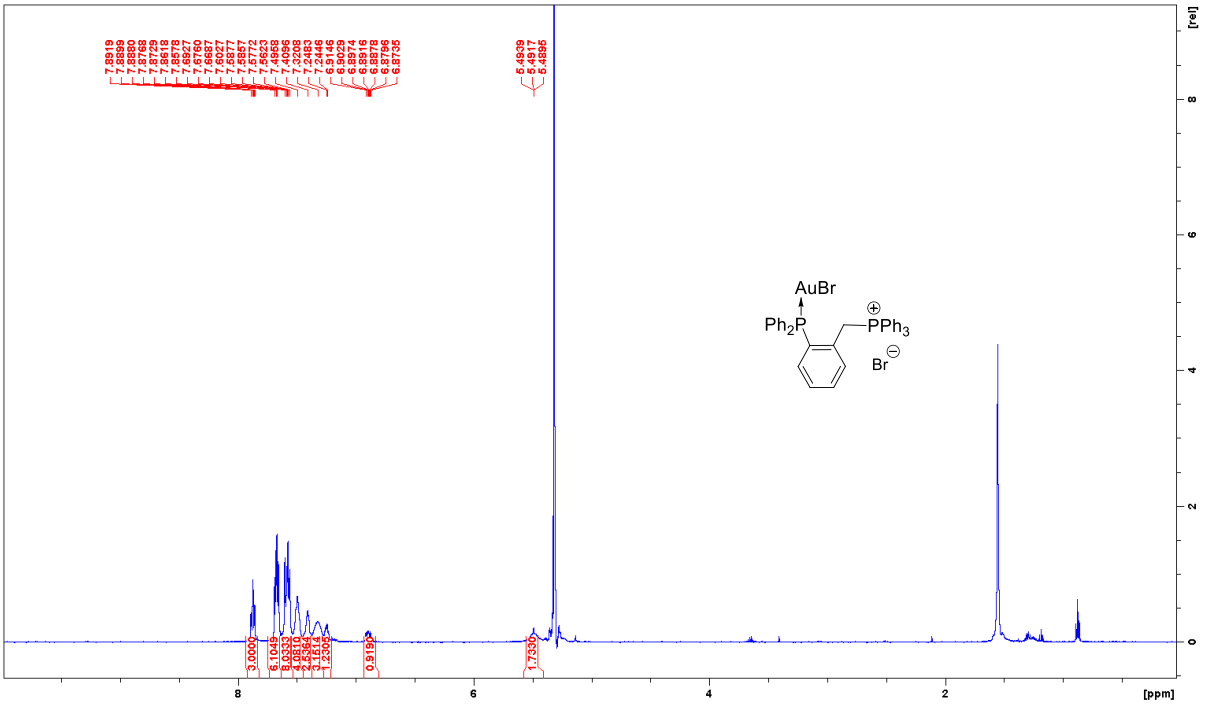

^{1}H NMR (500 MHz, Methylene Chloride-d_2)

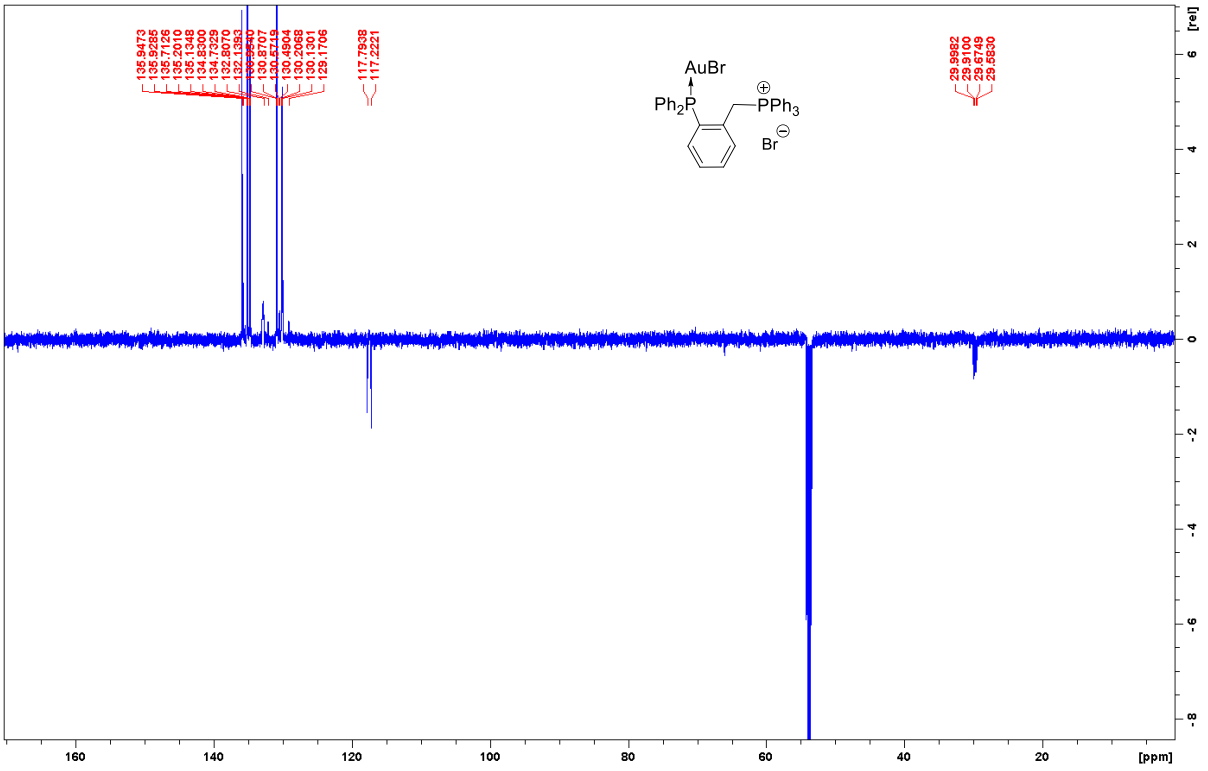

$^{13}C\{^{1}H\}$ J-mod NMR (151 MHz, Methylene Chloride-d_2)

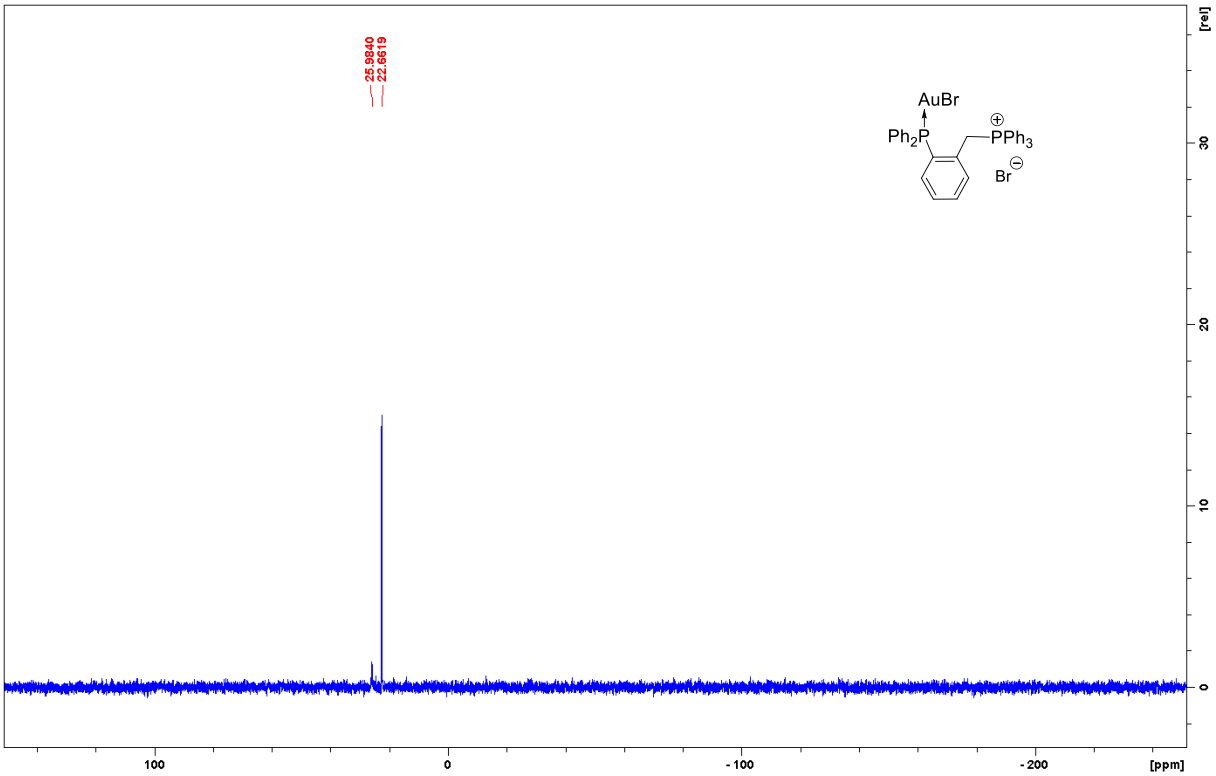

$^{31}P\{^{1}H\}$ NMR (202 MHz, Methylene Chloride-d_2)

11. ^{1}H, $^{13}C\{^{1}H\}$ and $^{31}P\{^{1}H\}$ NMR spectra of compound **Ib**

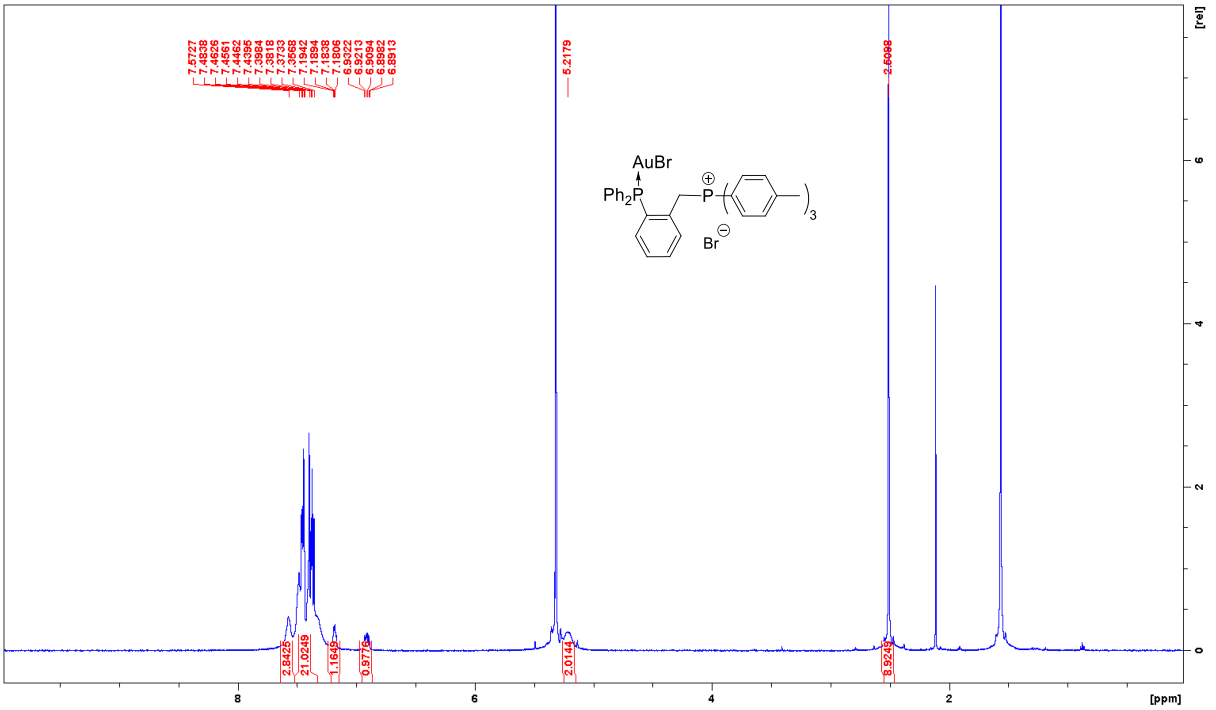

^{1}H NMR (500 MHz, Methylene Chloride-d_2)

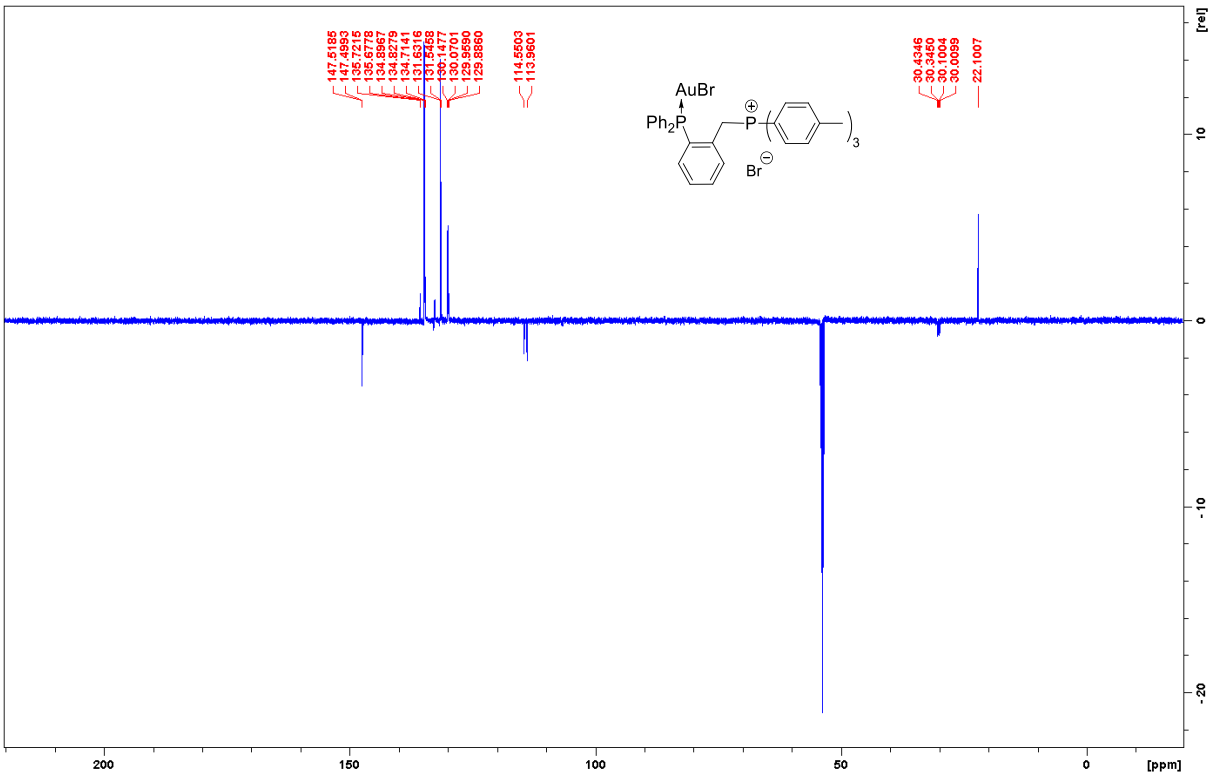

$^{13}C\{^{1}H\}$ J-mod NMR (151 MHz, Methylene Chloride-d_2)

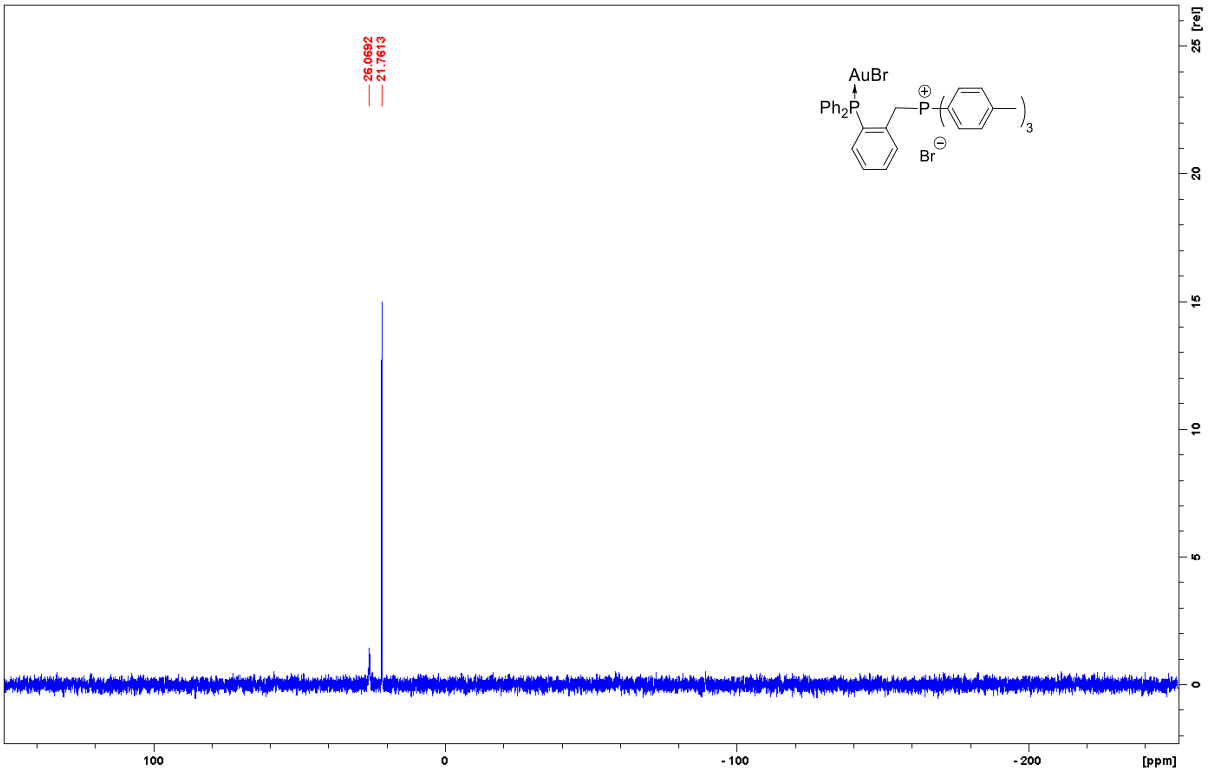

$^{31}P\{^{1}H\}$ NMR (202 MHz, Methylene Chloride-d_2)

12. ^{1}H, $^{13}C\{^{1}H\}$ and $^{31}P\{^{1}H\}$ NMR spectra of compound **Ic**

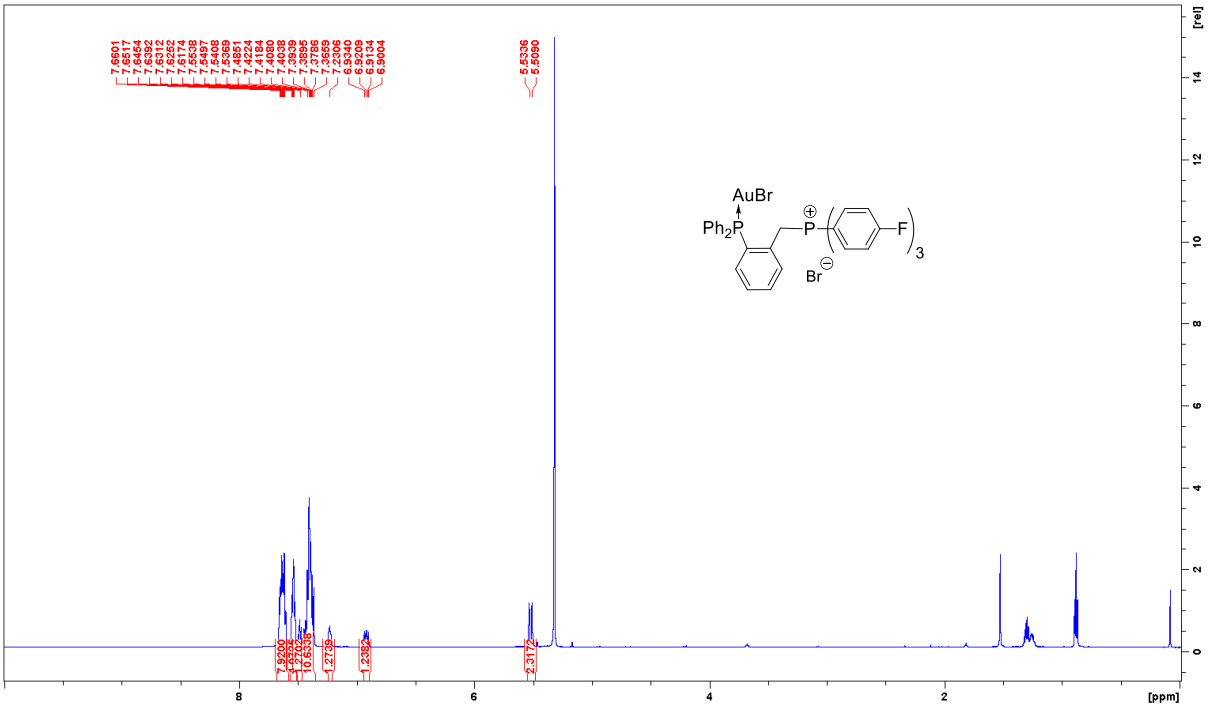

^{1}H NMR (600 MHz, Methylene Chloride-d_2)

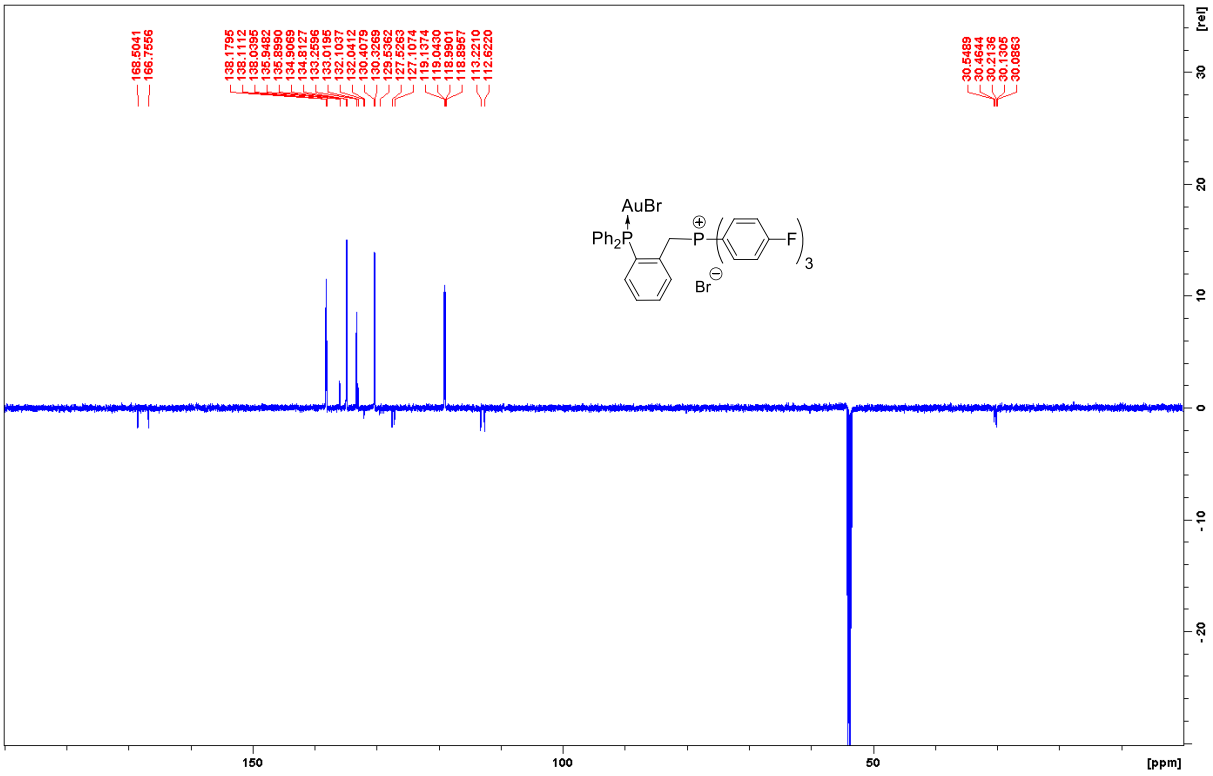

$^{13}C\{^{1}H\}$ J-mod NMR (151 MHz, Methylene Chloride-d_2)

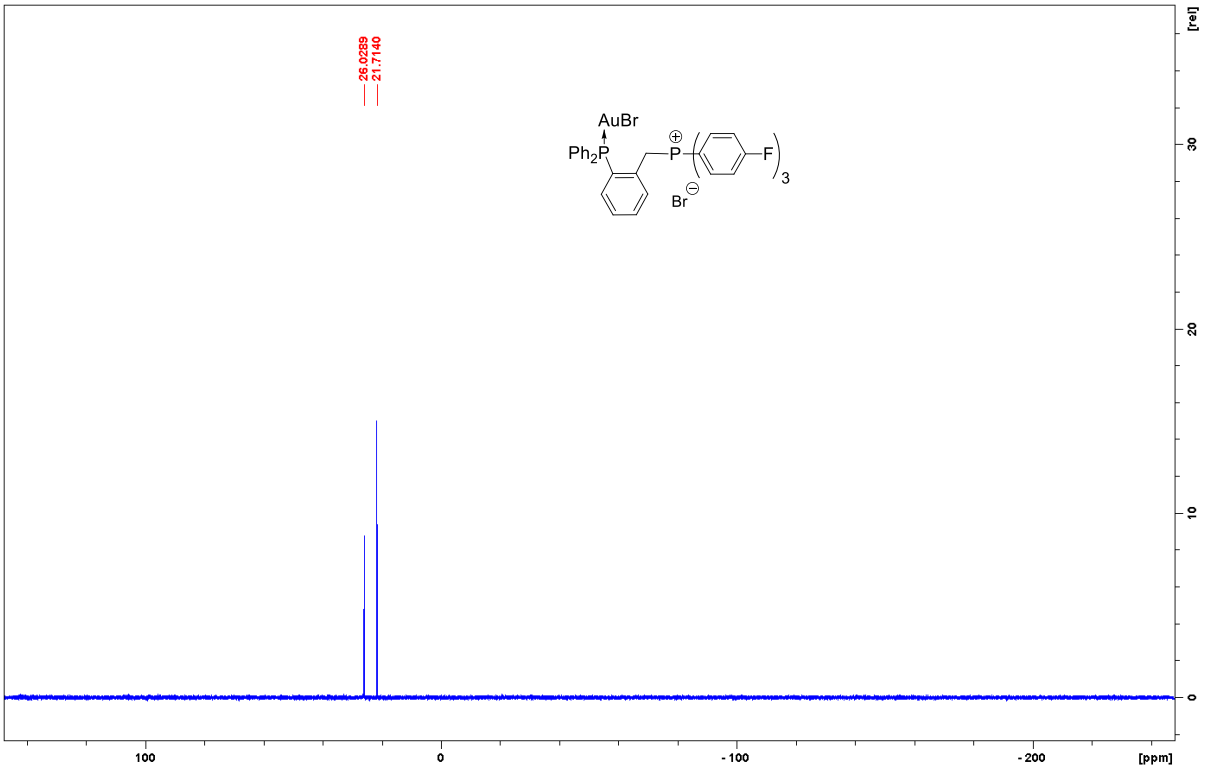

$^{31}P\{^{1}H\}$ NMR (243 MHz, Methylene Chloride-d_2)

13. ^{1}H, $^{13}C\{^{1}H\}$ and $^{31}P\{^{1}H\}$ NMR spectra of compound **Id**

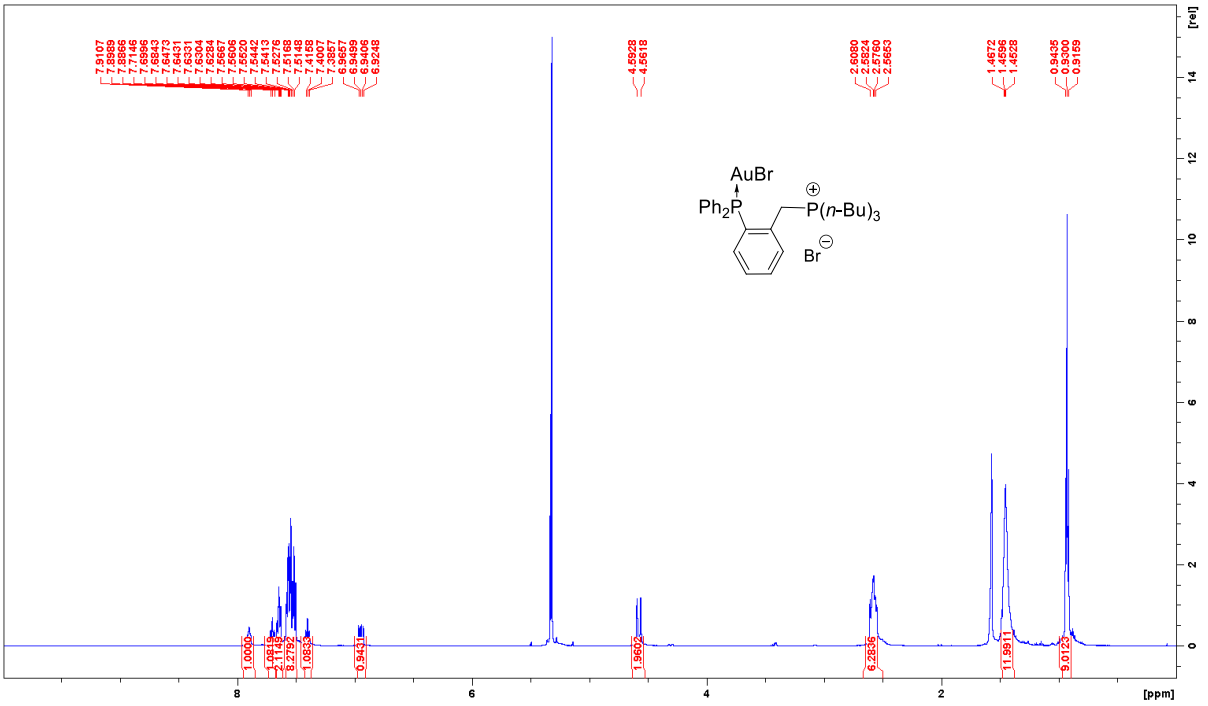

^{1}H NMR (500 MHz, Methylene Chloride-d_2)

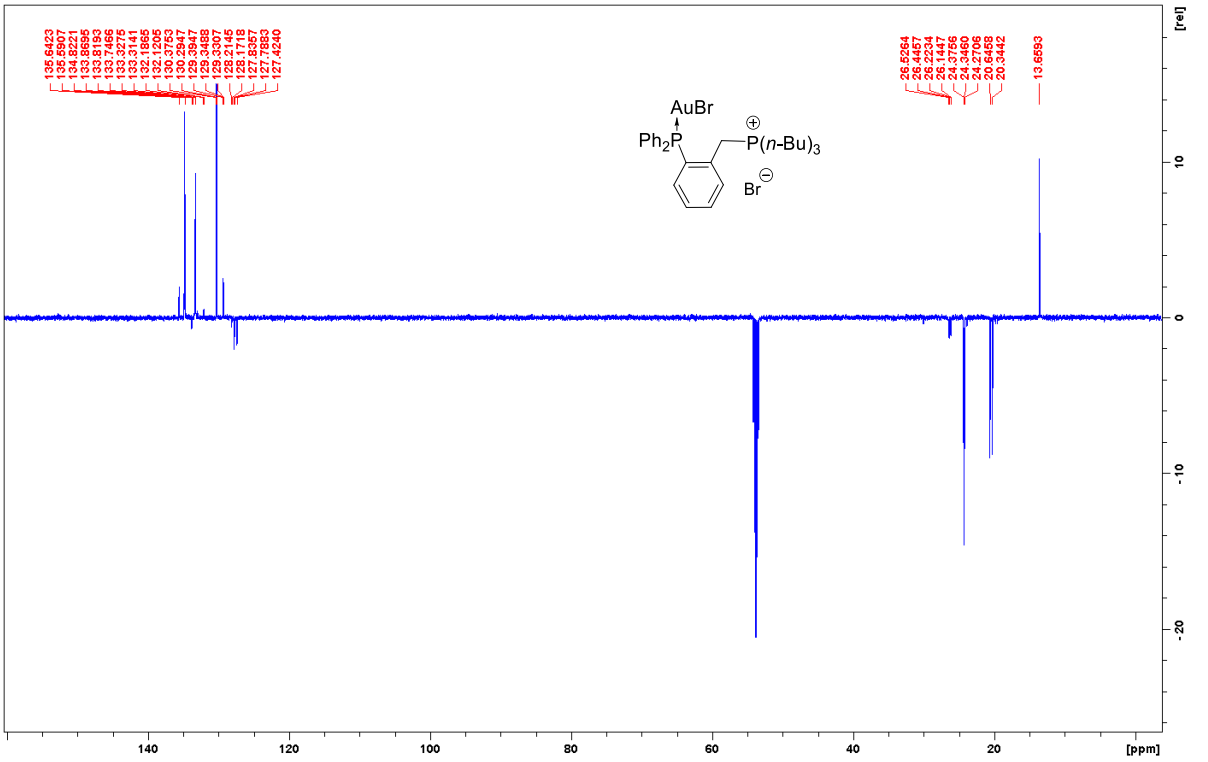

$^{13}C\{^{1}H\}$ J-mod NMR (151 MHz, Methylene Chloride-d_2)

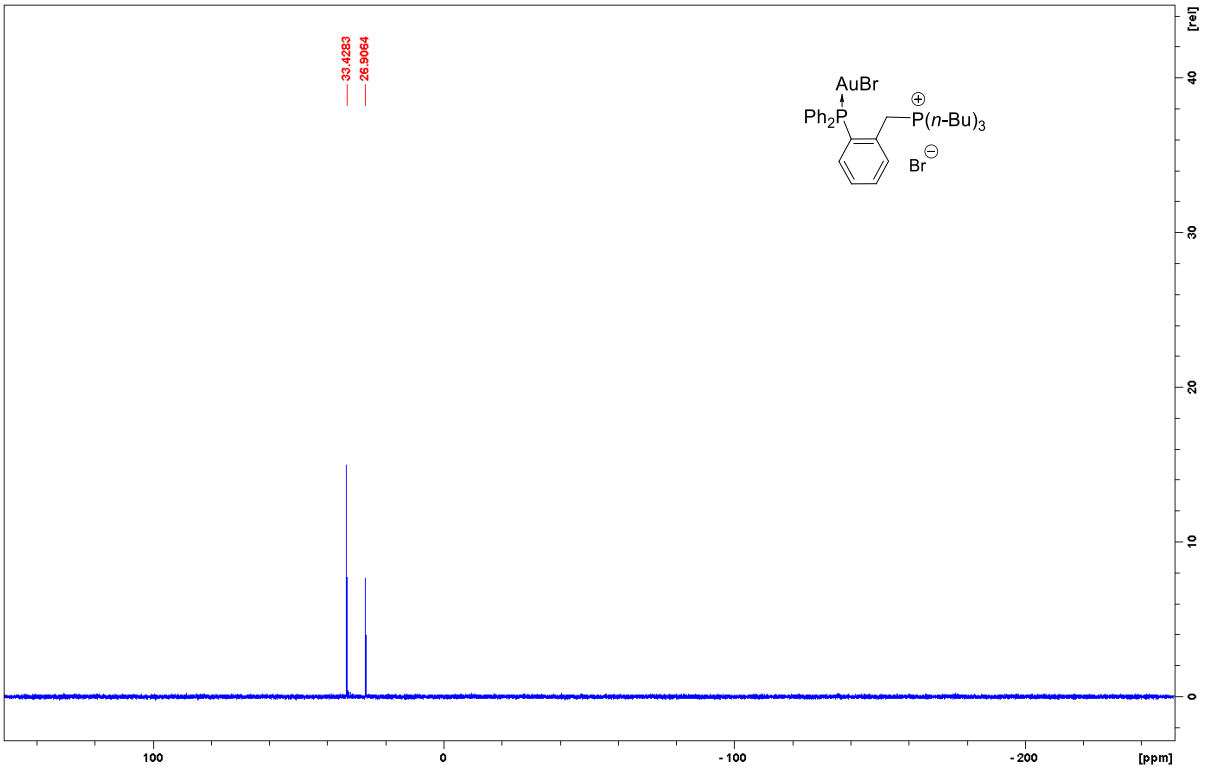

$^{31}P\{^{1}H\}$ NMR (202 MHz, Methylene Chloride-d_2)

14. ^{1}H, $^{13}C\{^{1}H\}$ and $^{31}P\{^{1}H\}$ NMR spectra of compound **Ie**

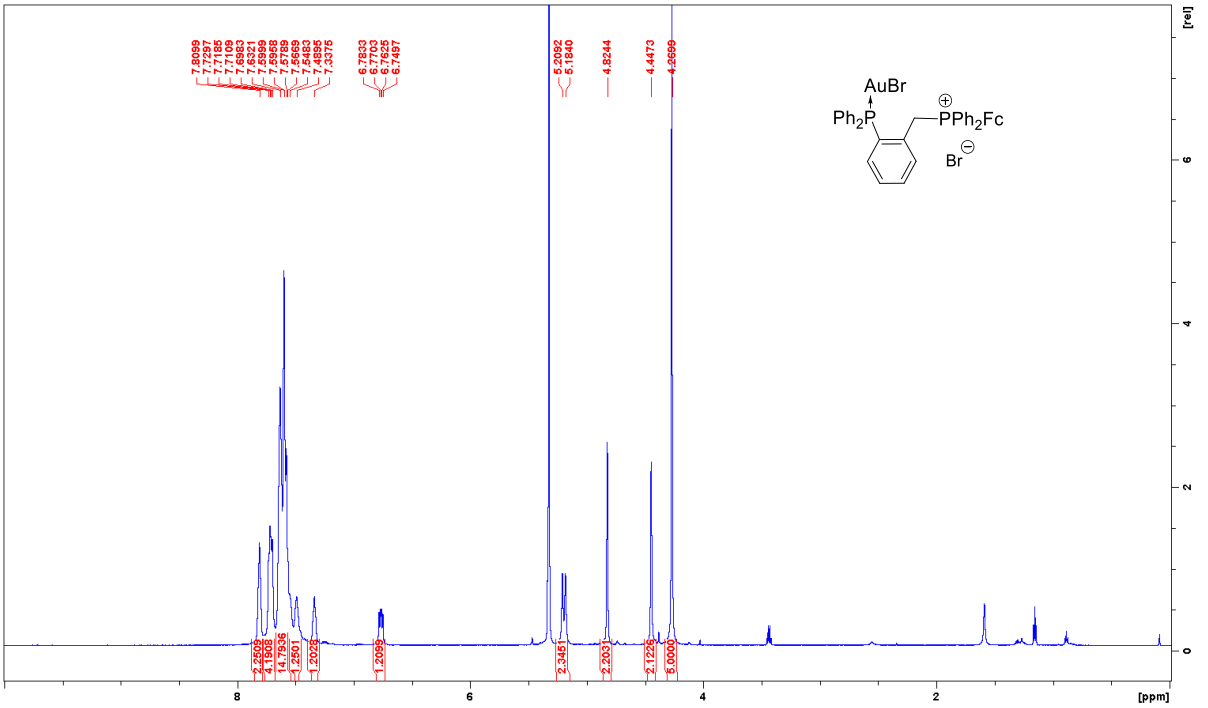

^{1}H NMR (600 MHz, Methylene Chloride-d_2)

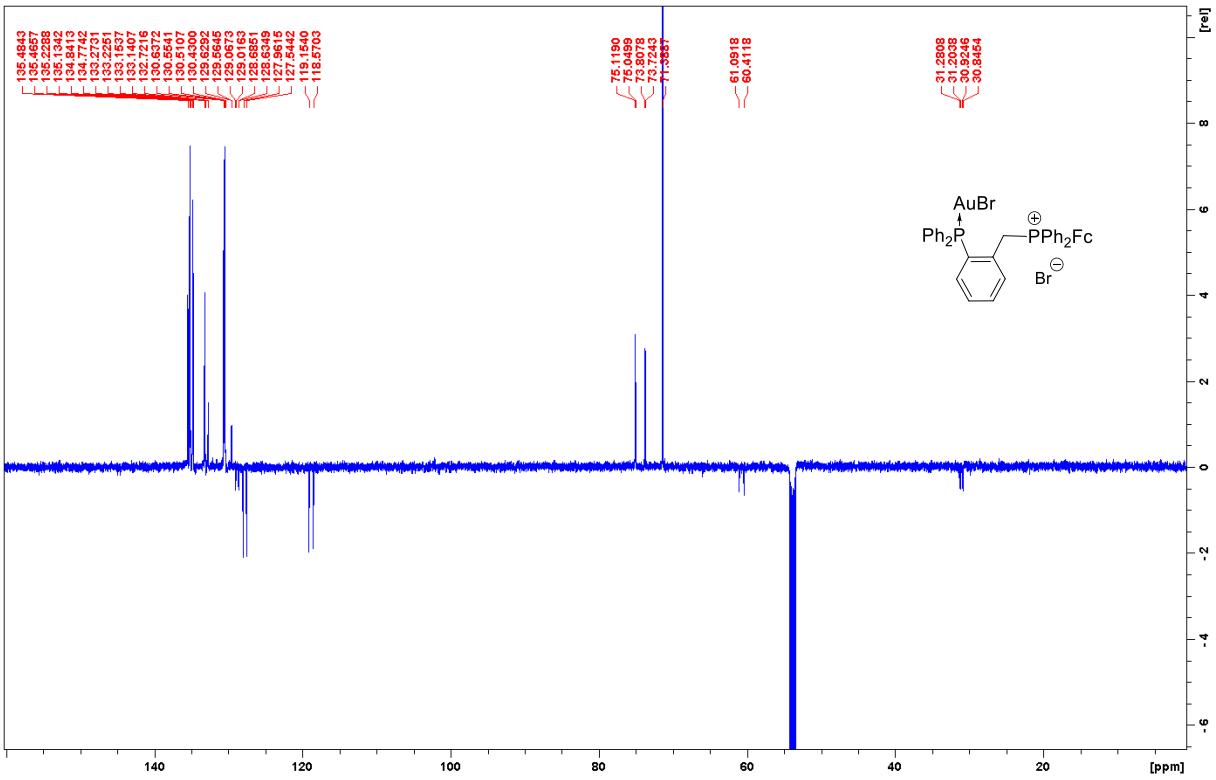

$^{13}C\{^{1}H\}$ J-mod NMR (151 MHz, Methylene Chloride-d_2)

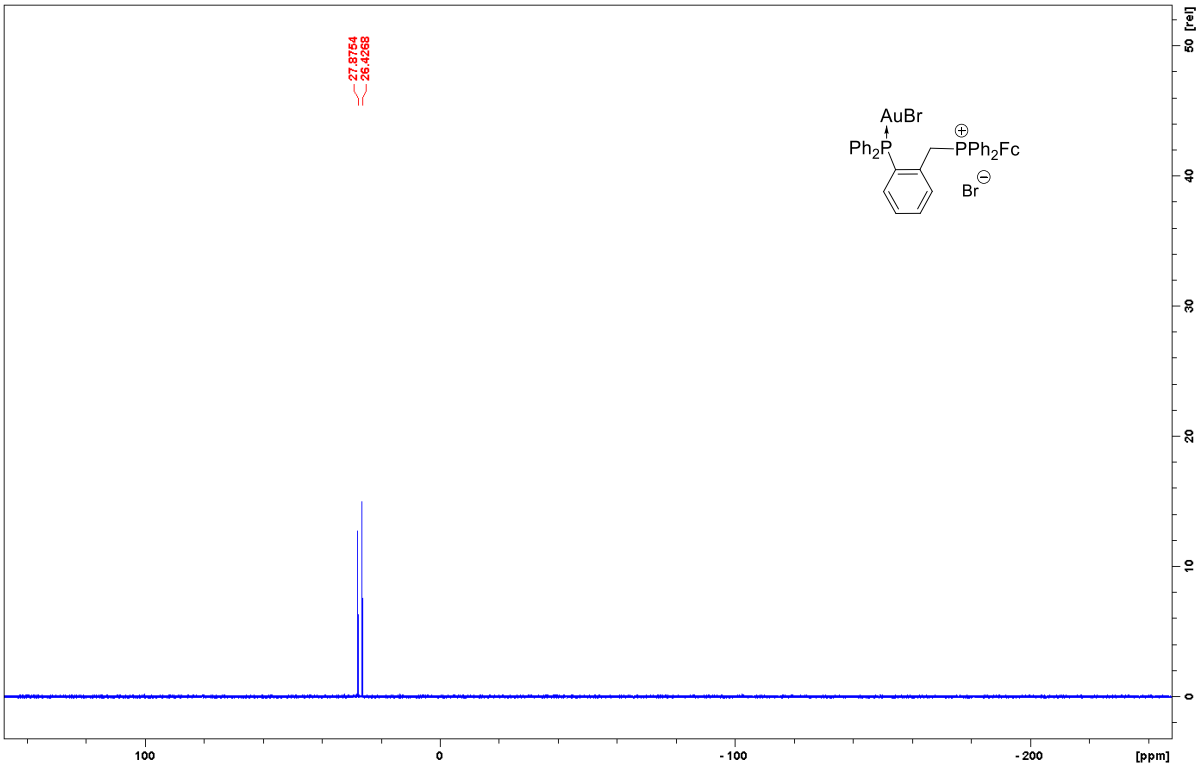

$^{31}P\{^{1}H\}$ NMR (243 MHz, Methylene Chloride-d_2)

15. ^{1}H, $^{13}C\{^{1}H\}$ and $^{31}P\{^{1}H\}$ NMR spectra of compound **If**

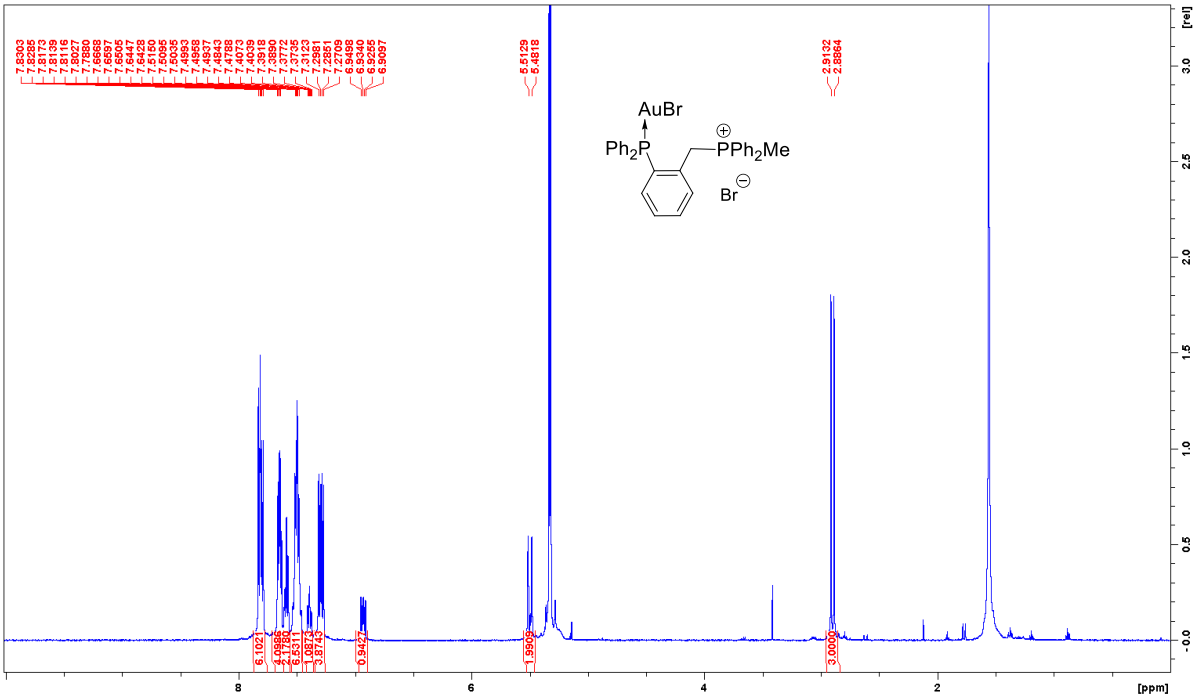

^{1}H NMR (500 MHz, Methylene Chloride-d_2)

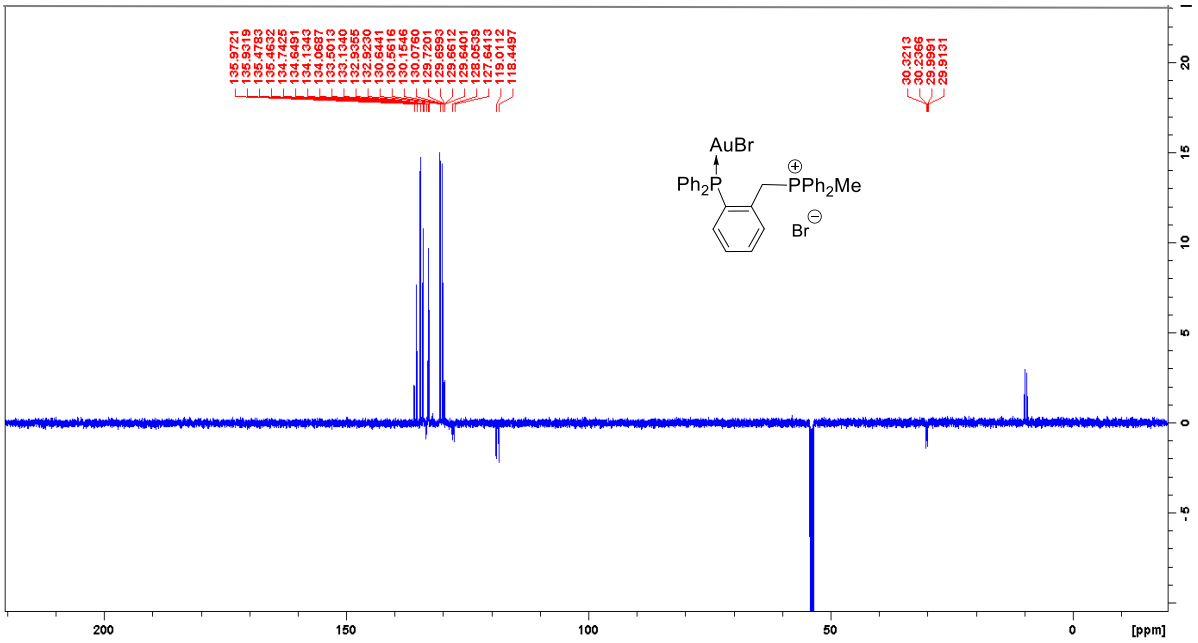

$^{13}C\{^{1}H\}$ J-mod NMR (151 MHz, Methylene Chloride-d_2)

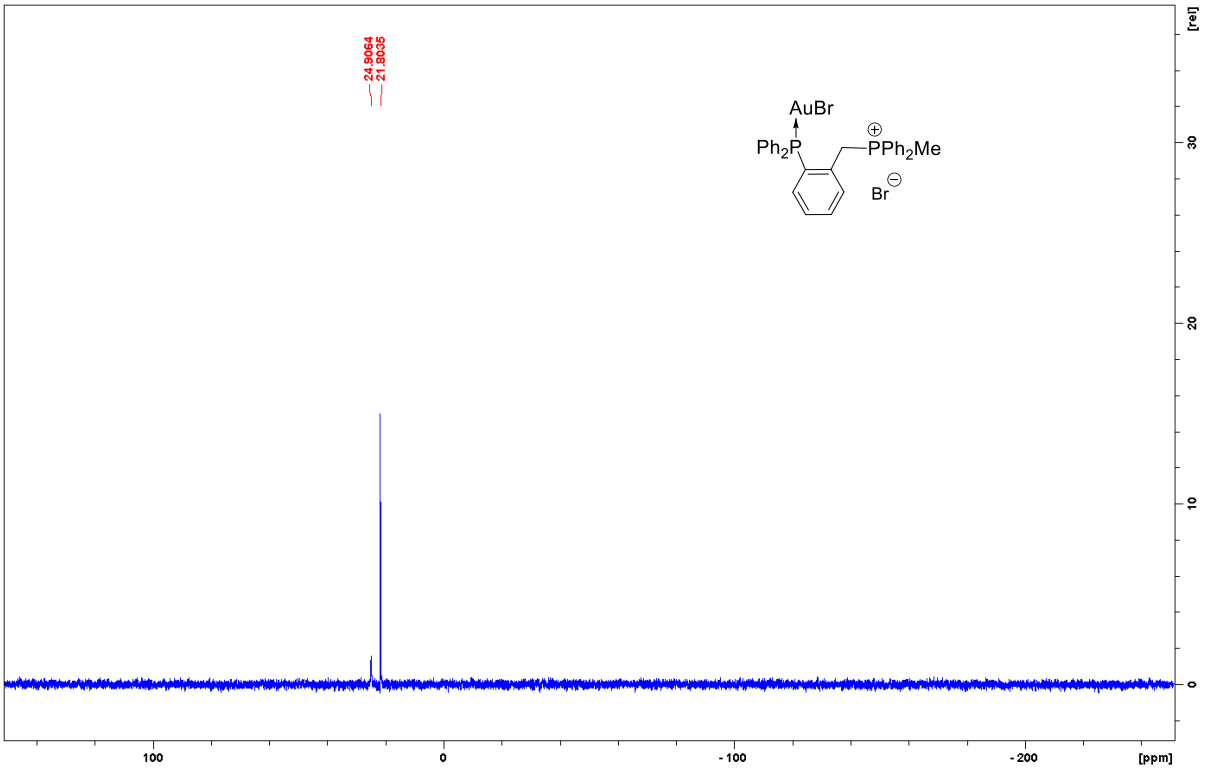

$^{31}P\{^{1}H\}$ NMR (202 MHz, Methylene Chloride-d_2)

16. ^{1}H, $^{13}C\{^{1}H\}$ and $^{31}P\{^{1}H\}$ NMR spectra of compound **4**

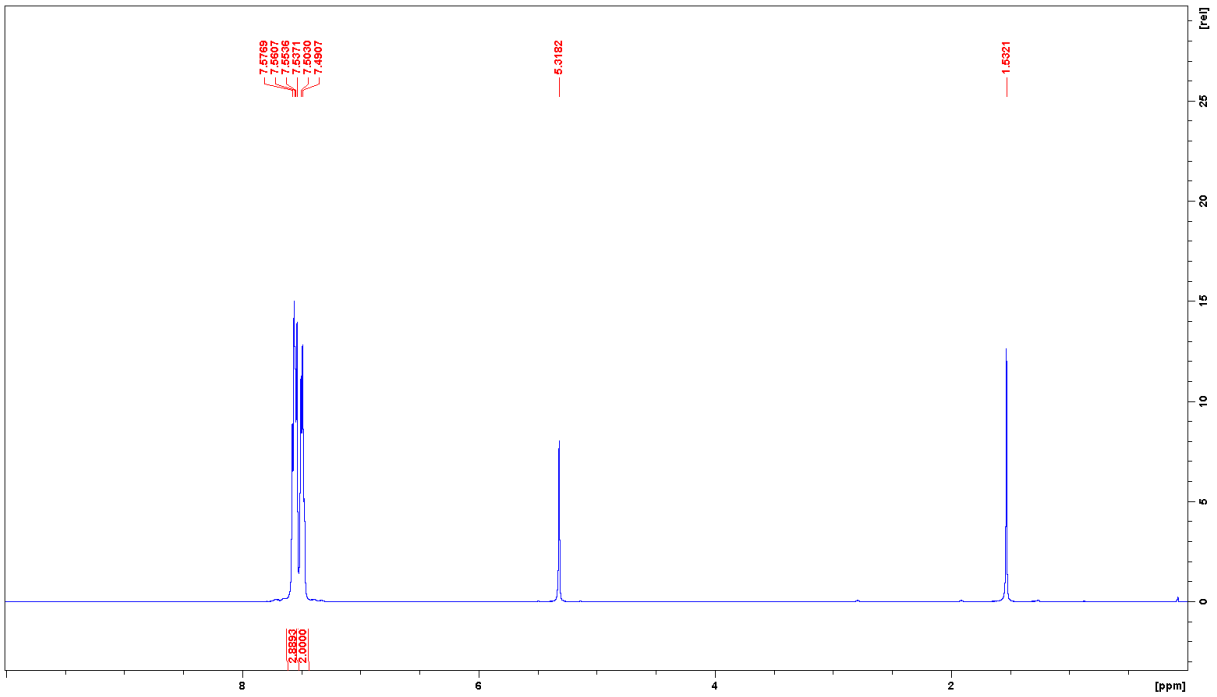

^{1}H NMR (500 MHz, Methylene Chloride-d_2) of PPh_3AuBr (**Ig**)

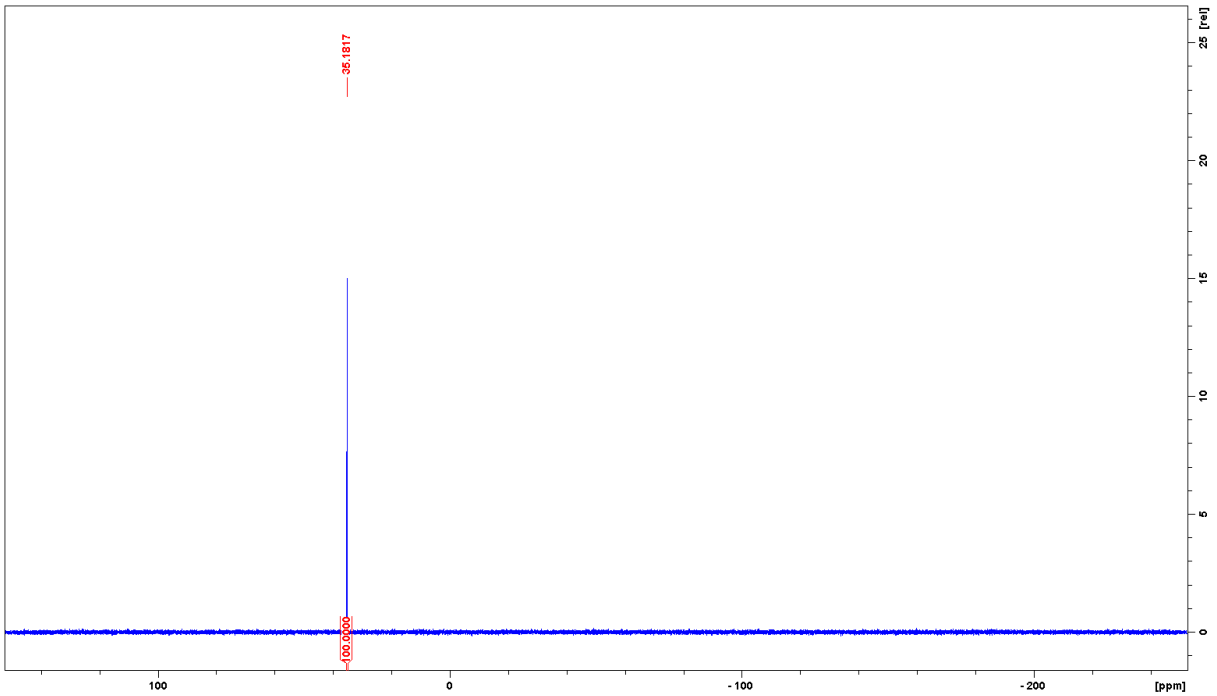

$^{31}P\{^{1}H\}$ NMR (202 MHz, Methylene Chloride-d_2) of PPh_3AuBr (**Ig**)

17. Crystal structure and table of crystal data of compound **Ie**

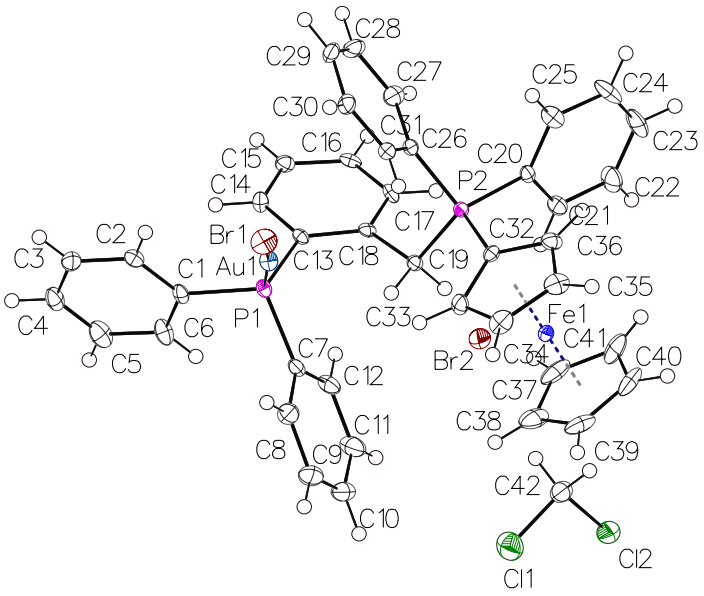

Experimental. Single clear light orange block-shaped crystals of compound **Ie** were recrystallized from diethyl ether by slow evaporation. A suitable crystal 0.74x0.42x0.27 mm^3 was selected and mounted on a MITIGEN holder oil on a Bruker D8 VENTURE diffractometer. The crystal was kept at T = 100(1) K during data collection. Using **Olex2** (Dolomanov et al., 2009), the structure was solved with the **ShelXT** (Sheldrick, 2015) structure solution program, using the Intrinsic Phasing solution method. The model was refined with version 2018/1 of **ShelXL** (Sheldrick, 2015) using Least Squares minimization.

Crystal Data. $C_{42}H_{37}AuBr_2Cl_2FeP_2$, M_r = 1087.19, orthorhombic, *P*bca (No. 61), a = 18.7538(15) Å, b = 17.9377(14) Å, c = 23.5541(17) Å, $\alpha = \beta = \gamma = 90^\circ$, V = 7923.6(11) Å^3, T = 100(1) K, Z = 8, Z' = 1, μ(MoK$_\alpha$) = 6.328, 122695 reflections measured, 9105 unique (R_{int} = 0.0561) which were used in all calculations. The final wR_2 was 0.0609 (all data) and R_1 was 0.0291 (I > 2σ(I)).

Compound	**Ie**
CCDC	2036897
Internal reference	20180104BR114
Formula	$C_{42}H_{37}AuBr_2Cl_2FeP_2$
$D_{calc.}$/ g cm^{-3}	1.823
μ/mm^{-1}	6.328
Formula Weight	1087.19
Colour	clear light orange
Shape	block
Size/mm^3	0.74x0.42x0.27
T/K	100(1)
Crystal System	orthorhombic
Space Group	*P*bca
a/Å	18.7538(15)
b/Å	17.9377(14)
c/Å	23.5541(17)
α/°	90
β/°	90
γ/°	90
V/Å^3	7923.6(11)
Z	8
Z'	1
Wavelength/Å	0.710760
Radiation type	MoK$_\alpha$
θ_{min}/°	3.000
θ_{max}/°	27.547
Measured Refl.	122695
Independent Refl.	9105
Reflections Used	7686
R_{int}	0.0561
Parameters	451
Restraints	0
Largest Peak	0.976
Deepest Hole	-1.242
GooF	1.066
wR_2 (all data)	0.0609
wR_2	0.0576
R_1 (all data)	0.0408
R_1	0.0291

Structure Quality Indicators

Reflections:	d min (Mo) 0.77	I/σ 31.4	Rint 5.61%	complete 100%
Refinement:	Shift -0.003	Max Peak 1.0	Min Peak -1.2	GooF 1.066

A clear light orange block-shaped crystal with dimensions 0.74x0.42x0.27 mm^3 was mounted on a MITIGEN holder oil. X-ray diffraction data were collected using a Bruker D8 VENTURE diffractometer equipped with an Oxford Cryosystems low-temperature device, operating at T = 100(1) K. Data were measured using ϕ and ω scans using MoK_α radiation (X-ray tube, 50 kV, 30 mA). The total number of runs and images was based on the strategy calculation from the program **APEX3** (Bruker, 2015). The maximum resolution achieved was Θ = 27.547°. Cell parameters were retrieved using the **SAINT** (Bruker, V8.38A, after 2013) software and refined using **SAINT** (Bruker, V8.38A, after 2013) on 8936 reflections, 7 % of the observed reflections. Data reduction was performed using the **SAINT** (Bruker, V8.38A, after 2013) software which corrects for Lorentz polarisation. The final completeness is 99.70 % out to 27.547° in Θ. A multi-scan absorption correction was performed using **SADABS-2016/2** (Bruker,2016) was used for absorption correction. wR_2(int) was 0.1054 before and 0.0559 after correction. The Ratio of minimum to maximum transmission is 0.5910. The absorption coefficient μ of this material is 6.328 mm^{-1} at this wavelength (λ = 0.71073Å) and the minimum and maximum transmissions are 0.0721 and 0.1220. The structure was solved in the space group *P*bca (# 61) by Intrinsic Phasing using the **ShelXT** (Sheldrick, 2015) structure solution program and refined by Least Squares using version 2018/1 of **ShelXL** (Sheldrick, 2015). All non-hydrogen atoms were refined anisotropically. Hydrogen atom positions were calculated geometrically and refined using the riding model. There is a single molecule in the asymmetric unit,

Table 1: Bond Lengths in Å for **Ie**.

Atom	Atom	Length/Å	Atom	Atom	Length/Å
Au1	Br1	2.4026(4)	P2	C32	1.765(3)
Au1	P1	2.2373(9)	P2	C19	1.807(3)
Fe1	C33	2.035(4)	P2	C26	1.789(3)
Fe1	C32	2.022(3)	P2	C20	1.798(3)
Fe1	C34	2.045(4)	Cl2	C42	1.764(4)
Fe1	C35	2.048(4)	Cl1	C42	1.771(4)
Fe1	C36	2.039(4)	C33	C32	1.442(5)
Fe1	C41	2.043(4)	C33	C34	1.421(5)
Fe1	C40	2.037(4)	C13	C18	1.405(5)
Fe1	C37	2.050(4)	C13	C14	1.400(5)
Fe1	C38	2.049(4)	C18	C17	1.394(5)
Fe1	C39	2.038(4)	C18	C19	1.518(5)
P1	C13	1.825(3)	C32	C36	1.436(5)
P1	C1	1.818(3)	C34	C35	1.411(6)
P1	C7	1.814(4)	C2	C1	1.392(5)

Atom	Atom	Length/Å	Atom	Atom	Length/Å
C2	C3	1.389(5)	C20	C25	1.390(5)
C1	C6	1.397(5)	C29	C28	1.383(6)
C17	C16	1.383(5)	C35	C36	1.416(5)
C7	C8	1.401(5)	C4	C5	1.379(6)
C7	C12	1.392(5)	C4	C3	1.376(6)
C14	C15	1.385(5)	C21	C22	1.383(5)
C30	C31	1.381(5)	C9	C10	1.383(6)
C30	C29	1.386(5)	C41	C40	1.410(6)
C8	C9	1.390(5)	C41	C37	1.421(6)
C27	C26	1.398(5)	C40	C39	1.407(6)
C27	C28	1.389(5)	C10	C11	1.383(6)
C31	C26	1.397(5)	C37	C38	1.401(6)
C16	C15	1.385(5)	C38	C39	1.425(6)
C12	C11	1.393(5)	C22	C23	1.379(6)
C6	C5	1.389(5)	C23	C24	1.384(6)
C20	C21	1.401(5)	C25	C24	1.395(6)

Table 2: Bond Angles in ° for **Ie**.

Atom	Atom	Atom	Angle/°	Atom	Atom	Atom	Angle/°
P1	Au1	Br1	172.73(2)	C32	Fe1	C35	68.86(14)
C33	Fe1	C34	40.78(15)	C32	Fe1	C36	41.42(13)
C33	Fe1	C35	68.75(16)	C32	Fe1	C41	122.41(16)
C33	Fe1	C36	69.63(15)	C32	Fe1	C40	153.81(17)
C33	Fe1	C41	157.13(16)	C32	Fe1	C37	112.76(14)
C33	Fe1	C40	161.30(16)	C32	Fe1	C38	130.68(15)
C33	Fe1	C37	122.12(16)	C32	Fe1	C39	165.77(17)
C33	Fe1	C38	108.69(17)	C34	Fe1	C35	40.32(16)
C33	Fe1	C39	125.03(17)	C34	Fe1	C37	153.41(18)
C32	Fe1	C33	41.63(13)	C34	Fe1	C38	117.46(18)
C32	Fe1	C34	68.92(14)	C35	Fe1	C37	166.27(18)

Atom	Atom	Atom	Angle/°
C35	Fe1	C38	149.30(17)
C36	Fe1	C34	68.44(16)
C36	Fe1	C35	40.55(15)
C36	Fe1	C41	109.43(18)
C36	Fe1	C37	131.59(17)
C36	Fe1	C38	169.59(16)
C41	Fe1	C34	161.64(16)
C41	Fe1	C35	126.28(17)
C41	Fe1	C37	40.64(17)
C41	Fe1	C38	67.88(19)
C40	Fe1	C34	122.98(16)
C40	Fe1	C35	104.27(16)
C40	Fe1	C36	117.05(17)
C40	Fe1	C41	40.43(16)
C40	Fe1	C37	67.99(16)
C40	Fe1	C38	67.95(18)
C40	Fe1	C39	40.40(18)
C38	Fe1	C37	39.97(18)
C39	Fe1	C34	103.71(17)
C39	Fe1	C35	113.94(16)
C39	Fe1	C36	148.71(16)
C39	Fe1	C41	68.18(19)
C39	Fe1	C37	68.10(17)
C39	Fe1	C38	40.80(16)
C13	P1	Au1	119.10(11)
C1	P1	Au1	109.81(12)
C1	P1	C13	104.03(15)
C7	P1	Au1	111.42(12)
C7	P1	C13	106.39(15)

Atom	Atom	Atom	Angle/°
C7	P1	C1	105.00(16)
C32	P2	C19	108.26(16)
C32	P2	C26	108.83(16)
C32	P2	C20	107.98(16)
C26	P2	C19	109.75(15)
C26	P2	C20	108.70(16)
C20	P2	C19	113.23(16)
C32	C33	Fe1	68.73(19)
C34	C33	Fe1	70.0(2)
C34	C33	C32	107.0(3)
C18	C13	P1	123.3(3)
C14	C13	P1	118.0(2)
C14	C13	C18	118.7(3)
C13	C18	C19	122.6(3)
C17	C18	C13	119.1(3)
C17	C18	C19	118.3(3)
P2	C32	Fe1	129.01(18)
C33	C32	Fe1	69.64(19)
C33	C32	P2	127.4(3)
C36	C32	Fe1	69.90(19)
C36	C32	P2	124.6(3)
C36	C32	C33	107.8(3)
C33	C34	Fe1	69.2(2)
C35	C34	Fe1	70.0(2)
C35	C34	C33	109.0(3)
C3	C2	C1	119.4(3)
C2	C1	P1	119.9(3)
C2	C1	C6	119.8(3)
C6	C1	P1	120.3(3)

Atom	Atom	Atom	Angle/°
C16	C17	C18	121.3(3)
C8	C7	P1	118.4(3)
C12	C7	P1	122.9(3)
C12	C7	C8	118.7(3)
C15	C14	C13	121.3(3)
C18	C19	P2	114.7(2)
C31	C30	C29	119.9(4)
C9	C8	C7	121.2(4)
C28	C27	C26	119.5(4)
C30	C31	C26	119.8(3)
C17	C16	C15	119.8(3)
C27	C26	P2	120.4(3)
C31	C26	P2	119.5(3)
C31	C26	C27	120.1(3)
C7	C12	C11	120.0(4)
C5	C6	C1	120.1(4)
C21	C20	P2	120.9(3)
C25	C20	P2	118.7(3)
C25	C20	C21	120.2(3)
C28	C29	C30	120.7(3)
C34	C35	Fe1	69.7(2)
C34	C35	C36	108.6(3)
C36	C35	Fe1	69.4(2)
C3	C4	C5	120.7(4)
C29	C28	C27	120.0(4)
C32	C36	Fe1	68.67(19)
C35	C36	Fe1	70.1(2)
C35	C36	C32	107.6(3)

Atom	Atom	Atom	Angle/°
C4	C5	C6	119.6(4)
C22	C21	C20	119.3(4)
C14	C15	C16	119.6(3)
C4	C3	C2	120.5(4)
C10	C9	C8	119.3(4)
C40	C41	Fe1	69.6(2)
C40	C41	C37	107.6(4)
C37	C41	Fe1	69.9(2)
C41	C40	Fe1	70.0(2)
C39	C40	Fe1	69.8(2)
C39	C40	C41	108.6(4)
C9	C10	C11	120.2(4)
C41	C37	Fe1	69.4(2)
C38	C37	Fe1	70.0(2)
C38	C37	C41	108.1(4)
C37	C38	Fe1	70.0(2)
C37	C38	C39	108.2(4)
C39	C38	Fe1	69.2(2)
Cl2	C42	Cl1	110.3(2)
C10	C11	C12	120.6(4)
C23	C22	C21	120.5(4)
C22	C23	C24	120.7(4)
C40	C39	Fe1	69.8(2)
C40	C39	C38	107.5(4)
C38	C39	Fe1	70.0(2)
C20	C25	C24	119.8(4)
C23	C24	C25	119.6(4)

Table 3: Torsion Angles in ° for **Ie**.

Atom	Atom	Atom	Atom	Angle/°
Au1	P1	C13	C18	71.4(3)
Au1	P1	C13	C14	-109.1(2)
Au1	P1	C1	C2	26.2(3)
Au1	P1	C1	C6	-155.9(3)
Au1	P1	C7	C8	34.0(3)
Au1	P1	C7	C12	-146.4(3)
Fe1	C33	C32	P2	124.2(3)
Fe1	C33	C32	C36	-59.7(2)
Fe1	C33	C34	C35	58.8(3)
Fe1	C32	C36	C35	-59.5(2)
Fe1	C34	C35	C36	58.6(3)
Fe1	C35	C36	C32	58.6(2)
Fe1	C41	C40	C39	59.4(3)
Fe1	C41	C37	C38	-59.5(3)
Fe1	C40	C39	C38	60.1(3)
Fe1	C37	C38	C39	-58.8(3)
Fe1	C38	C39	C40	-60.0(3)
P1	C13	C18	C17	174.7(2)
P1	C13	C18	C19	-3.5(4)
P1	C13	C14	C15	-177.2(3)
P1	C1	C6	C5	-177.8(3)
P1	C7	C8	C9	178.5(3)
P1	C7	C12	C11	-179.7(3)
P2	C32	C36	Fe1	-124.2(3)
P2	C32	C36	C35	176.3(3)
P2	C20	C21	C22	-174.8(3)
P2	C20	C25	C24	173.8(3)
C33	C32	C36	Fe1	59.6(2)
C33	C32	C36	C35	0.0(4)

Atom	Atom	Atom	Atom	Angle/°
C33	C34	C35	Fe1	-58.4(3)
C33	C34	C35	C36	0.2(4)
C13	P1	C1	C2	-102.3(3)
C13	P1	C1	C6	75.5(3)
C13	P1	C7	C8	165.3(3)
C13	P1	C7	C12	-15.1(3)
C13	C18	C17	C16	3.6(5)
C13	C18	C19	P2	-113.3(3)
C13	C14	C15	C16	1.5(5)
C18	C13	C14	C15	2.4(5)
C18	C17	C16	C15	0.3(5)
C32	P2	C19	C18	159.7(2)
C32	P2	C26	C27	163.5(3)
C32	P2	C26	C31	-18.1(3)
C32	P2	C20	C21	91.6(3)
C32	P2	C20	C25	-82.7(3)
C32	C33	C34	Fe1	-59.0(2)
C32	C33	C34	C35	-0.2(4)
C34	C33	C32	Fe1	59.8(2)
C34	C33	C32	P2	-176.0(3)
C34	C33	C32	C36	0.1(4)
C34	C35	C36	Fe1	-58.8(3)
C34	C35	C36	C32	-0.2(4)
C2	C1	C6	C5	0.1(6)
C1	P1	C13	C18	-166.0(3)
C1	P1	C13	C14	13.5(3)
C1	P1	C7	C8	-84.8(3)
C1	P1	C7	C12	94.8(3)
C1	C2	C3	C4	0.0(5)

Atom	Atom	Atom	Atom	Angle/°
C1	C6	C5	C4	-0.3(6)
C17	C18	C19	P2	68.5(3)
C17	C16	C15	C14	-2.8(5)
C7	P1	C13	C18	-55.5(3)
C7	P1	C13	C14	124.1(3)
C7	P1	C1	C2	146.1(3)
C7	P1	C1	C6	-36.1(3)
C7	C8	C9	C10	1.3(6)
C7	C12	C11	C10	1.2(6)
C14	C13	C18	C17	-4.9(5)
C14	C13	C18	C19	176.9(3)
C19	P2	C32	Fe1	56.2(3)
C19	P2	C32	C33	-37.0(3)
C19	P2	C32	C36	147.5(3)
C19	P2	C26	C27	-78.2(3)
C19	P2	C26	C31	100.2(3)
C19	P2	C20	C21	-28.3(3)
C19	P2	C20	C25	157.5(3)
C19	C18	C17	C16	-178.1(3)
C30	C31	C26	P2	-178.3(3)
C30	C31	C26	C27	0.1(5)
C30	C29	C28	C27	-1.3(6)
C8	C7	C12	C11	-0.1(5)
C8	C9	C10	C11	-0.2(7)
C31	C30	C29	C28	2.1(6)
C26	P2	C32	Fe1	175.5(2)
C26	P2	C32	C33	82.3(3)
C26	P2	C32	C36	-93.3(3)
C26	P2	C19	C18	41.0(3)

Atom	Atom	Atom	Atom	Angle/°
C26	P2	C20	C21	-150.5(3)
C26	P2	C20	C25	35.3(3)
C26	C27	C28	C29	-0.2(6)
C12	C7	C8	C9	-1.1(6)
C20	P2	C32	Fe1	-66.7(3)
C20	P2	C32	C33	-159.9(3)
C20	P2	C32	C36	24.6(3)
C20	P2	C19	C18	-80.6(3)
C20	P2	C26	C27	46.2(3)
C20	P2	C26	C31	-135.5(3)
C20	C21	C22	C23	1.5(6)
C20	C25	C24	C23	0.7(6)
C29	C30	C31	C26	-1.5(5)
C28	C27	C26	P2	179.2(3)
C28	C27	C26	C31	0.8(5)
C5	C4	C3	C2	-0.2(6)
C21	C20	C25	C24	-0.4(6)
C21	C22	C23	C24	-1.2(7)
C3	C2	C1	P1	177.9(3)
C3	C2	C1	C6	0.0(5)
C3	C4	C5	C6	0.3(6)
C9	C10	C11	C12	-1.0(7)
C41	C40	C39	Fe1	-59.5(3)
C41	C40	C39	C38	0.6(5)
C41	C37	C38	Fe1	59.2(3)
C41	C37	C38	C39	0.4(4)
C40	C41	C37	Fe1	59.6(3)
C40	C41	C37	C38	0.0(4)
C37	C41	C40	Fe1	-59.8(3)

Atom	Atom	Atom	Atom	Angle/°
C37	C41	C40	C39	-0.4(4)
C37	C38	C39	Fe1	59.4(3)
C37	C38	C39	C40	-0.6(5)
C22	C23	C24	C25	0.2(7)
C25	C20	C21	C22	-0.6(5)

18. Crystal structure and table of crystal data of compound **If**

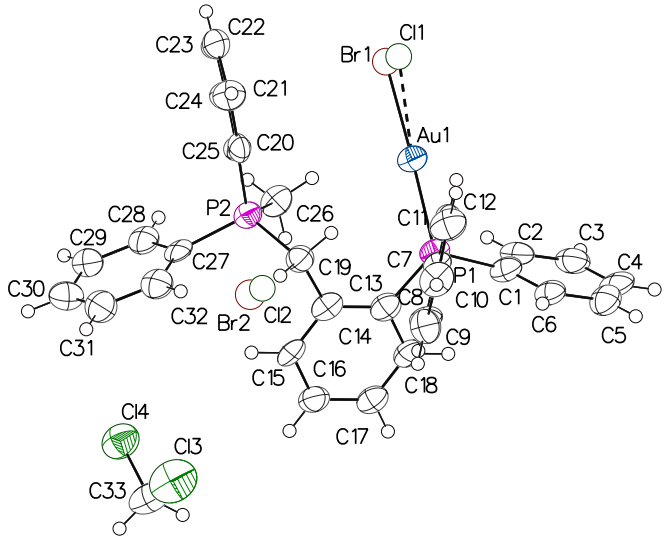

Experimental. Single clear light colourless prism-shaped crystals of compound **If** were recrystallised from DCM by slow evaporation. A suitable crystal 0.11x0.11x0.07 mm^3 was selected and mounted on a MITIGEN holder oil on a Nonius Kappa Apex II diffractometer. The crystal was kept at T = 110.0(1) K during data collection. Using **Olex2** (Dolomanov et al., 2009), the structure was solved with the **ShelXT** (Sheldrick, 2015) structure solution program, using the Intrinsic Phasing solution method. The model was refined with version 2018/3 of **ShelXL** (Sheldrick, 2015) using Least Squares minimisation.

Crystal Data. $C_{33}H_{29}AuBr_{0.83}Cl_{3.17}P_2$, M_r = 863.06, orthorhombic, Pna2$_1$ (No. 33), a = 25.312(2) Å, b = 9.6184(7) Å, c = 13.5131(9) Å, α = β = γ = 90°, V = 3289.9(4) Å^3, T = 110(1) K, Z = 4, Z' = 1, μ(MoK$_\alpha$) = 5.854, 17639 reflections measured, 5751 unique (R_{int} = 0.1236) which were used in all calculations. The final wR_2 was 0.1461 (all data) and R_1 was 0.0644 (I > 2σ(I)).

Compound	**If**
CCDC	**2036898**
Internal reference	17br88
Formula	$C_{33}H_{29}AuBr_{0.83}Cl_{3.17}P_2$
$D_{calc.}$/ g cm^{-3}	1.742
μ/mm^{-1}	5.854
Formula Weight	863.06
Colour	clear light colourless
Shape	prism
Size/mm^3	0.11x0.11x0.07
T/K	110.0(1)
Crystal System	orthorhombic
Flack Parameter	0.055(14)
Hooft Parameter	0.041(14)
Space Group	Pna2$_1$
a/Å	25.312(2)
b/Å	9.6184(7)
c/Å	13.5131(9)
α/°	90
β/°	90
γ/°	90
V/Å^3	3289.9(4)
Z	4
Z'	1
Wavelength/Å	0.710730
Radiation type	MoK$_\alpha$
θ_{min}/°	2.660
θ_{max}/°	25.000
Measured Refl.	17639
Independent Refl.	5751
Reflections Used	3381
R_{int}	0.1236
Parameters	312
Restraints	268
Largest Peak	1.416
Deepest Hole	-1.097
GooF	0.986
wR_2 (all data)	0.1461
wR_2	0.1227
R_1 (all data)	0.1258
R_1	0.0644

Structure Quality Indicators

Reflections:	d min (Mo) 2θ=50.0°	0.84	I/σ(I)	7.4	Rint	12.36%	Full 50.0°	99.7	
Refinement:	Shift	-0.001	Max Peak	1.4	Min Peak	-1.1	GooF	0.986	Flack	.055(14)

A clear light colourless prism-shaped crystal with dimensions 0.11x0.11x0.07 mm^3 was mounted on a MITIGEN holder oil. X-ray diffraction data were collected using a Nonius Kappa Apex II diffractometer equipped with an Oxford Cryosystems low-temperature device, operating at T = 110.0(1) K. Data were measured using ϕ and ω scans using MoK$_\alpha$ radiation (X-ray tube, 50 kV, 32 mA). The total number of runs and images was based on the strategy calculation from the program **APEX3** (Bruker, 2015). The maximum resolution achieved was Θ = 25°. Cell parameters were retrieved using the **SAINT** (Bruker, V8.38A, after 2013) software and refined using **SAINT** (Bruker, V8.38A, after 2013) on 917 reflections, 5 % of the observed reflections. Data reduction was performed using the **SAINT** (Bruker, V8.38A, after 2013) software which corrects for Lorentz polarisation. The final completeness is 99.70 % out to 25° in Θ. A multi-scan absorption correction was performed using **SADABS-2016/2** (Bruker,2016/2) was used for absorption correction. wR_2(int) was 0.1002 before and 0.0807 after correction. The Ratio of minimum to maximum transmission is 0.4338. The absorption coefficient μ of this material is 5.854 mm^{-1} at this wavelength (λ = 0.71073Å) and the minimum and maximum transmissions are 0.005 and 0.021. The structure was solved in the space group Pna2$_1$ (# 33) by Intrinsic Phasing using the **ShelXT** (Sheldrick, 2015) structure solution program and refined by Least Squares using version 2016/6 of **ShelXL** (Sheldrick, 2015). Counterions were found disordered as a mixture of Bromine/Chlorine with a s.o.f of 53.4%/46.6% and 29.4%/70.6% for Br1/Cl1 and Br2/Cl2 respectively. All non-hydrogen atoms were refined anisotropically, excepted disordered Br/Cl. Hydrogen atom positions were calculated geometrically and refined using the riding model. Some rigid bond restraints with esds 0.002 for 1,2-distances and 0.002 for 1,3 were employed by using RIGU (Sheldrick, 2015) restraints to maintain a reasonable model. Poor diffraction was observed beyond 2θ = 50°, these reflections were ignored totally from the refinement by using OMIT -2 50. High R_{int} value was observed because crystals weakly diffracting and exhibits many weak reflections at higher theta values.

Table 4: Bond Lengths in Å for **If**.

Atom	Atom	Length/Å	Atom	Atom	Length/Å
Au1	Br1	2.371(5)	C20	C25	1.42(4)
Au1	P1	2.250(5)	C19	C14	1.47(2)
Au1	Cl1	2.390(15)	C21	C22	1.37(3)
P1	C13	1.798(14)	C14	C15	1.3900
P1	C1	1.834(15)	C14	C13	1.3900
P1	C7	1.806(16)	C15	C16	1.3900
P2	C20	1.78(2)	C16	C17	1.3900
P2	C26	1.78(2)	C17	C18	1.3900
P2	C19	1.81(3)	C18	C13	1.3900
P2	C27	1.796(15)	C22	C23	1.28(4)
C20	C21	1.42(3)	C23	C24	1.41(3)

Atom	Atom	Length/Å	Atom	Atom	Length/Å
C27	C32	1.3900	C3	C2	1.3900
C27	C28	1.3900	Cl4	C33	1.74(3)
C32	C31	1.3900	Cl3	C33	1.69(3)
C31	C30	1.3900	C24	C25	1.37(3)
C30	C29	1.3900	C7	C12	1.3900
C29	C28	1.3900	C7	C8	1.3900
C1	C6	1.3900	C12	C11	1.3900
C1	C2	1.3900	C11	C10	1.3900
C6	C5	1.3900	C10	C9	1.3900
C5	C4	1.3900	C9	C8	1.3900
C4	C3	1.3900			

Table 5: Bond Angles in ° for **If**.

Atom	Atom	Atom	Angle/°	Atom	Atom	Atom	Angle/°
P1	Au1	Br1	178.3(3)	C25	C20	C21	119(2)
P1	Au1	Cl1	171.8(5)	C14	C19	P2	116.0(16)
C13	P1	Au1	117.0(6)	C22	C21	C20	119(2)
C13	P1	C1	106.0(9)	C15	C14	C19	116.8(15)
C13	P1	C7	103.7(9)	C15	C14	C13	120.0
C1	P1	Au1	109.1(7)	C13	C14	C19	123.2(15)
C7	P1	Au1	111.8(7)	C14	C15	C16	120.0
C7	P1	C1	108.9(9)	C17	C16	C15	120.0
C20	P2	C26	109.9(12)	C16	C17	C18	120.0
C20	P2	C19	108.9(13)	C13	C18	C17	120.0
C20	P2	C27	107.8(10)	C14	C13	P1	121.1(10)
C26	P2	C19	108.3(12)	C18	C13	P1	118.6(10)
C26	P2	C27	110.3(11)	C18	C13	C14	120.0
C27	P2	C19	111.6(11)	C23	C22	C21	123(2)
C21	C20	P2	121.7(19)	C22	C23	C24	119(3)
C25	C20	P2	119.4(19)	C32	C27	P2	120.9(10)

Atom	Atom	Atom	Angle/°
C32	C27	C28	120.0
C28	C27	P2	118.8(10)
C31	C32	C27	120.0
C32	C31	C30	120.0
C31	C30	C29	120.0
C28	C29	C30	120.0
C29	C28	C27	120.0
C6	C1	P1	121.0(10)
C6	C1	C2	120.0
C2	C1	P1	118.7(10)
C5	C6	C1	120.0
C6	C5	C4	120.0
C3	C4	C5	120.0

Atom	Atom	Atom	Angle/°
C4	C3	C2	120.0
C3	C2	C1	120.0
C25	C24	C23	123(2)
C12	C7	P1	118.7(9)
C12	C7	C8	120.0
C8	C7	P1	121.2(9)
C11	C12	C7	120.0
C12	C11	C10	120.0
C11	C10	C9	120.0
C10	C9	C8	120.0
C9	C8	C7	120.0
C24	C25	C20	117(2)
Cl3	C33	Cl4	117.2(18)

Table 6: Torsion Angles in ° for **If**.

Atom	Atom	Atom	Atom	Angle/°
Au1	P1	C13	C14	-57.9(11)
Au1	P1	C13	C18	128.3(7)
Au1	P1	C1	C6	127.0(9)
Au1	P1	C1	C2	-46.7(11)
Au1	P1	C7	C12	-24.5(12)
Au1	P1	C7	C8	152.5(8)
P1	C1	C6	C5	-173.6(13)
P1	C1	C2	C3	173.8(13)
P1	C7	C12	C11	177.1(13)
P1	C7	C8	C9	-177.0(14)
P2	C20	C21	C22	176(2)
P2	C20	C25	C24	-179(2)
P2	C19	C14	C15	-68.2(19)
P2	C19	C14	C13	111.4(16)

Atom	Atom	Atom	Atom	Angle/°
P2	C27	C32	C31	173.7(12)
P2	C27	C28	C29	-173.8(12)
C20	P2	C19	C14	-162.1(17)
C20	P2	C27	C32	-82.7(12)
C20	P2	C27	C28	91.0(12)
C20	C21	C22	C23	3(5)
C26	P2	C20	C21	27(3)
C26	P2	C20	C25	-154(2)
C26	P2	C19	C14	-43(2)
C26	P2	C27	C32	157.2(11)
C26	P2	C27	C28	-29.0(13)
C19	P2	C20	C21	146(2)
C19	P2	C20	C25	-35(3)
C19	P2	C27	C32	36.8(13)
C19	P2	C27	C28	-149.5(11)
C19	C14	C15	C16	179.6(15)
C19	C14	C13	P1	6.8(15)
C19	C14	C13	C18	-179.6(16)
C21	C20	C25	C24	1(4)
C21	C22	C23	C24	0(5)
C14	C15	C16	C17	0.0
C15	C14	C13	P1	-173.7(12)
C15	C14	C13	C18	0.0
C15	C16	C17	C18	0.0
C16	C17	C18	C13	0.0
C17	C18	C13	P1	173.8(11)
C17	C18	C13	C14	0.0
C13	P1	C1	C6	-106.2(11)
C13	P1	C1	C2	80.1(11)
C13	P1	C7	C12	-151.4(10)

Atom	Atom	Atom	Atom	Angle/°
C13	P1	C7	C8	25.6(12)
C13	C14	C15	C16	0.0
C22	C23	C24	C25	-3(5)
C23	C24	C25	C20	2(4)
C27	P2	C20	C21	-93(2)
C27	P2	C20	C25	86(2)
C27	P2	C19	C14	79.0(19)
C27	C32	C31	C30	0.0
C32	C27	C28	C29	0.0
C32	C31	C30	C29	0.0
C31	C30	C29	C28	0.0
C30	C29	C28	C27	0.0
C28	C27	C32	C31	0.0
C1	P1	C13	C14	-179.7(9)
C1	P1	C13	C18	6.5(11)
C1	P1	C7	C12	96.0(11)
C1	P1	C7	C8	-86.9(12)
C1	C6	C5	C4	0.0
C6	C1	C2	C3	0.0
C6	C5	C4	C3	0.0
C5	C4	C3	C2	0.0
C4	C3	C2	C1	0.0
C2	C1	C6	C5	0.0
C7	P1	C13	C14	65.6(10)
C7	P1	C13	C18	-108.1(10)
C7	P1	C1	C6	4.8(12)
C7	P1	C1	C2	-168.9(9)
C7	C12	C11	C10	0.0
C12	C7	C8	C9	0.0
C12	C11	C10	C9	0.0

Atom	Atom	Atom	Atom	Angle/°
C11	C10	C9	C8	0.0
C10	C9	C8	C7	0.0
C8	C7	C12	C11	0.0
C25	C20	C21	C22	-3(4)

Table 7: Atomic Occupancies for all atoms that are not fully occupied in **17br88a**.

Atom	Occupancy
Br1	0.534
Br2	0.294
Cl1	0.466
Cl2	0.706

Citations

O.V. Dolomanov and L.J. Bourhis and R.J. Gildea and J.A.K. Howard and H. Puschmann, Olex2: A complete structure solution, refinement and analysis program, *J. Appl. Cryst.*, (2009), **42**, 339-341.

Sheldrick, G.M., Crystal structure refinement with ShelXL, *Acta Cryst.*, (2015), **C71**, 3-8.

Sheldrick, G.M., ShelXT-Integrated space-group and crystal-structure determination, *Acta Cryst.*, (2015), **A71**, 3-8.

Software for the Integration of CCD Detector System Bruker Analytical X-ray Systems, Bruker axs, Madison, WI (after 2013).

19. Stability studies of compounds Ia-f in DMSO and in presence of water

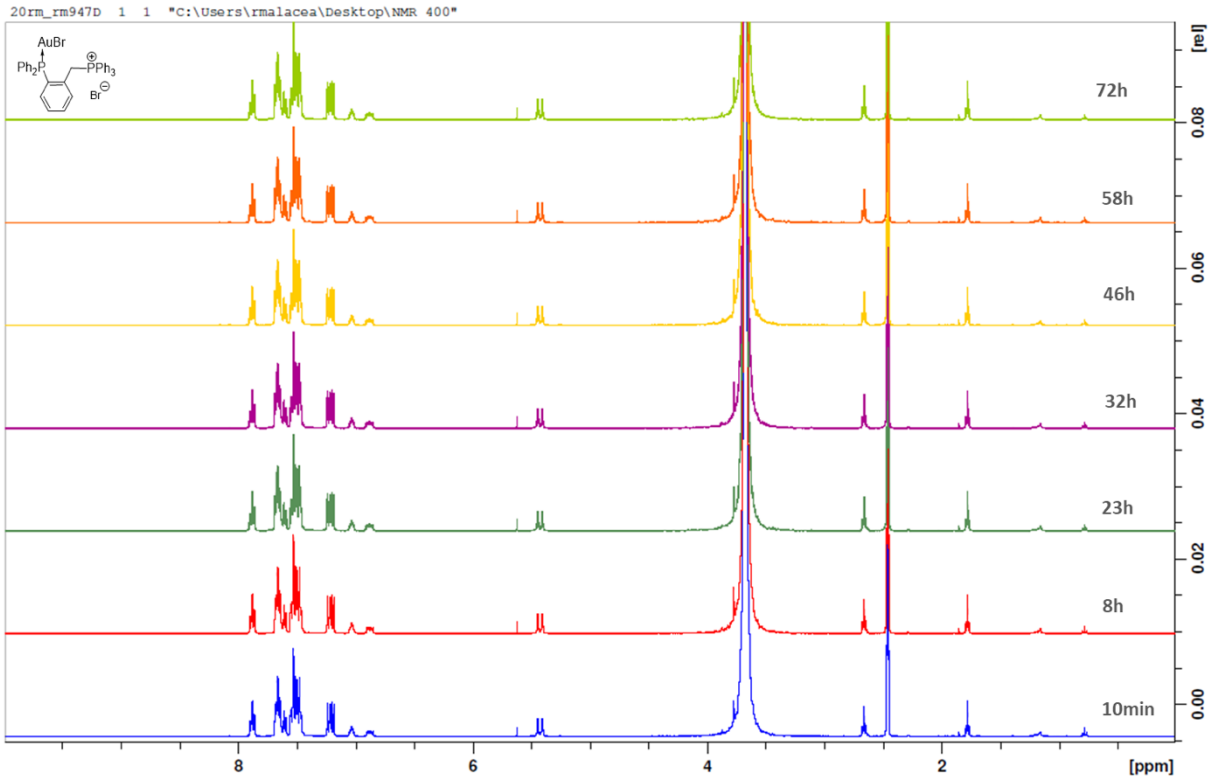

Stability of **Ia** in DMSO-D_6 followed by ^{1}H NMR (400MHz)

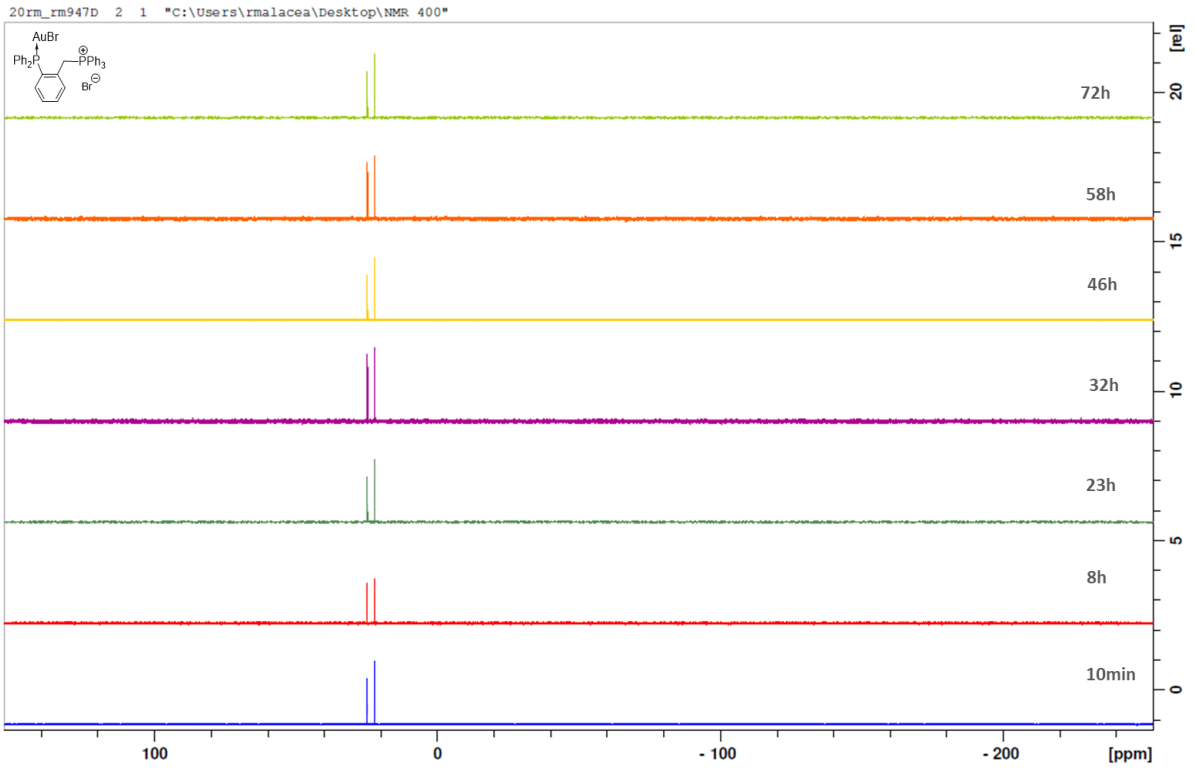

Stability of **Ia** in DMSO-D_6 followed by ^{31}P NMR (162MHz)

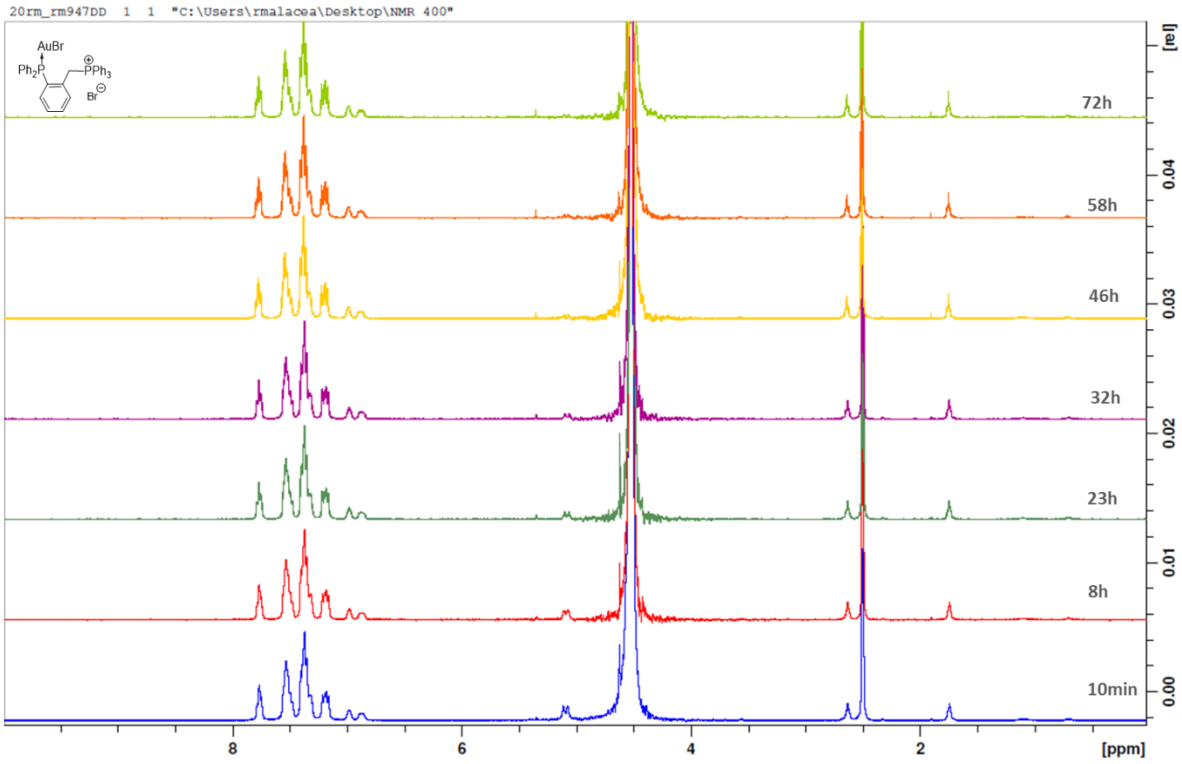

Stability of **Ia** in DMSO-D_6/D_2O followed by ^{1}H NMR (400MHz)

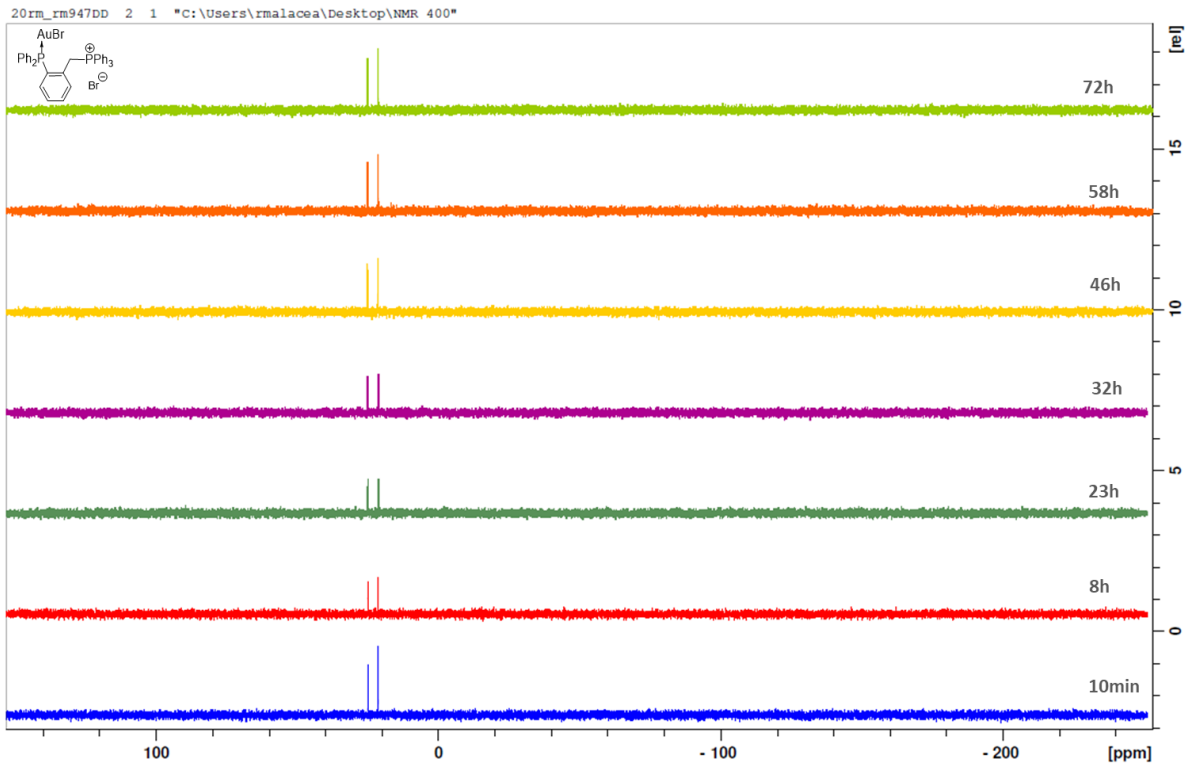

Stability of **Ia** in DMSO-D_6/D_2O followed by ^{31}P NMR (162MHz)

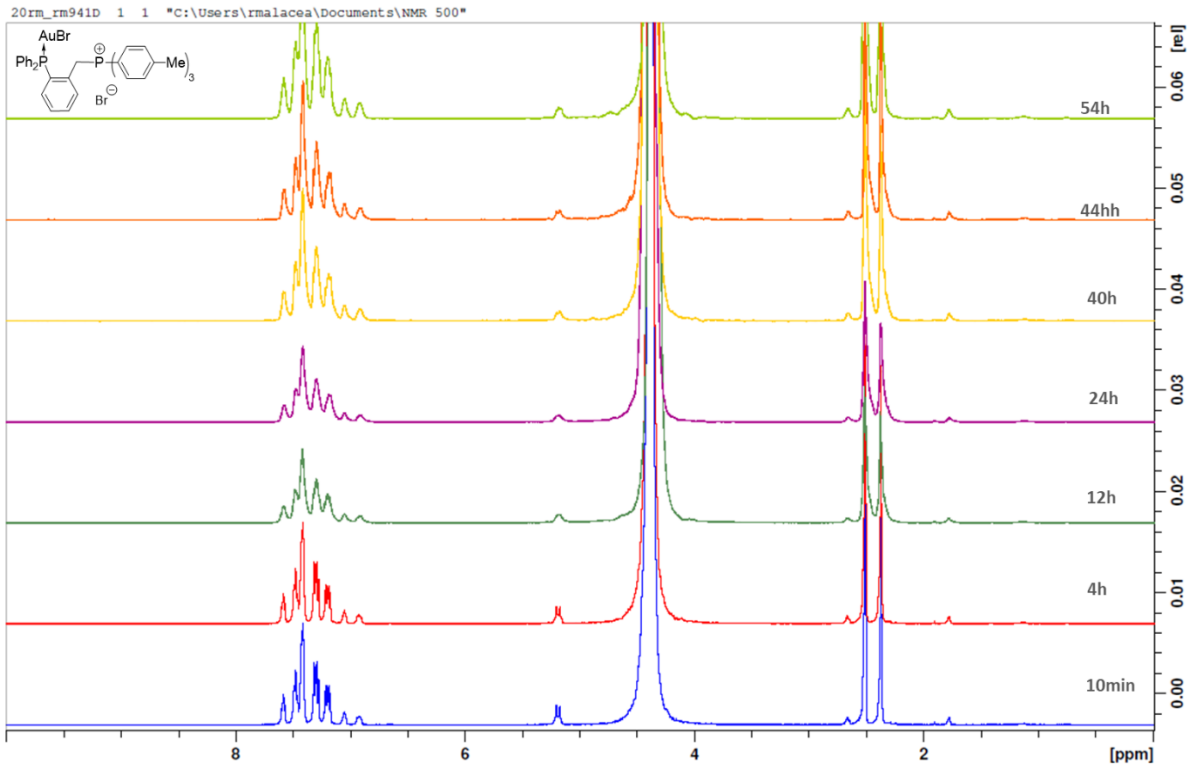

Stability of **Ib** in DMSO-D_6 followed by ^{1}H NMR (500MHz)

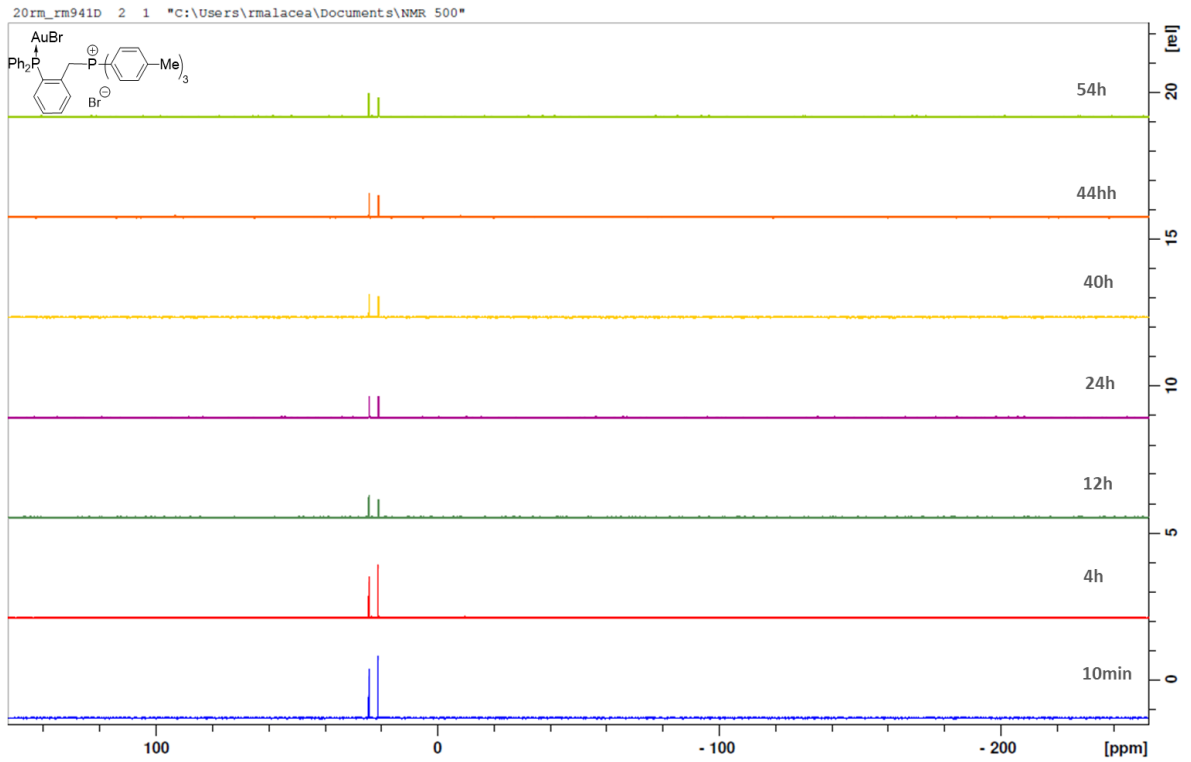

Stability of **Ib** in DMSO-D_6 followed by ^{31}P NMR (202MHz)

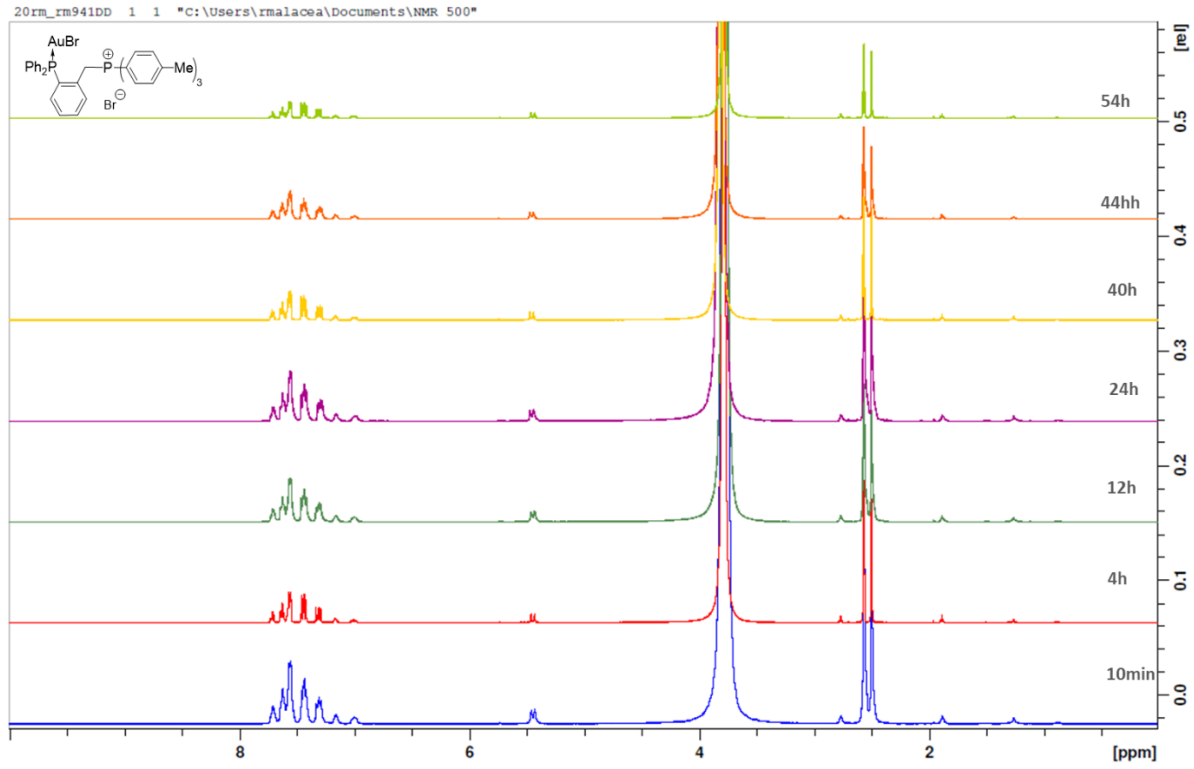

Stability of **Ib** in DMSO-D_6/D_2O followed by ^{1}H NMR (500MHz)

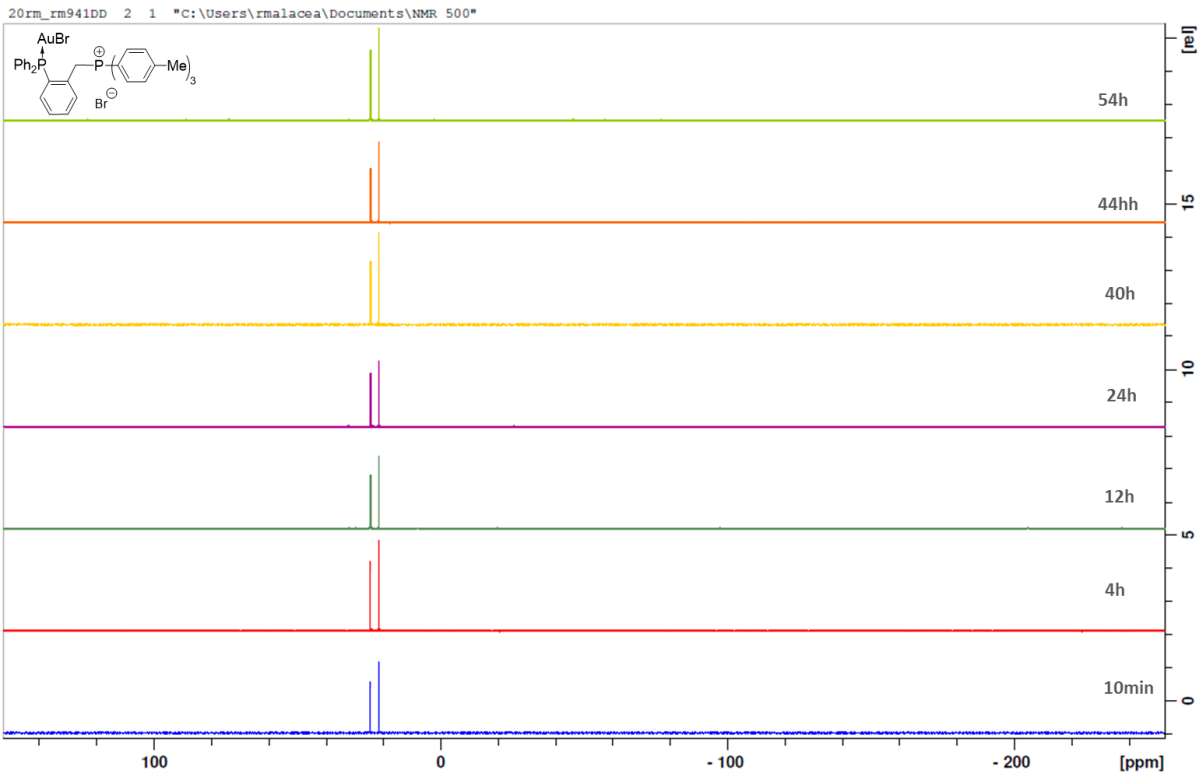

Stability of **Ib** in DMSO-D_6/D_2O followed by ^{31}P NMR (202MHz)

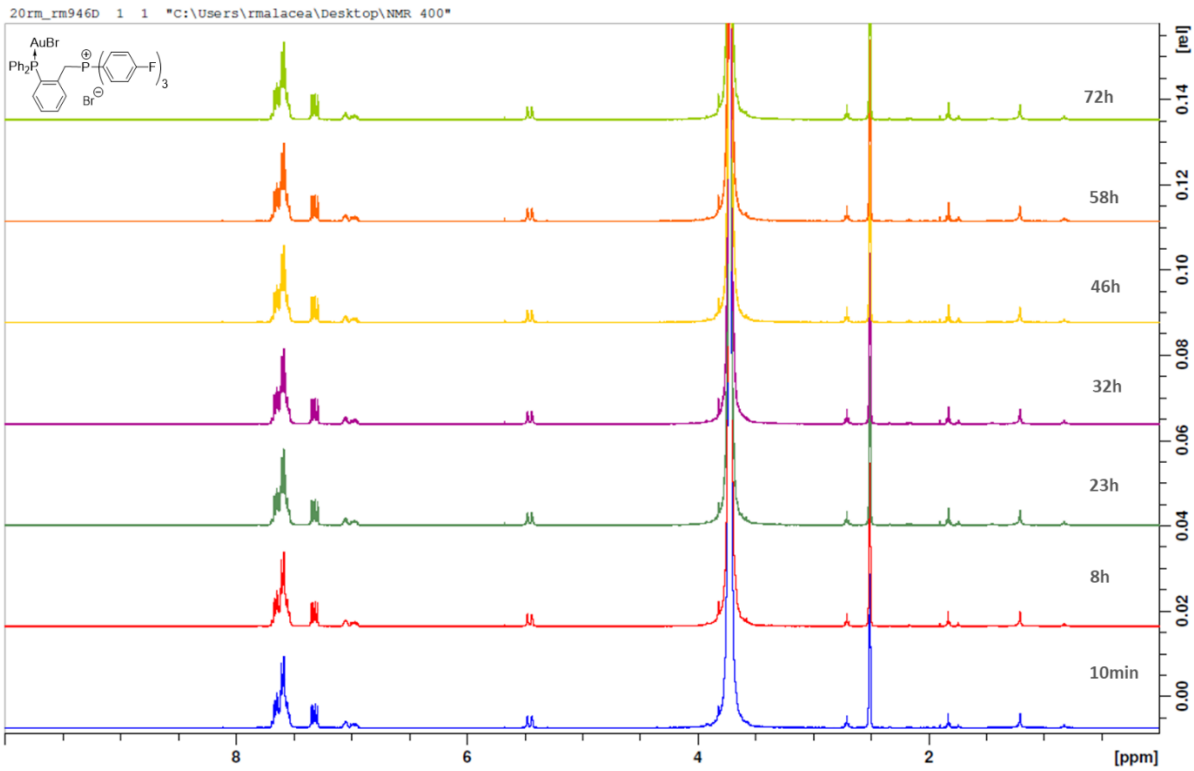

Stability of **Ic** in DMSO-D_6 followed by ^{1}H NMR (400MHz)

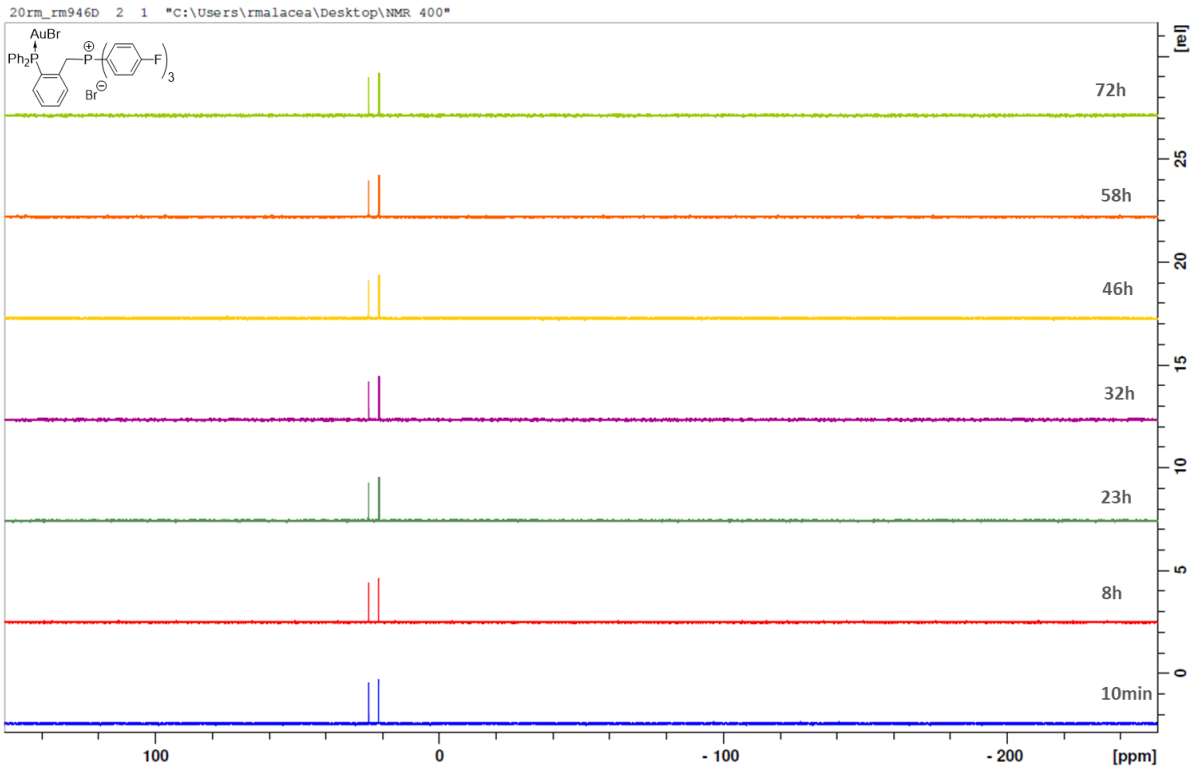

Stability of **Ic** in DMSO-D_6 followed by ^{31}P NMR (162MHz)

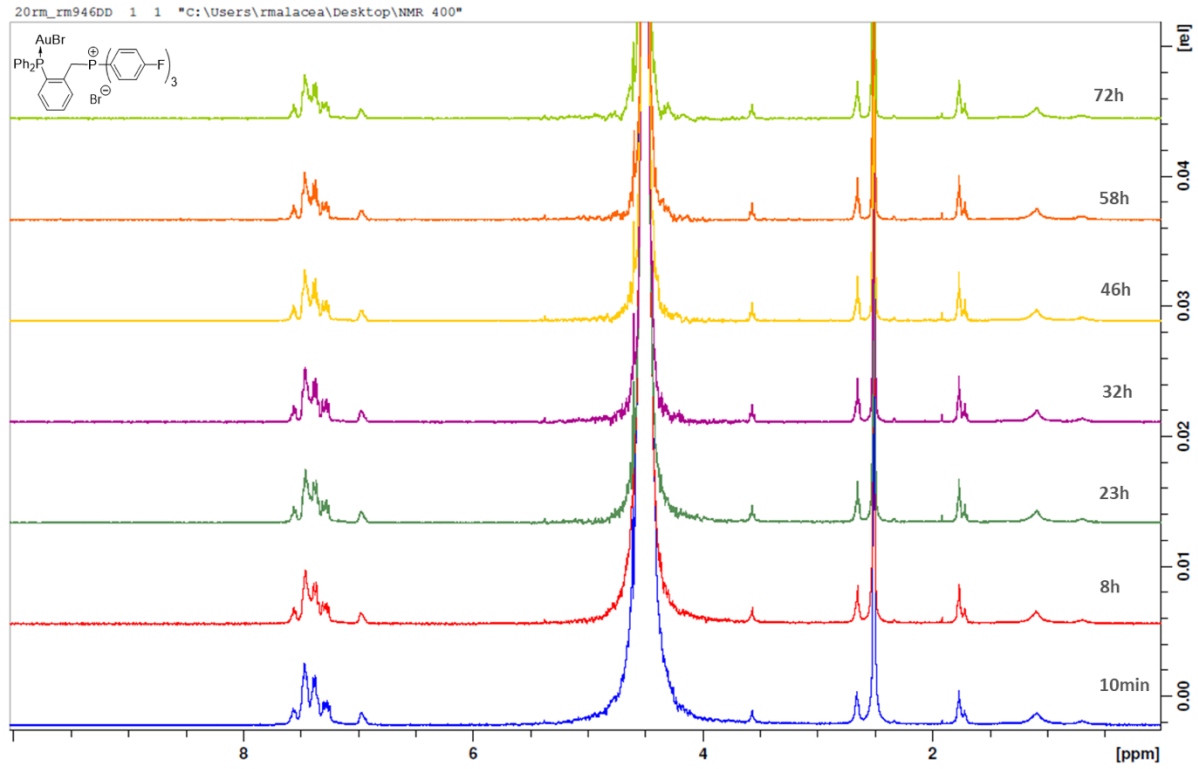

Stability of **Ic** in DMSO-D_6/D_2O followed by ^{1}H NMR (400MHz)

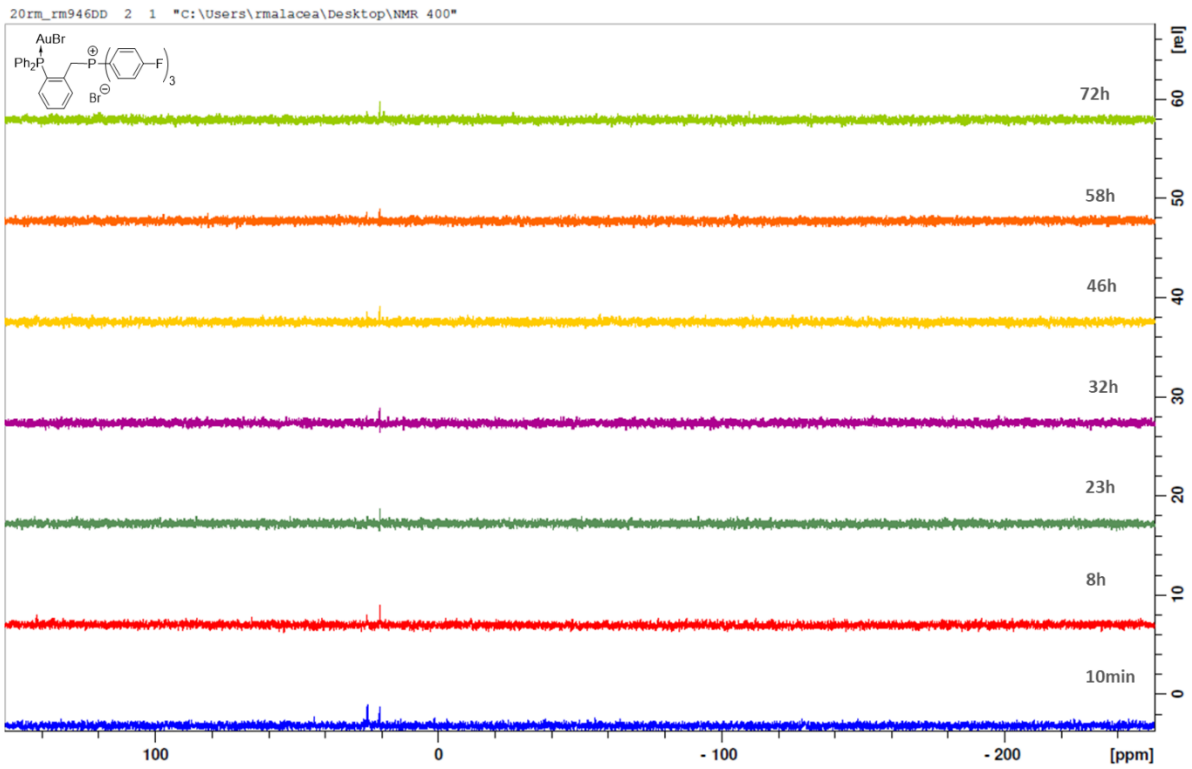

Stability of **Ic** in DMSO-D_6/D_2O followed by ^{31}P NMR (162MHz)

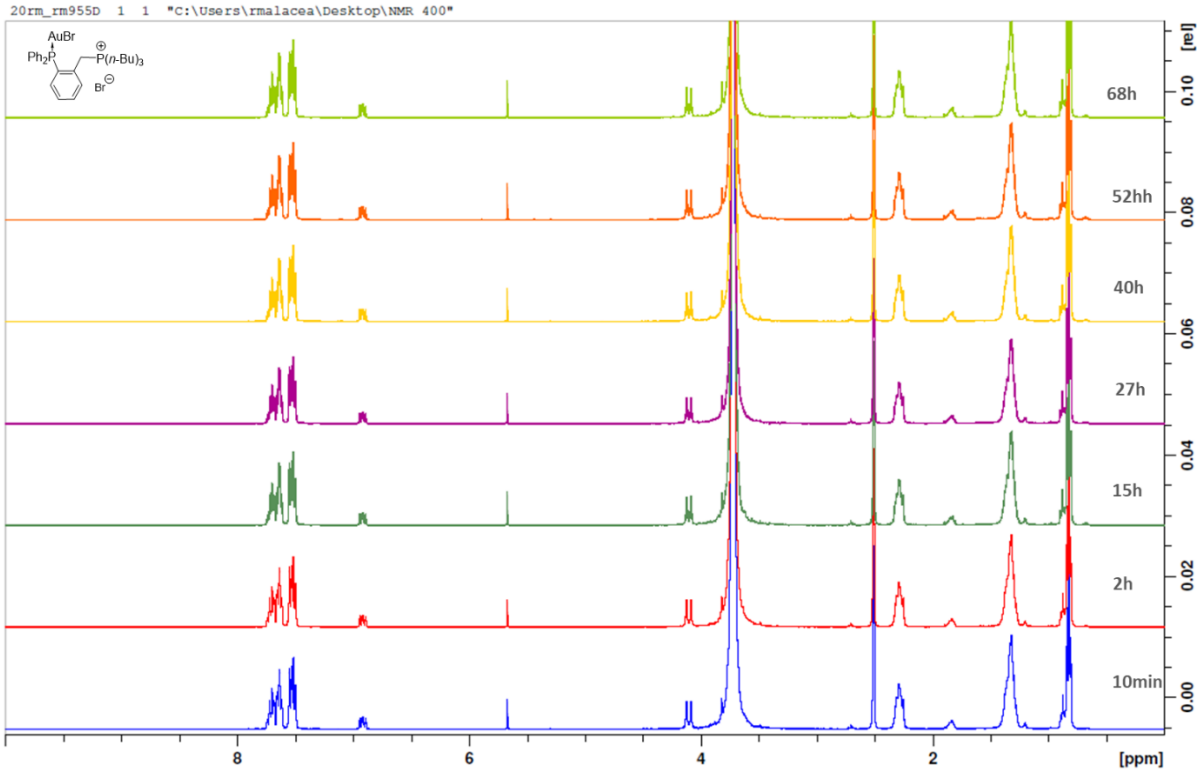

Stability of **Id** in DMSO-D_6 followed by ^{1}H NMR (400MHz)

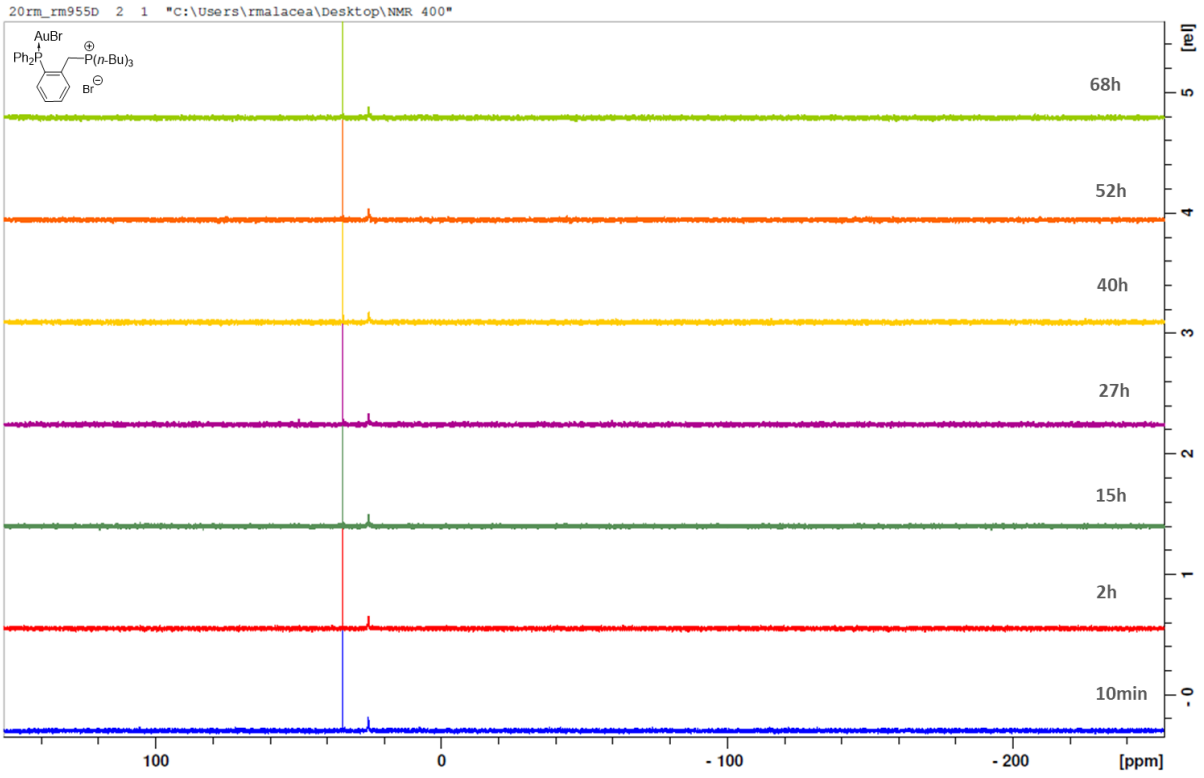

Stability of **Id** in DMSO-D_6 followed by ^{31}P NMR (162MHz)

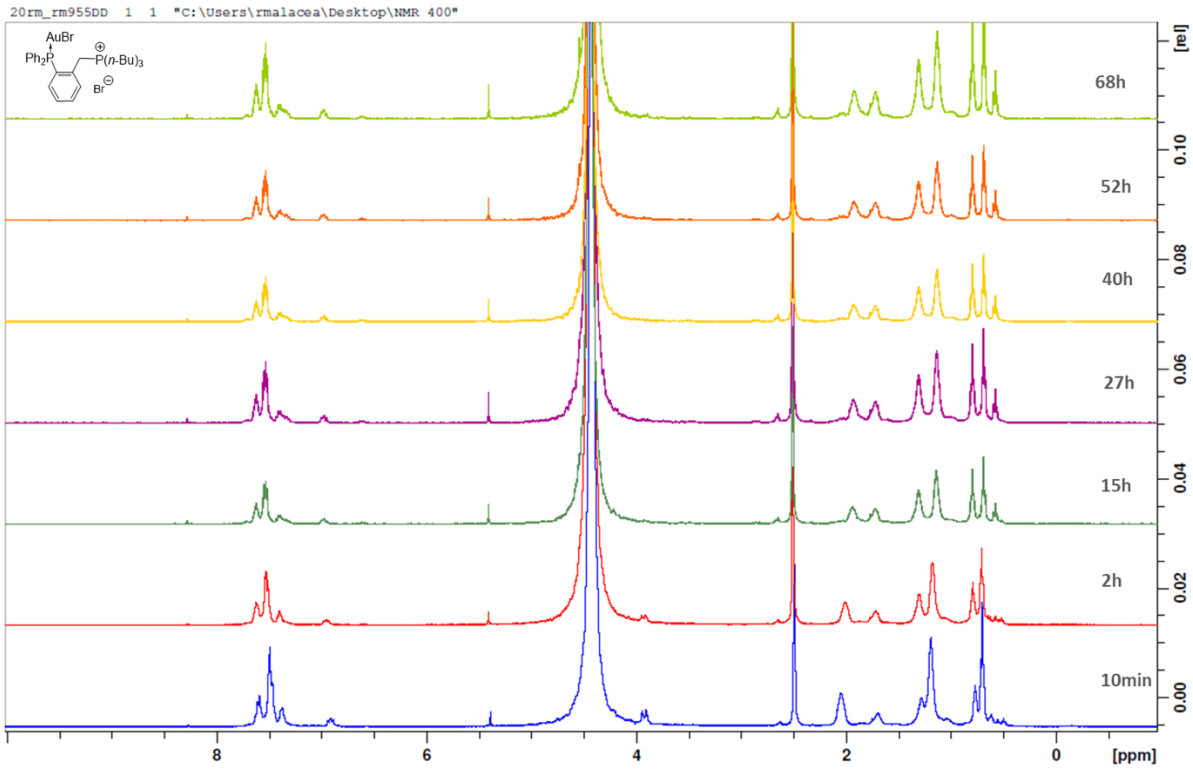

Stability of **Id** in DMSO-D_6/D_2O followed by ^{1}H NMR (400MHz)

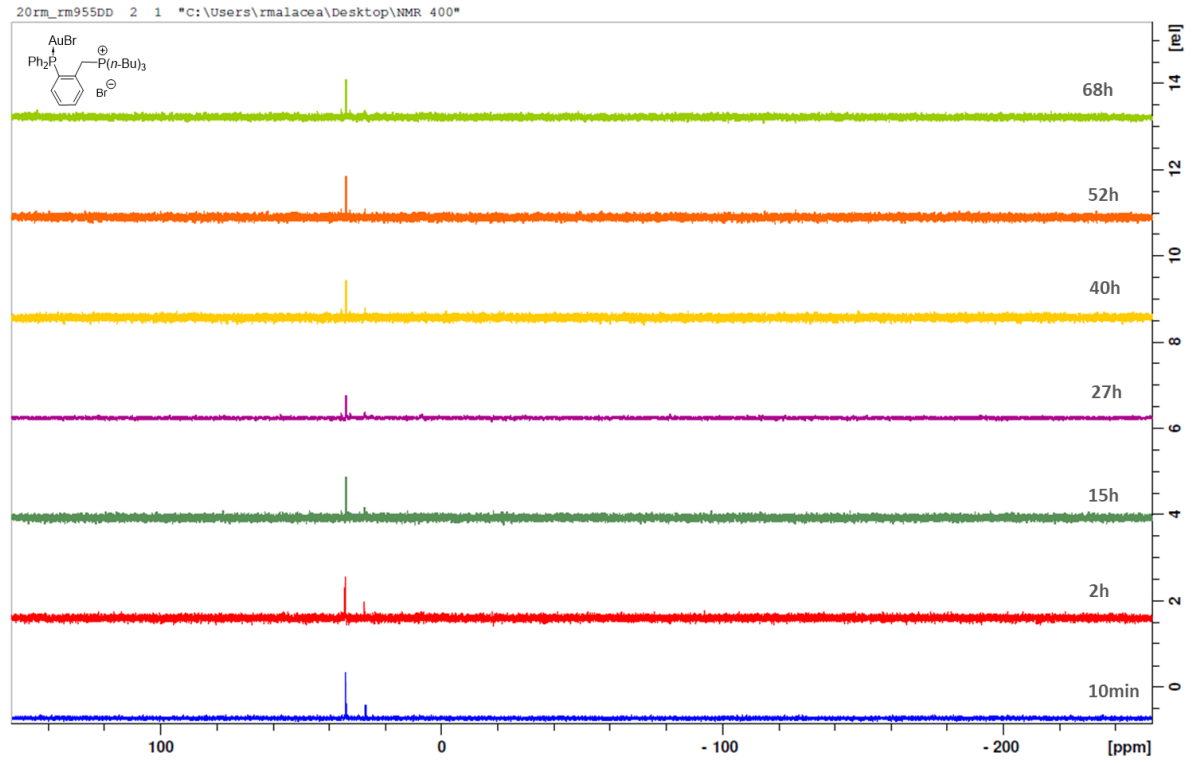

Stability of **Id** in DMSO-D_6/D_2O followed by ^{31}P NMR (162MHz)

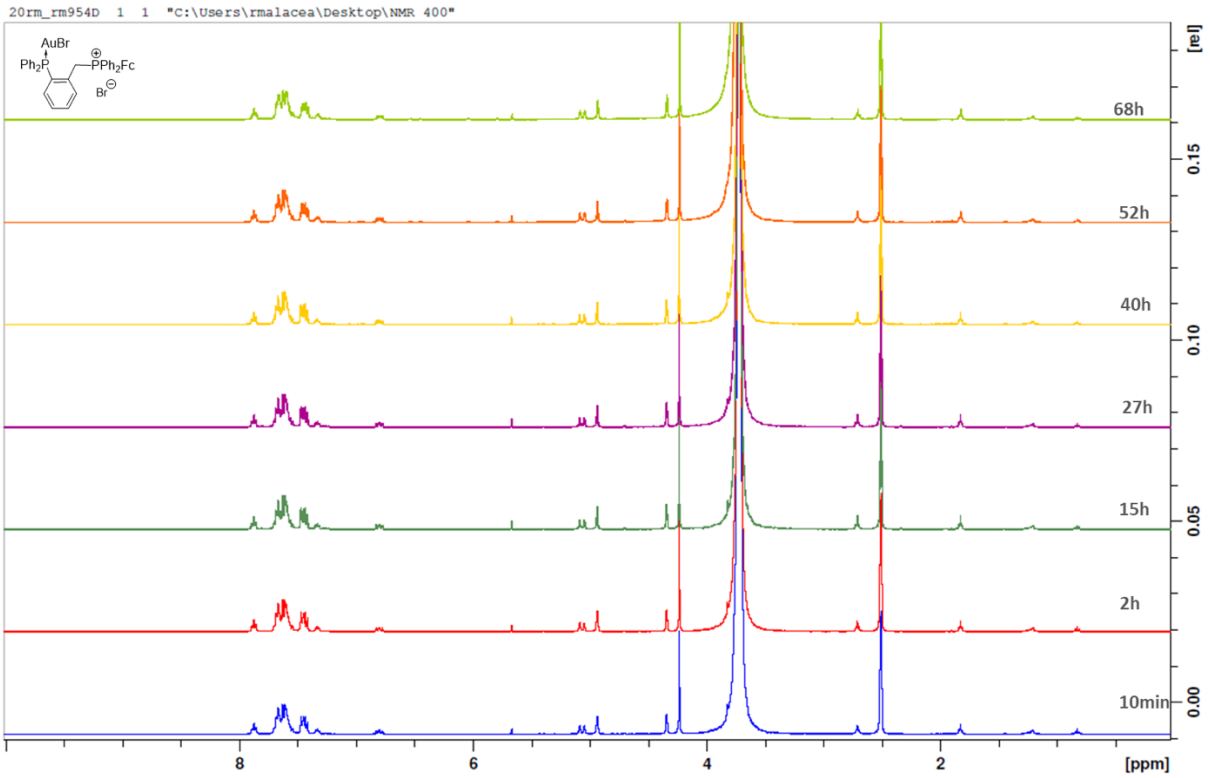

Stability of **Ie** in DMSO-D_6 followed by ^{1}H NMR (400MHz)

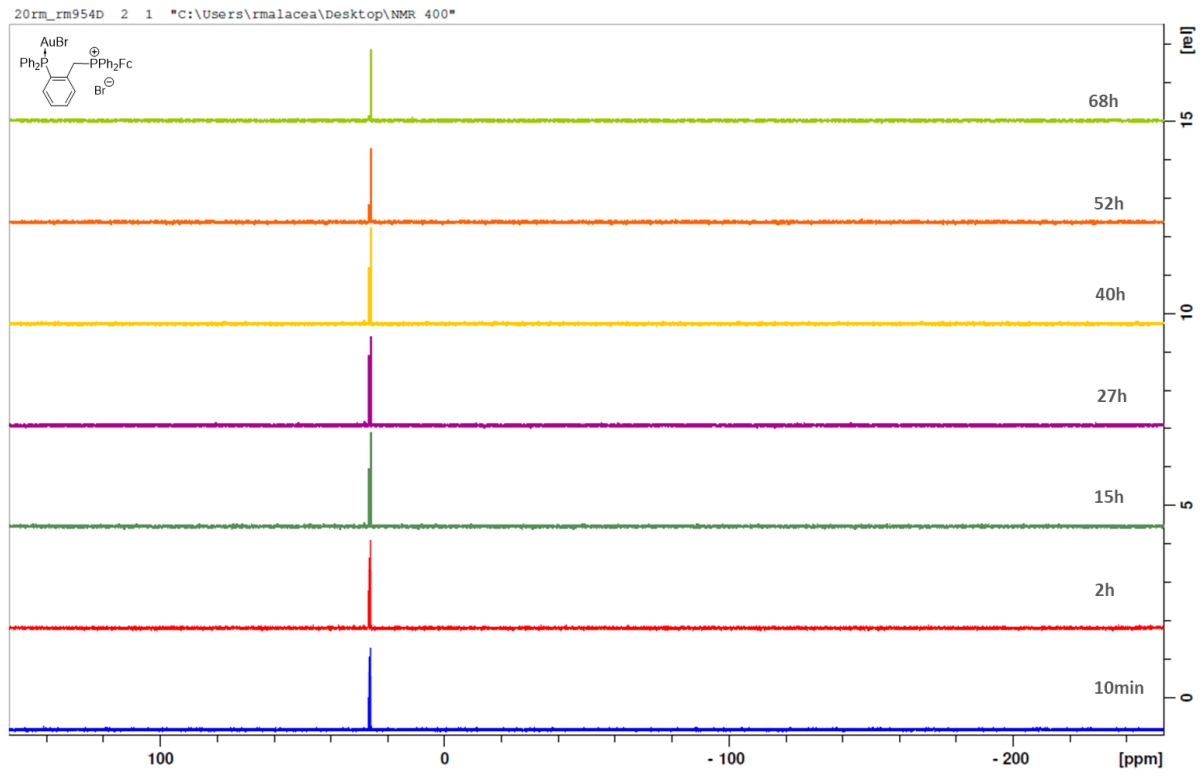

Stability of **Ie** in DMSO-D_6 followed by ^{31}P NMR (162MHz)

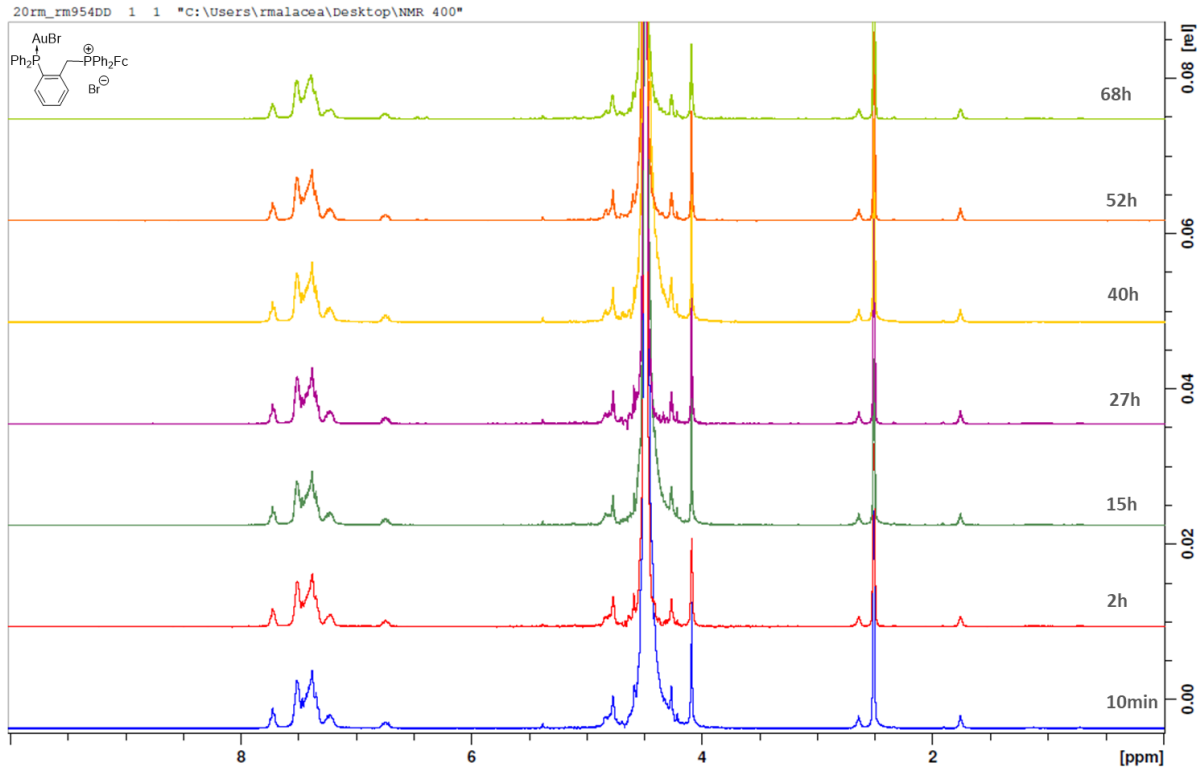

Stability of **Ie** in DMSO-D_6/D_2O followed by ^{1}H NMR (400MHz)

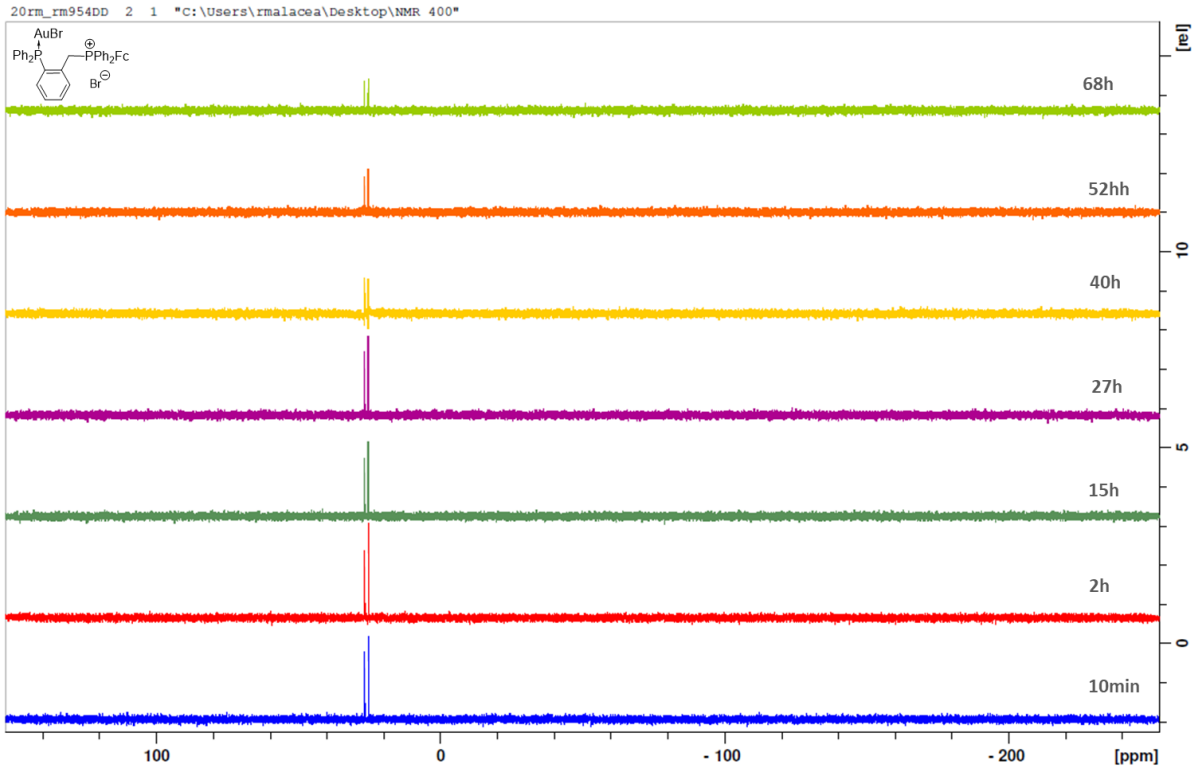

Stability of **Ie** in DMSO-D_6/D_2O followed by ^{31}P NMR (162MHz)

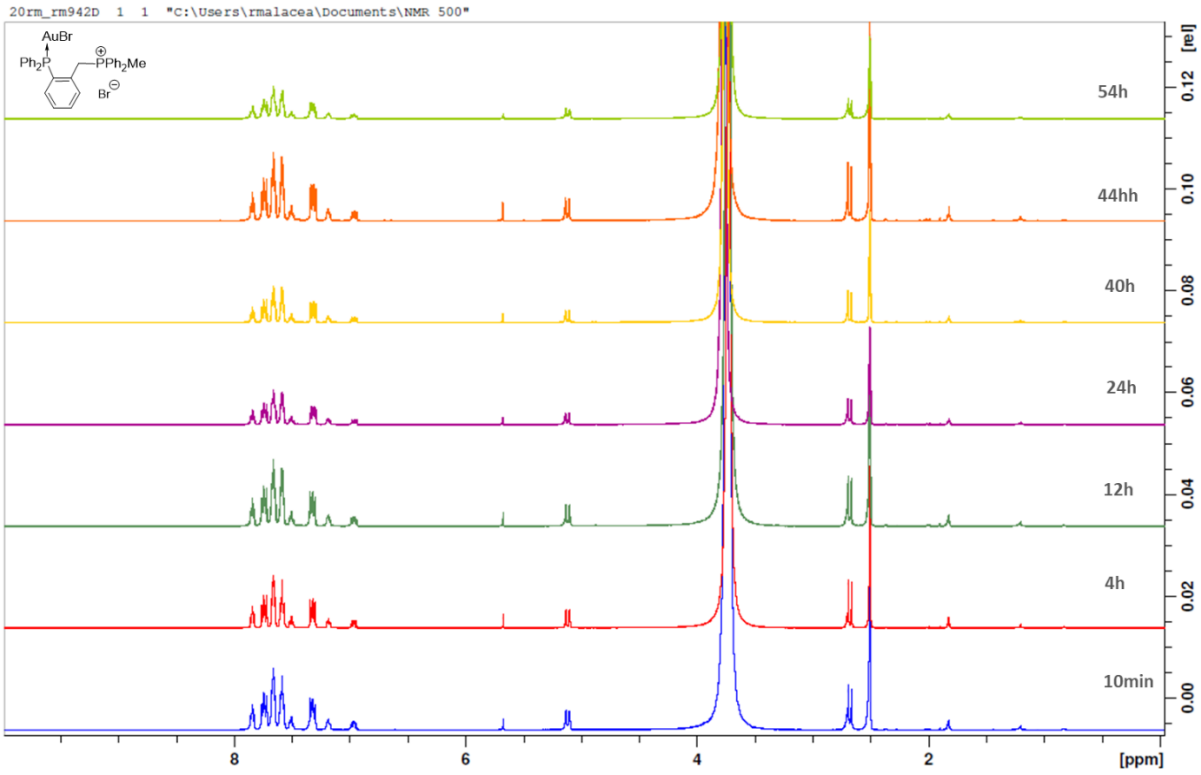

Stability of **If** in DMSO-D_6 followed by ^{1}H NMR (500MHz)

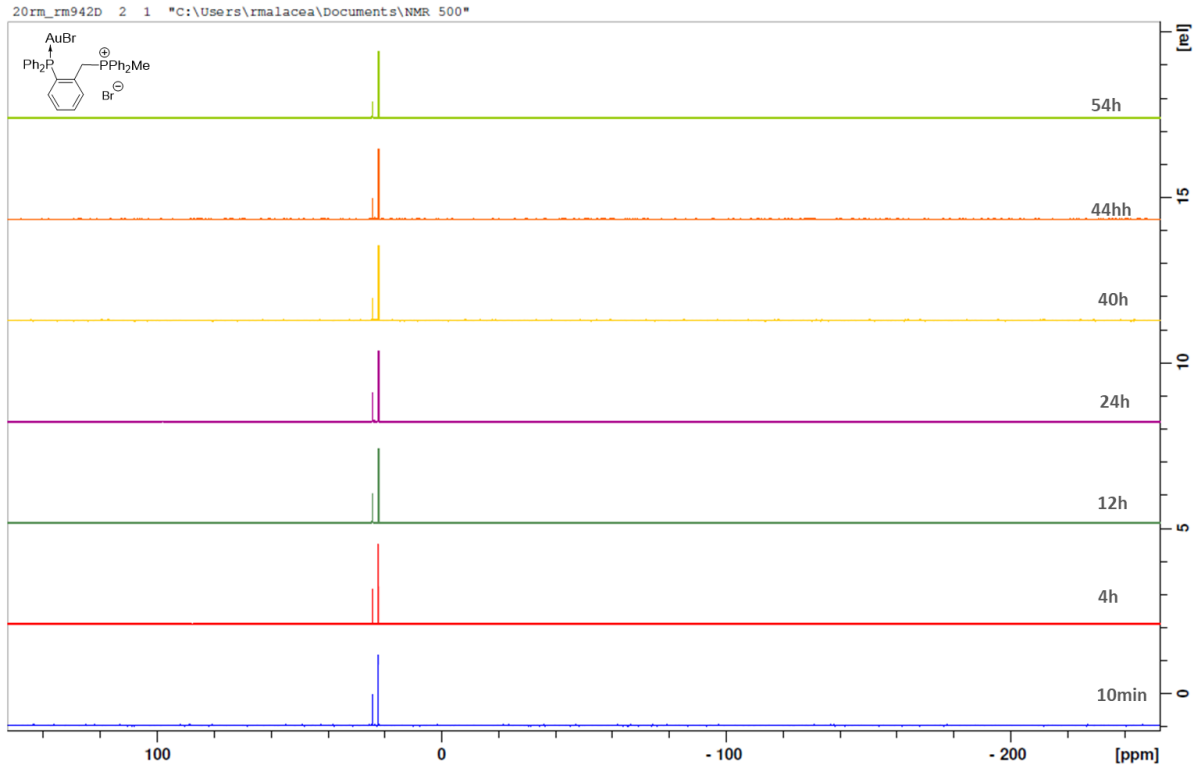

Stability of **If** in DMSO-D_6 followed by ^{31}P NMR (202MHz)

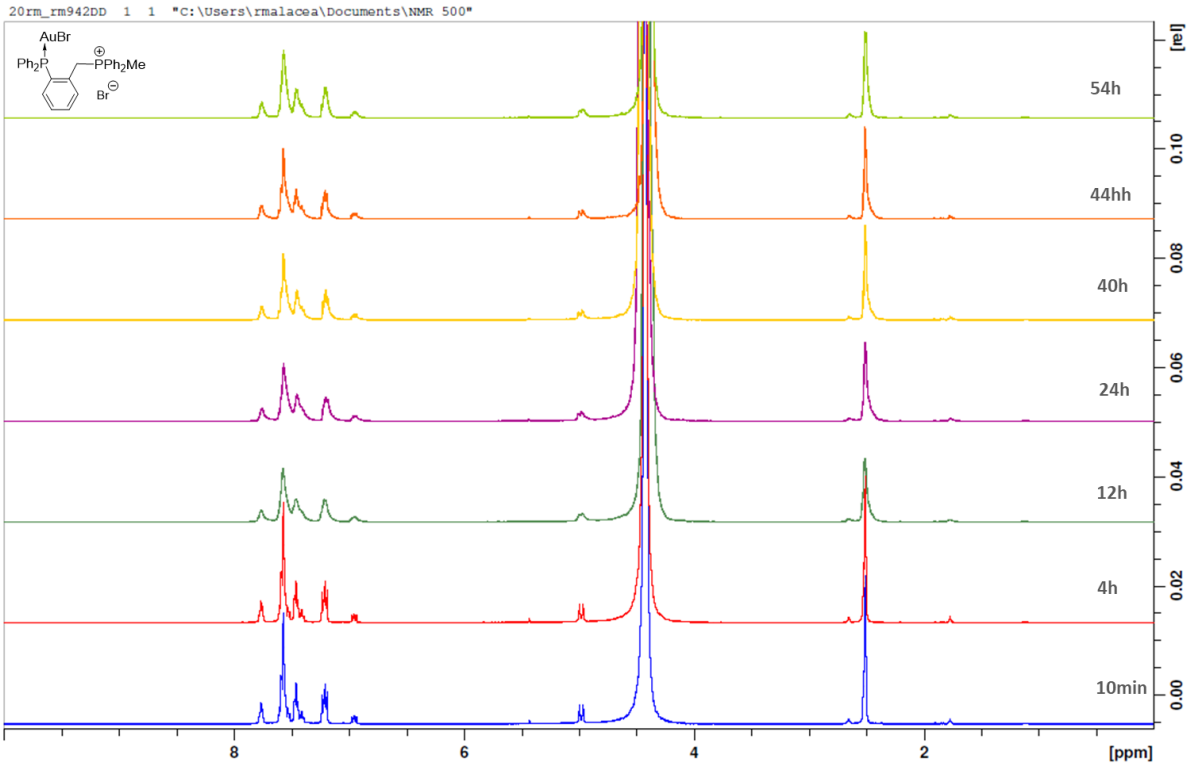

Stability of **If** in DMSO-D_6/D_2O followed by ^{1}H NMR (500MHz)

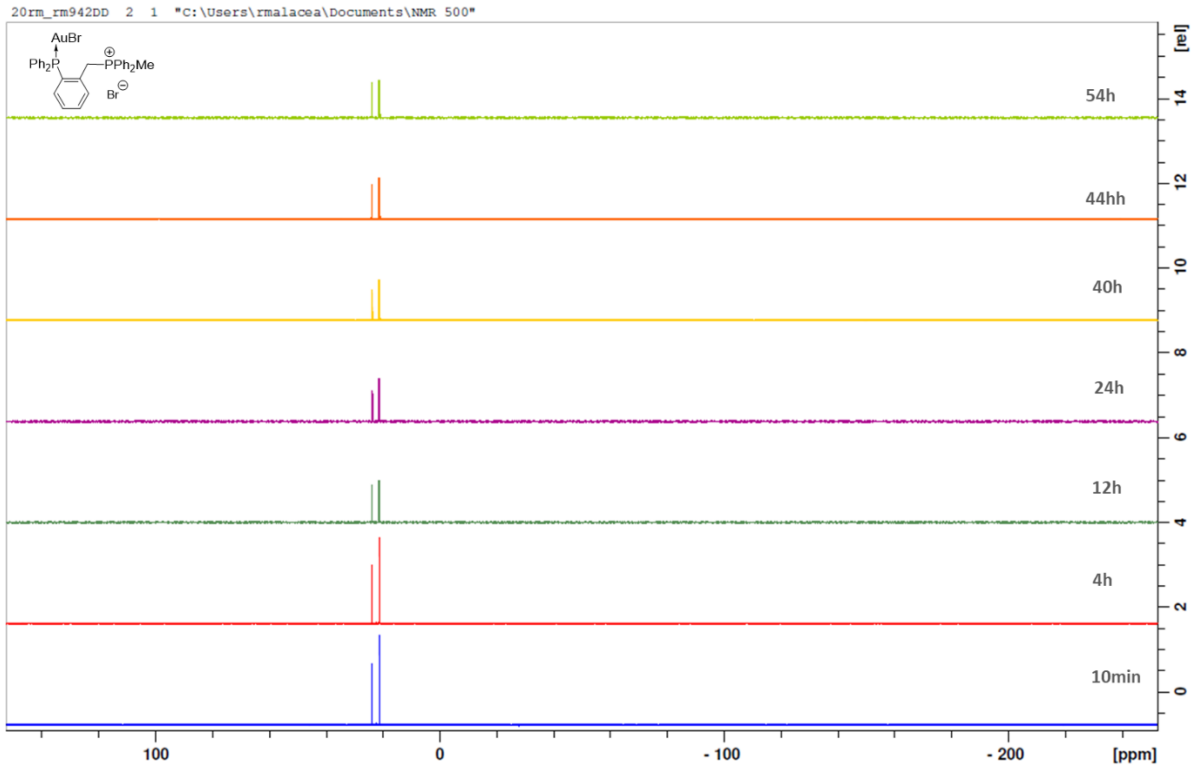

Stability of **If** in DMSO-D_6/D_2O followed by ^{31}P NMR (202MHz)

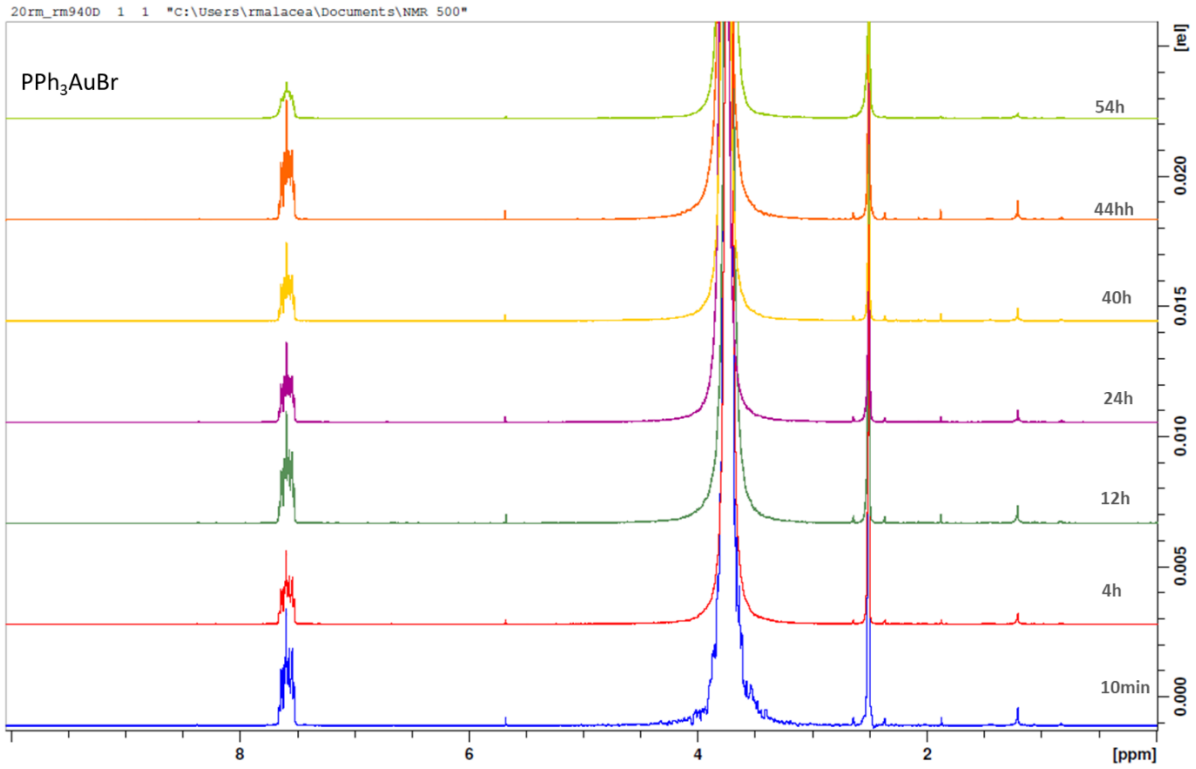

Stability of **Ig** in DMSO-D_6 followed by ^{1}H NMR (500MHz)

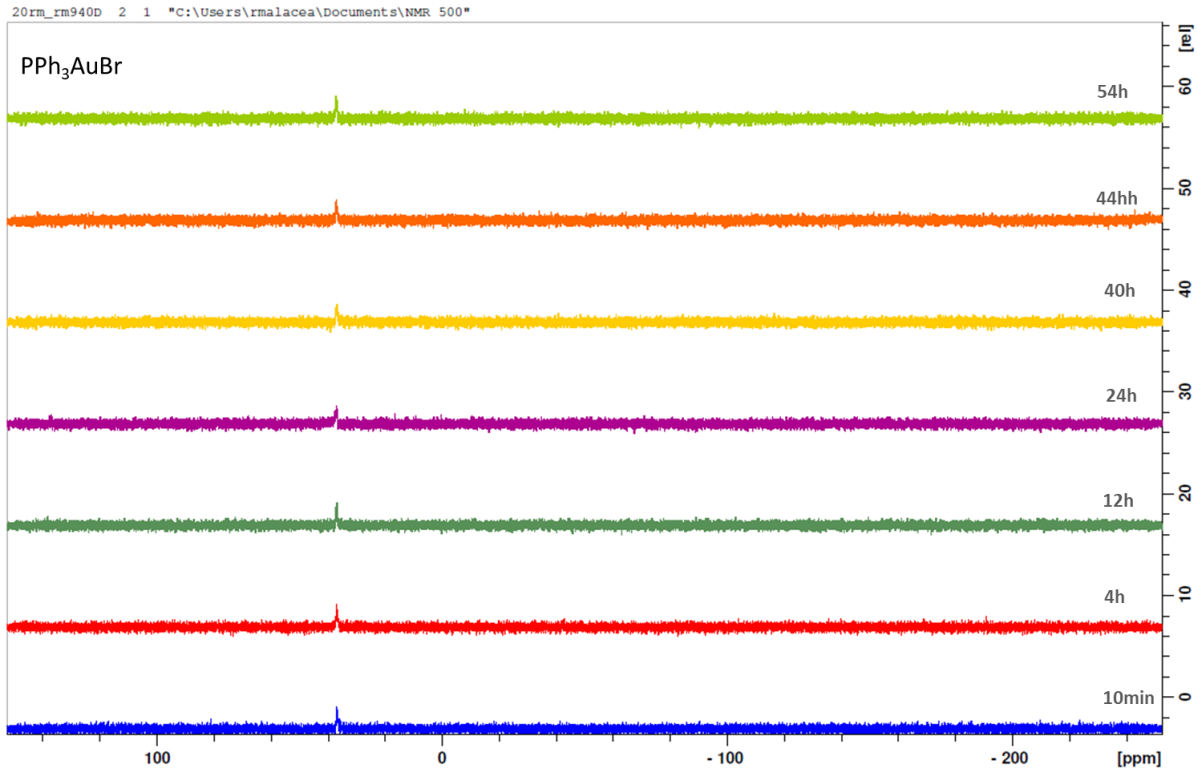

Stability of **Ig** in DMSO-D_6 followed by ^{31}P NMR (202MHz)

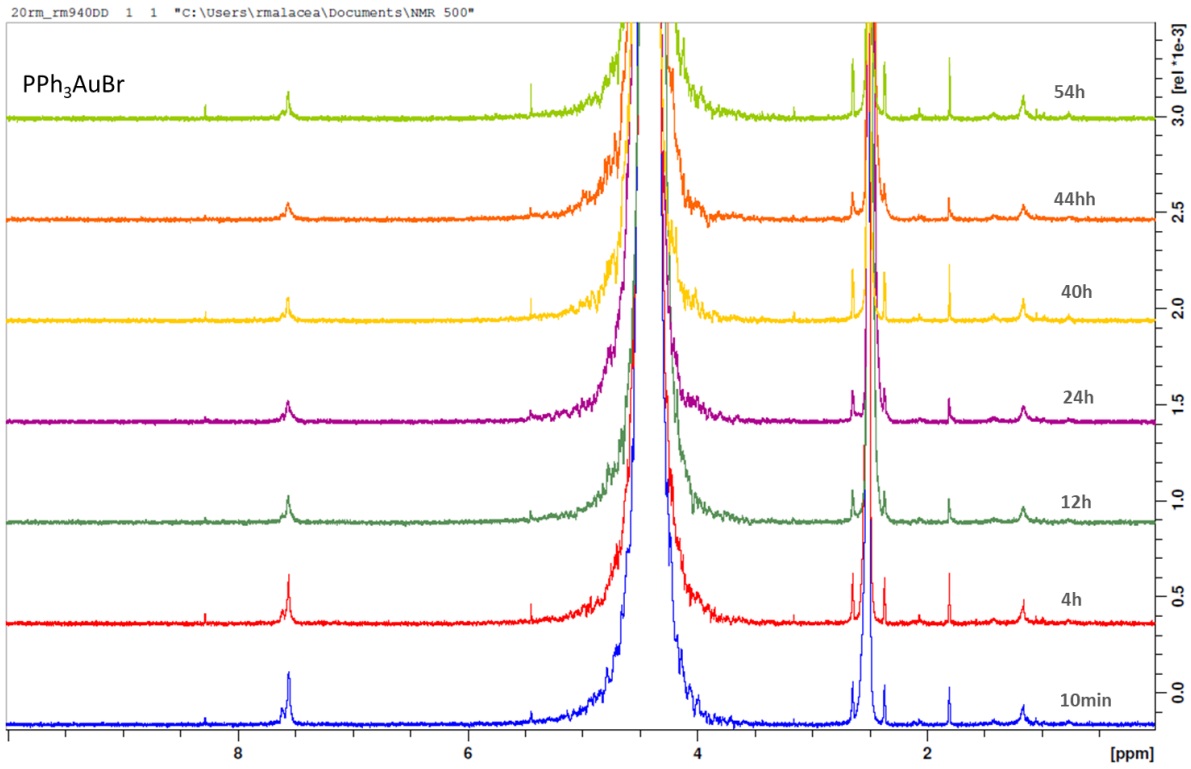

Stability of **Ig** in DMSO-D_6/D_2O followed by ^{1}H NMR (500MHz)

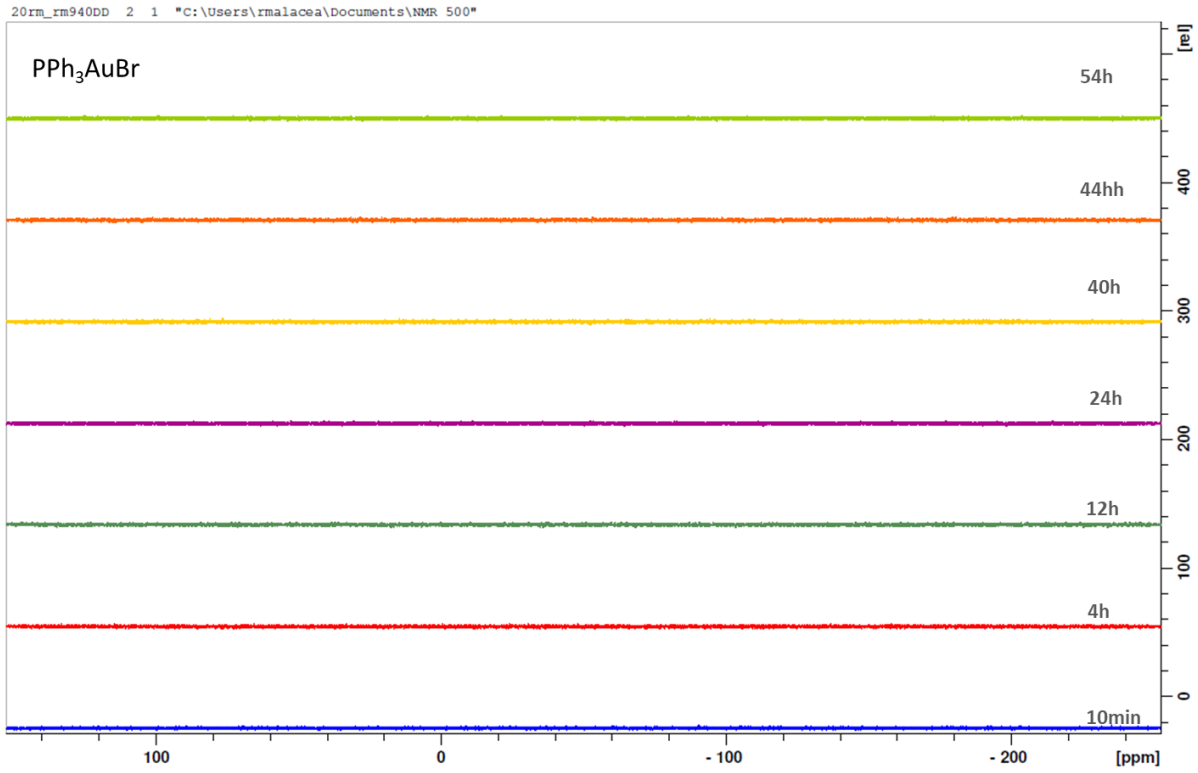

Stability of **Ig** in DMSO-D_6/D_2O followed by ^{31}P NMR (202MHz)

20. Water solubility of gold complexes **Ia-Ig** determined by ICP-AES

Procedure : Approximately 1 mg of each product is dissolved in 5 mL of ultra pure water. After one hour of stirring, the suspension was filtered through a 0.45 mm filter and mineralized by mMW with concentrated Trace Metal quality HCl. The gold concentration in solution was further measured by ICP-AES Thermo Electron (ICAP-7000).

Gold complexes	**Mass sample dissolved in 5ml water**	**Elemental analysis**	**Total Au in the initial sample**	**Measured Au in solution**	**Dissolved compound**
	mg	% Au	mg	mg	%
Ia	1.11	22.02	0.24	0.121	49.38
Ib	1.08	21.03	0.23	0.153	67.46
Ic	1.06	20.77	0.22	0.101	46.04
Id	1.5	23.61	0.35	0.172	48.47
Ie	1.05	19.65	0.21	0.130	62.80
If	1.14	23.67	0.27	0.207	76.63
Ig	1.18	36.53	0.43	0.002	0.43

21. Cells cytotoxity curves of Ia-g. DMSO. oxaliplatin. 5-FU. paclitaxel (A549)

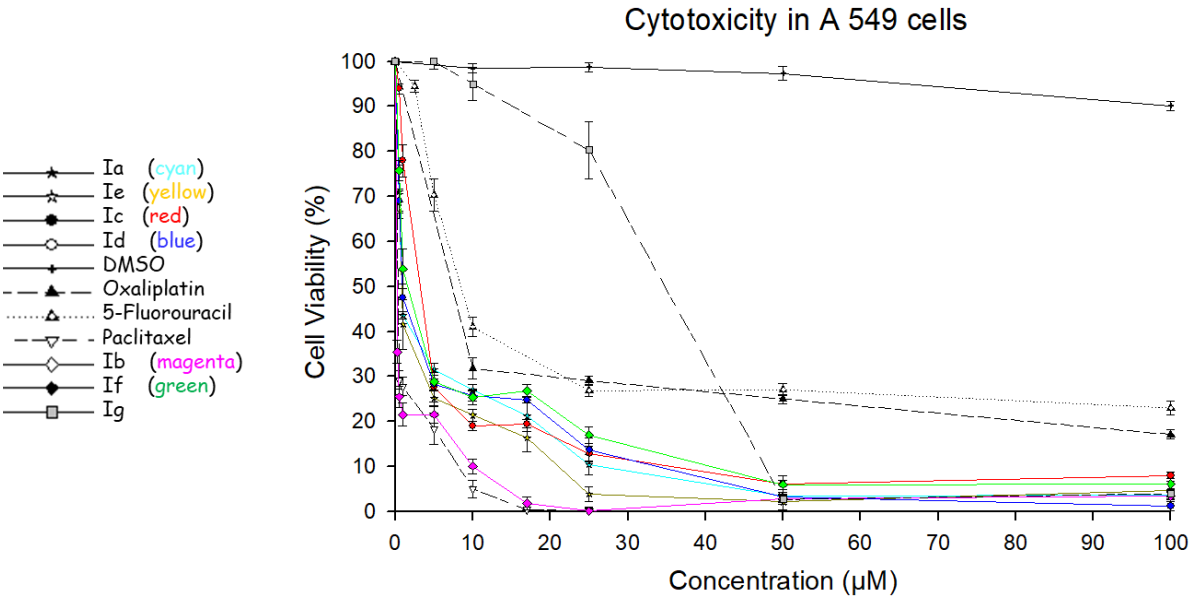

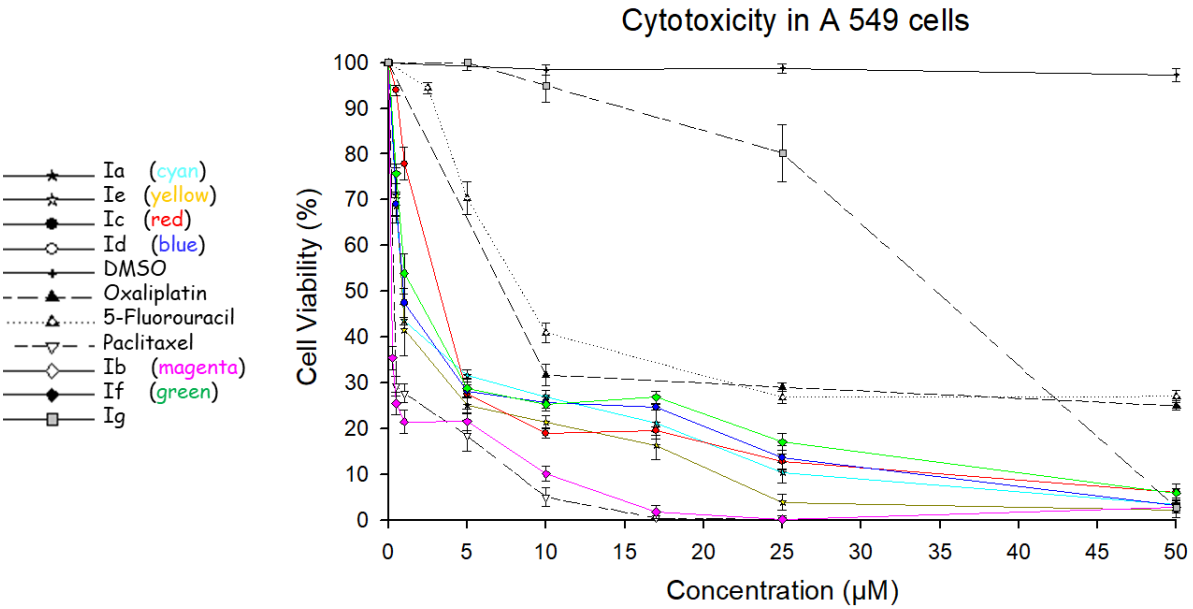

22. Cells cytotoxity curves of Ia-g. DMSO. oxaliplatin. 5-FU. paclitaxel (MDA-MB-231)

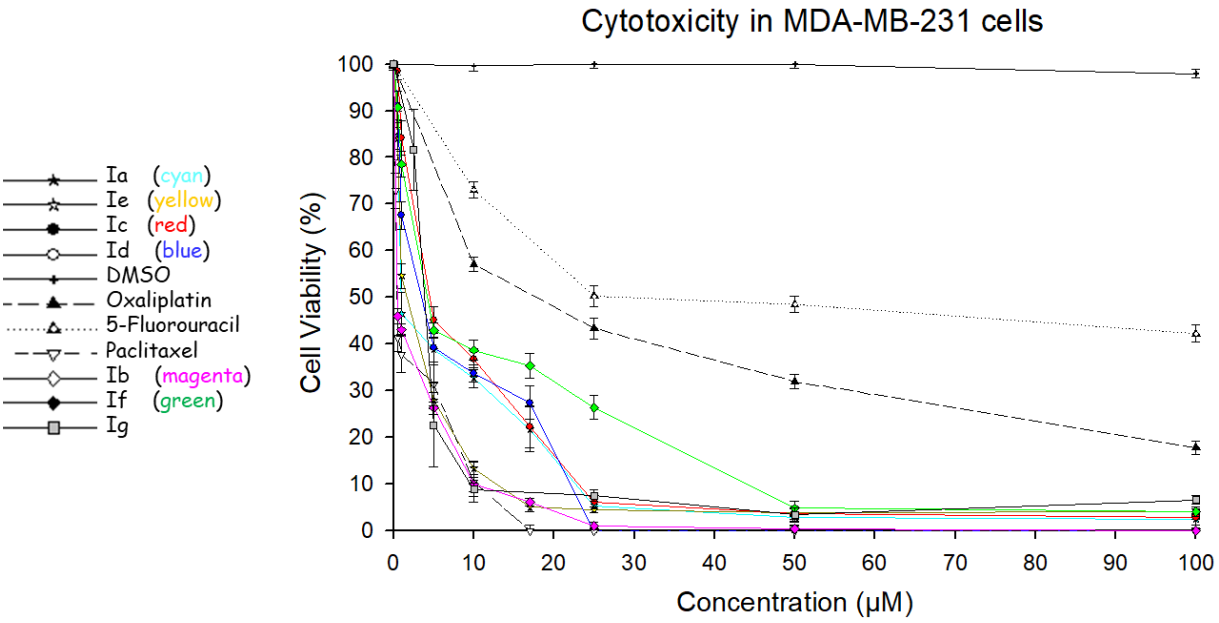

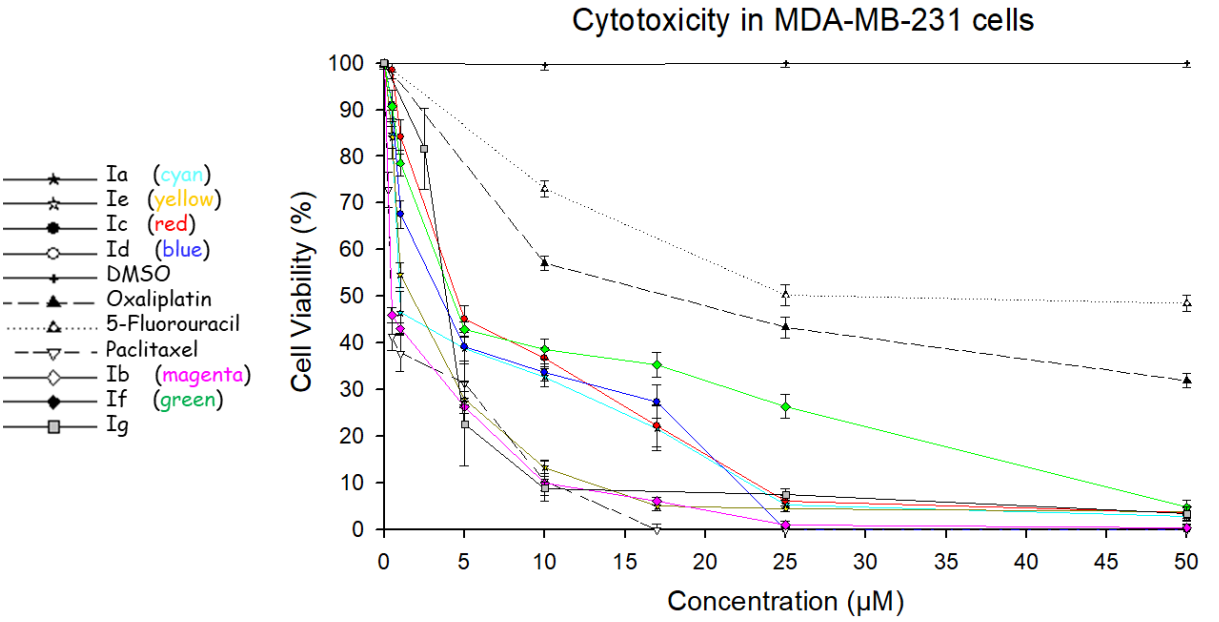

23. Cells cytotoxity curves of Ia-g. DMSO. oxaliplatin. 5-FU. paclitaxel (SW480)